~~Contains Security-Sensitive Information -~~
~~Withhold from public disclosure under 10 CFR 2.390(d)~~

ML14139A175

Enclosure 1

Validation of HRR Breach Hydrograph for Jocassee Dam

by Joseph L. Ehasz, P.E. and
Dr. David S., Bowles, P.E.,

April 2014

VALIDATION OF HRR BREACH HYDROGRAPH FOR JOCASSEE DAM

(Through an In-Depth Review of the Xu and Zhang Breach Parameter Estimation Methodology)

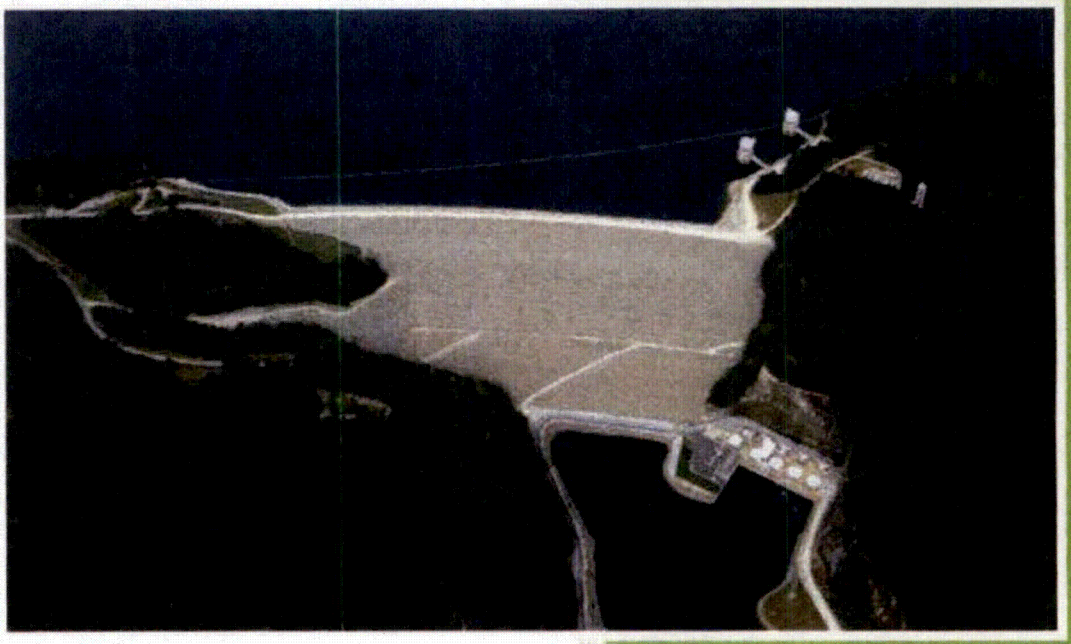

April 2014

By

Joseph L. Ehasz, P.E.

Dr. David S. Bowles, P.E.

VALIDATION OF HRR BREACH HYDROGRAPH FOR JOCASSEE DAM

(THROUGH AN IN-DEPTH REVIEW OF THE XU AND ZHANG BREACH PARAMETER ESTIMATION METHODOLOGY)

APRIL 2014

BY

JOSEPH L. EHASZ, P.E.
URS CIVIL CONSTRUCTION & MINING, INC.

APRIL 30, 2014

DR. DAVID S. BOWLES, P.E.
RAC ENGINEERS AND ECONOMISTS, LLC

APRIL 30, 2014

TABLE OF CONTENTS

APPENDICES

1.0 OBJECTIVE

1.1 Authorization

The authorization for this review was attached in an e-mail dated June 20, 2013 from Mr. Dean Hubbard, Duke Energy, to Mr. Joseph Ehasz, URS Civil Construction & Mining

1.2 Objective of the Validation Report

The objective of this report is to respond to questions raised by the FERC and the NRC about the use of the Xu and Zhang (2009) regression equations for estimating breach parameters to develop the breach hydrograph for a deterministic sunny-day breach of the Jocassee Dam. The agency questions are presented in Section 2.2. The implications of these responses and a detailed review of the Xu and Zhang (2009) methodology provide support for the breach hydrograph submitted to the NRC by Duke (2013) in the Hydrologic Reevaluation Report (HRR).

2.0 INTRODUCTION

2.1 HRR (Duke 2013) Breach Hydrograph

The HRR breach hydrographs (Duke 2013) for a deterministic sunny-day breach of the Jocassee Dam were developed as follows:

- The predicted median breach dimensions obtained from the Xu and Zhang (2009) best exact regression equations for a low erosion category were input to the HEC-RAS model.
- The values of the orifice and weir coefficients and the breach progression relationship in HEC-RAS were iteratively changed within reasonable ranges of values to match the predicted peak breach flow rate and the failure time from Xu and Zhang (2009). Consistent with the definition of failure time by Xu and Zhang (2009), the predicted value of failure time was used in HEC-RAS as a combination of breach initiation and breach formation.

An independent review, entitled "Jocassee and Keowee Dams Breach Parameter Review", dated February 2013, was performed on the Jocassee Dam postulated breach parameter estimates and underlying assumptions by Joseph L. Ehasz and Dr. David S. Bowles (Ehasz and Bowles 2013). That review focused on the appropriateness of estimating potential piping breach parameters for the Jocassee Dam based on the Xu and Zhang (2009) regression equations. Duke Energy and its consultant HDR Engineering had selected the dam breach parameter estimation methodology proposed by Y. Xu and L. M. Zhang in their technical paper entitled "Breaching Parameters for Earth and Rockfill Dams" published in the American Society of Civil Engineers (ASCE) Journal of Geotechnical and Geoenvironmental Engineering in December 2009 and in Xu (2010). This is a "state of knowledge" paper and is specifically applicable for consideration of a piping breach in a zoned embankment dam. The main objective of the paper is to develop robust empirical formulas for estimating dam breach parameters that consider physical characteristics of the dam such as the erodibility of the embankment materials in addition to the dam height and reservoir volume, which most other regression methods rely on.

The physical features of embankment dam design and construction strongly influence both the likelihood of a piping dam breach occurring and the breach characteristics in the event that a breach occurs. Therefore, our February 2013 report (Ehasz and Bowles 2013) began with a summary of some important physical features of the Jocassee Dam. It continued with an evaluation of, if piping should initiate, would detection and successful intervention be likely to prevent a failure. It discussed what piping failure modes might apply to Jocassee Dam based on a potential failure modes analysis and some general breach parameter considerations.

Finally, it evaluated, using the "state of knowledge," what are the appropriate breach parameters for Jocassee Dam? Those parameters were then used by HDR to simulate the downstream conditions that might result from a breach of Jocassee Dam caused by a piping failure.

The basis of the breach parameters that were used to represent the Jocassee Dam for a piping breach and the resulting breach hydrograph were developed based on the breach parameter estimation methodology developed by Xu and Zhang (2009). Significant factors in selecting the Xu and Zhang (2009) methodology included its distinction between modes of failure, namely either overtopping or piping, and its consideration of the erodibility of the embankment materials. In fact, erodibility was found to be the most significant control variable in the Xu and Zhang (2009) regression equations for all five breach parameters.

The conclusions from our February 2013 (Ehasz and Bowles 2013) review of the basis for the HRR breach hydrograph (Duke 2013) are summarized as follows:

- Xu and Zhang (2009) is considered to be a "state-of-the-practice" regression method for estimating piping dam breach parameters. Unlike most other methods, it includes erodibility as a control variable. This variable was found to be the most important variable in the Xu and Zhang (2009) regression analysis. The capability to consider erodibility is particularly important for predicting breach parameters for Jocassee Dam to account for the influence of its modern dense rockfill construction.
- The HRR (Duke 2013) breach hydrograph is a realistic but conservative breach hydrograph that has good defendablity based on the validity of the Xu and Zhang (2009) method and the conservative nature of the median breach parameter estimates due to:
    - uni-directional breach formation due a postulated piping failure mode initiating in the (b)(7)(F)
    - the deposition of eroded rockfill immediately below the dam leading to a tailwater rise that would limit the rate of breach development; and
    - the robust characteristics of a modern zoned central core rockfill dam that were included in the design and construction of Jocassee Dam that make it more erosion resistant than other low erodibility dams in the Xu and Zhang (2009) case histories data set on which their regression analysis is based.

2.2 Agency Questions

Presentations of the estimated Jocassee Dam breach parameters and simulated downstream conditions were made to both the FERC and the NRC based on the review presented in our February 2013 report (Ehasz and Bowles 2013). In addition, a field trip was made to the Jocassee Dam site by representatives of both regulatory agencies to visually inspect the condition of the dam as well as the monitoring procedures and resulting observations.

Both the FERC and the NRC had questions about the use of the Xu and Zhang (2009) methodology for developing the breach parameter estimates. These questions are summarized as follows:

1) **Precedence** - where has use of the Xu and Zhang (2009) methodology been accepted?
2) **Chinese case histories** – about 43% of the dam failure case histories on which the Xu and Zhang (2009) methodology is based are for Chinese dams for which little information is available in the US.
3) **Representation of case histories for rockfill and other low erodibility dams** - the data set of dams used by Xu and Zhang (2009) to develop the regression equations has only three dams that are considered large (i.e. > 15 meters high) embankment dams with low erodibility and these dams are all outside of the US.
4) **Use of the Briaud erosion categories** – how were the erosion categories developed by Briaud (2008) applied in developing the Xu and Zhang (2009) methodology and are they applicable to dam breach?
5) **Breach time definition**[1] – the definition of time to failure used by Xu and Zhang (2009) includes at least part of the breach initiation phase in addition to the breach formation process unlike other regression methods that include only the breach formation process.

Therefore the objective of this report is to respond to these agency questions and to provide support for the appropriate use of the Xu and Zhang (2009) methodology for Jocassee Dam in developing the HRR breach hydrograph submitted to the NRC by Duke (2013).

2.3 Summary of Approach for This Review

The major activities conducted under this review were as follows:

- A four-day working session was held with Dr. Yao Xu, the principal author of the Xu and Zhang (2009) methodology. Professor Jean-Louis Briaud, the author of the erosion categorization methodology used by Xu and Zhang (2009) participated in the first two days. Dr. Xu responded to the agency questions and participated in a detailed case-by-case review of the 75 case histories that were used to develop the Xu and Zhang (2009) regression equations.
- Professor Briaud made a site visit to Jocassee Dam to become familiar with the properties of the rockfill material and other aspects of its construction. He addressed questions regarding the appropriateness of using his erosion categorization methodology in the Xu and Zhang (2009) breach parameter methodology. He also confirmed the low erosion category for Jocassee Dam.

[1] In this report the terms *breach development time* and *breach formation time* are used interchangeably.

Revised regression equations were developed by Dr. Xu for sensitivity studies on the Jocassee Dam HRR breach hydrograph based on changes that were made to the original Xu and Zhang (2009) case histories data set to address the agency questions and some other issues identified during our detailed review. The revised equations were also applied to Teton Dam to compare with the observed breach parameters and those obtained by Xu and Zhang (2009) and the observed breach parameters.

- Sensitivity studies were conducted based on the revised Xu and Zhang and the Froehlich (1995a and 2008) regression equations applied to Jocassee Dam. The resulting breach parameter estimates were used by HDR in the HEC-RAS model to obtain breach hydrographs for a deterministic sunny-day breach of the Jocassee Dam. A comparison of these hydrographs with the HRR breach hydrograph submitted to the NRC by Duke (2013) provided support for the HRR breach hydrograph.

2.4 Report Outline

- Section 3 of this report contains an update of the background discussion of Jocassee Dam that was provided in our February 2013 report (Ehasz and Bowles 2013).
- Section 4 presents the outcomes of Professor Briaud's visit to Jocassee Dam his confirmation of the low erosion category for the rockfill material for this dam.
- Section 5 refers to a summary of the original Xu and Zhang (2009) methodology and its original implementation for Jocassee Dam contained in Appendix B.
- Section 6 presents the findings of the review of the original Xu and Zhang (2009) methodology that we conducted with Dr. Xu, including the changes made to the case histories data set to address the FERC and NRC questions and the development of revised regression equations.
- Section 7 presents the sensitivity study using the revised regression equations for Jocassee Dam, which provides support for the breach hydrographs submitted in the Hydrologic Reevaluation Report (HRR) to the NRC by Duke on March 12, 2013 (Duke 2013).
- Section 8 presents the overall conclusions and responds to the questions presented by the FERC and NRC.
- Appendix A contains Professor Briaud's complete report.
- Appendix B summarizes the original Xu and Zhang (2009) methodology and its original implementation for Jocassee Dam on which the HRR hydrograph (Duke 2013) is based.
- Appendix C contains a bench marking/comparative analysis for rockfill dams and characteristics of recent failures relative to Jocassee Dam.
- Appendix D contains the detailed data supporting the revision to the Xu and Zhang regression equations.

- Appendix E contains a review of this report by Dr. Mark Morris, an internationally recognized European expert in dam breach analysis and breach hydrograph development.

The most significant outcome and conclusions of this report are the verification and revision of the data set utilized to develop the breach parameter regression equations presented in the Xu and Zhang (2009) and the verification of the interpretation of the erosion characteristics on which the Xu and Zhang (2009) methodology is based. Through sensitivity analyses based on the revised Xu and Zhang regression equations and the Froehlich (1995a and 2008) regression equations it is demonstrated that the HRR breach hydrograph (Duke 2013) for a deterministic sunny-day piping breach of the Jocassee Dam is a reasonable and conservative estimate.

3.0 BACKGROUND

Our February 2013 (Ehasz and Bowles 2013) report gave some details of the Jocassee Dam embankment, the general piping failure mechanism and the potential piping failure modes for the dam. As background and for continuity, this report will repeat some of this information in this section, especially with regard to the characterization of the dam and it's attributes as they affect erodibility during development of a postulated breach.

3.1 Characterization of Jocassee Dam

The following statements describe the detailed characteristics of the dam and are significant to dam performance and breach characteristics (see Figures 3.1 and 3.2):

- The dam was completed in 1967. It has been continuously monitored and has performed very well to the present; meeting or exceeding FERC standards. Even though the dam was designed and constructed in the mid-1960's it has all the modern and defensive measures of the rockfill dams designed and constructed today. A detailed review of the Jocassee Dam and it's performance was conducted 20 years after completion as described in the report entitled, "Jocassee Main Dam Design, Construction and Performance", by George F. Sowers, April 1987.

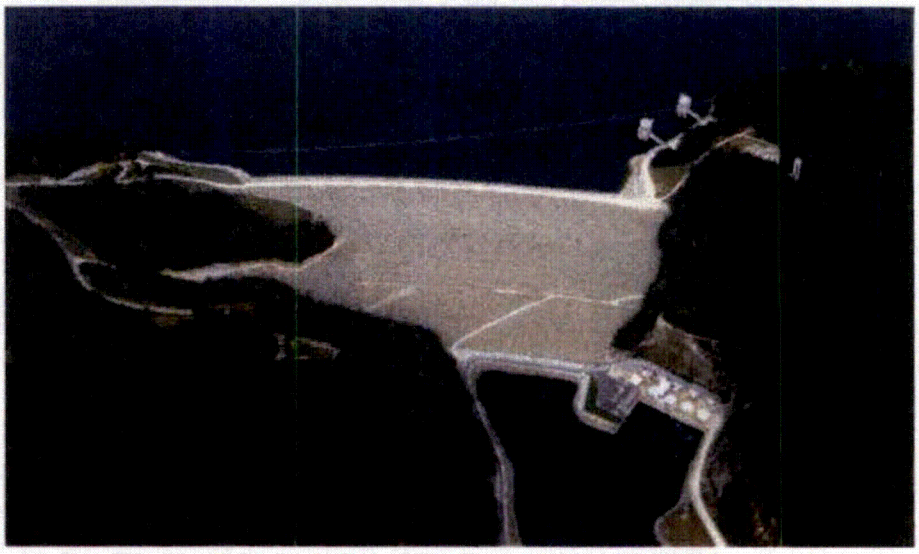

Figure 3.1. Google aerial view of Jocassee Dam

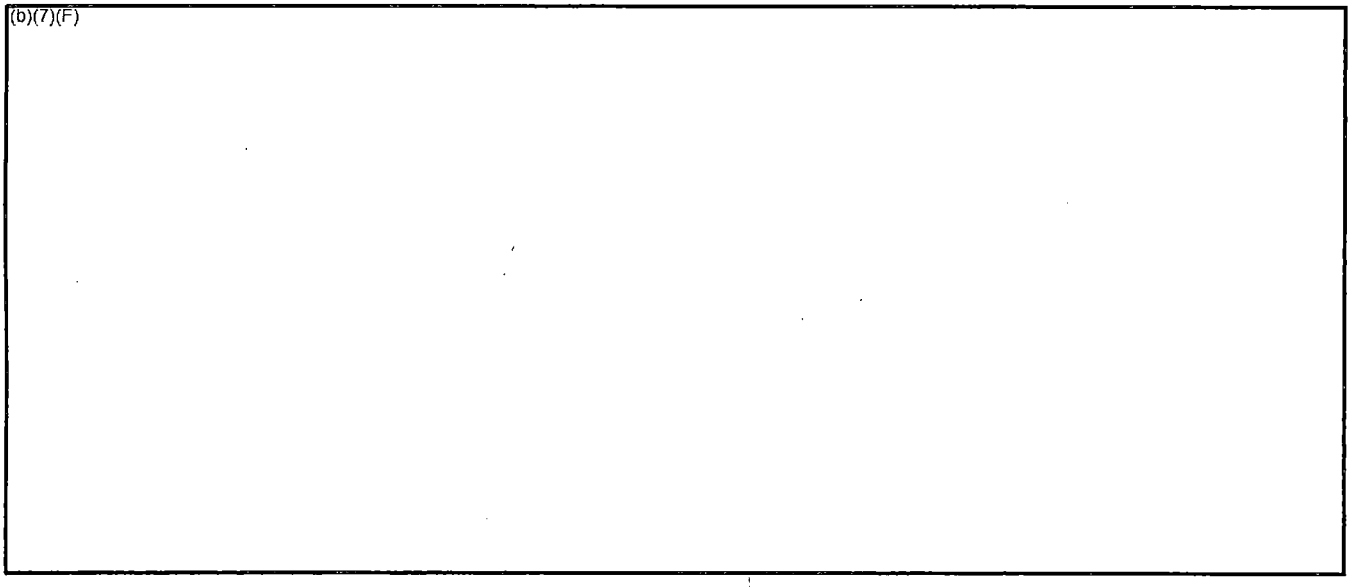

Figure 3.2. Jocassee Dam cross section (Sowers 1987)

Security sensitive information. Withhold from public disclosure under 10 CFR 2.390 (d)(1)

- Beginning at the rock foundation level, (b)(7)(F) (b)(7)(F)
- To decrease the hydraulic gradients as low as possible, (b)(7)(F) (b)(7)(F) (b)(7)(F) along the foundation contact.
- To protect the core materials from internal erosion, material movement and potential piping of the core, (b)(7)(F) (b)(7)(F) (b)(7)(F) into the larger rockfill materials.

- To establish a dense rockfill (b)(7)(F) (b)(7)(F) (b)(7)(F) embankment zone.
- Quality Control: selection of materials and documentation was enforced by the Resident Engineering staff and maintained as an important function during the construction. As indicated above, the selection and placement of the various zones was carefully done so as to maintain the compatibility of adjacent materials to eliminate migration of materials and maintain a stable embankment. Grain-size and density testing to verify selection of soil and rockfill materials properties and compaction were conducted at intervals to confirm and maintain control of the placements. Field inspection was maintained during construction with Duke Engineering staff observing and interfacing to ensure the design intent was maintained throughout construction.

All of the above facts are important when considering the potential for internal erosion and piping at Jocassee Dam. The materials and features employed during design and construction, as described above, were all designed to minimize the possibility of piping and failure of the embankment. Thus, it is even difficult to envision the development of a piping condition at the Jocassee Dam, given the defensive design measures incorporated and with the past 45 years of excellent performance. However, a deterministic approach is being used to postulate a sunny-day piping failure for Jocassee Dam.

Many of the above-listed facts also affect the breaching characteristics under the hypothesis that a piping failure occurs. Ideally these favorable physical properties would be taken into consideration in estimating breach parameters. Unfortunately regression methods for estimating breach parameters are somewhat limited in the degree to which this can be done. An exception is the Xu and Zhang (2009) methodology in which erodibility is considered.

3.2 Piping Failure Mechanism

For piping to occur, all four of the following conditions must exist:

1) there must be a source of water and a flow path;
2) there must be an unprotected exit for the eroded material;
3) there must be erodible material in the flow path; and
4) the material must support a roof for a pipe to enlarge and propagate.

The piping phenomenon must originate with internal erosion and material movement somewhere within the dam or its foundation, such as at the abutment-core contact, and exit downstream. The flow of water and materials must have an exit, to which the flow can carry materials and then progress upstream along some erosion path and move materials from

upstream. With increasing movement of large amounts of water carrying materials, the flow would eventually form a flow path within the downstream rockfill portion of the dam, referred to as a "pipe". If the process, called the "breach initiation phase", continues and the flows increase, it would progressively engage a larger and larger portion of the rockfill and eventually form a raveling condition within the rockfill large enough to make the downstream shell of the dam unstable. If it becomes unstable enough to move rockfill downstream or to cause pockets through collapses, it could then expose the core, which is the water retaining structure of the dam for the upstream reservoir. If support is removed from the downstream side of the core, it would become unstable and partially collapse. The breach of the dam would progress as it overtops the core and form an overtopping breach and failure of the dam; this is considered the start of the "breach formation phase".

The defensive measures within the Jocassee Dam are designed, constructed and incorporated, with consideration of all four of the necessary conditions for piping, to minimize any potential for the piping process to occur.

3.3 Potential Piping Failure Modes for Jocassee Dam

In a Potential Failure Modes Analysis (PFMA), which was facilitated by RAC Engineers & Economists and included engineers from Duke Hydro and HDR, the most likely (i.e. "least unlikely") piping failure mode was determined to be piping through (b)(7)(F) (b)(7)(F) piping through the rock foundation of the main dam is considered to be a significantly less likely piping failure mode due to the tight rock formations and low seepage rates in the (b)(7)(F) The potential for piping through the main dam embankment is extremely unlikely for the reasons described in our February 2013 report (Ehasz and Bowles 2013). Each of these failure modes is described in detail in Appendix A of our February 2013 report (Ehasz and Bowles 2013).

4.0 CONFIRMATION OF JOCASSEE DAM ERODIBILITY

4.1 Overview

Dam erodibility is described by Xu and Zhang (2009) as *a relative measure based on the embankment material compositions and compaction conditions, dam cross-sectional geometry, construction time and other relevant pieces of construction information*. In their regression analysis, Xu and Zhang (2009) found dam erodibility to be the most important control variable for predicting all five breach parameters. The three erosion categories (low, medium or high) used in the Xu and Zhang (2009) equations referenced the technical lecture paper by Briaud (2008), whereby soils and rocks are classified into various erosion resistance categories based on water velocity or hydraulic shear stress at the soil-water interface (see Figures 4.1a and 4b). Therefore it is significant to establish the compatibility of Xu and Zhang's application of the Briaud erosion categories with the categorization system developed by Briaud (2008).

To directly address the erodibility questions and to develop a clear explanation of the three erosion categories (low, medium and high) used by Xu and Zhang (2009) and the six erosion categories (non-erosive, very low, low, medium, high and very high) developed by Briaud (2008), Professor Briaud made a site visit to the Jocassee Dam and participated in a face-to-face meeting with Dr. Yao Xu in Denver. A summary of the Professor Briaud's responses to several questions about the use of his erosion categorization scheme by Xu and Zhang (2009) is provided in Section 4.2. A summary of Professor Briaud's independent evaluation of the erosion category for Jocassee Dam is contained in Section 4.3. Professor Briaud's complete report is contained in Appendix A.

4.2 Use of Briaud's Erosion Categorization Scheme by Xu and Zhang (2009)

The site meeting with Professor Briaud took place on October 3rd and 4th 2013 at the Jocassee Dam site in South Carolina and at the offices of Duke Energy at the Oconee Nuclear Plant. The purpose of the site visit was for Professor Briaud to become familiar with the Jocassee Dam and the materials used for construction. In addition, he was asked if his erosion categories are applicable to erosion during an earth dam breach and specifically:

- Is your (Briaud) work applicable to earth dam erosion?
- What is your (Briaud) characterization of Jocassee Dam erosion characteristics?
- Please comment on Xu and Zhang work on dam breach, and how the three erodibility classifications, used by Xu and Zhang, compare to your six classifications.

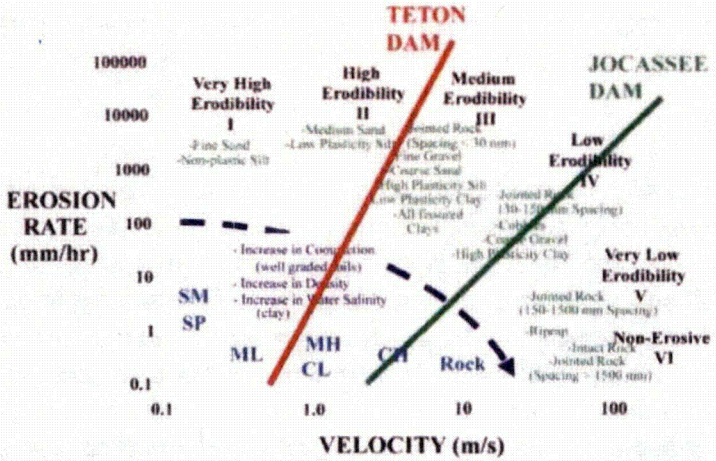

Figure 4.1a. Overall erosion category for Jocassee and Teton Dams (velocity based)

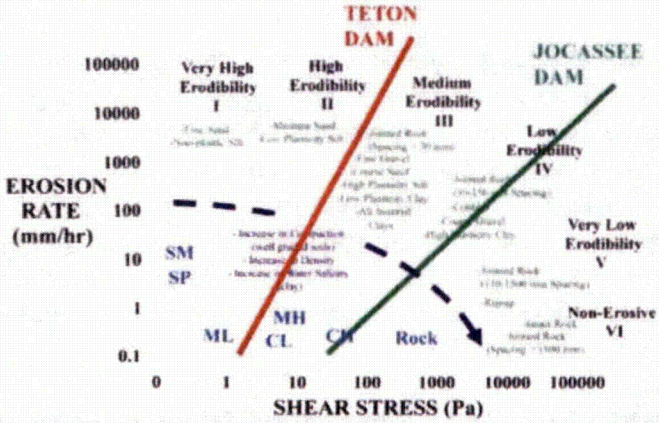

Figure 4.1b. Overall erosion category for Jocassee and Teton Dams (shear stress based)

Professor Briaud prepared a detailed report on his site visit to Jocassee Dam (Briaud 2013) and his answers to the above questions (see Appendix A). A summary of his responses is as follows:

- *Is your (Briaud) work applicable to earth dam erosion?* The erosion function is characterizing the behavior of the soil at the element level so it is broadly applicable to many erosion situations, including the erosion and breach process for earth and rockfill embankment dams. The erosion function is the curve which links the erosion rate to the water velocity or the hydraulic shear stress at the soil-water interface; it is to erosion studies what the stress strain curve is to deformation problems. It is a constitutive equation, which can be used in numerical methods as easily as in simple hand calculations.

- *What is your (Briaud) characterization of Jocassee Dam erosion characteristics?* The erodibility of the Jocassee Dam materials was evaluated; and the Jocassee cross-section materials are clearly and conservatively established to be "low erodibility" materials (see Section 4.3).
- *Please comment on Xu and Zhang work on dam breach, and how the three erodibility classifications, used by Xu and Zhang, compare to your six classifications.* The Xu and Zhang regression equations do show and consider that erodibility is the most significant factor in the development of embankment breach parameters. Thus, it is most important, in my evaluation of their equations, that I have found that Xu and Zhang have assigned the "low, medium or high" erodibility categories in a way that is consistent with my research findings for the various dams represented by the data used to establish their regression equations. The categorization reflects the fact that the types of materials typically used for the construction of earth dams fall into the Briaud erosion categories 2, 3, and 4 with some category 5 materials for rockfill dams. Indeed fine sands and non-plastic silts (Briaud category 1) and jointed and intact rock (Briaud category 6) are not used in earth dam engineering.

4.3 Confirmation of Low Erosion Category for Jocassee Dam

To evaluate the erosion category for the Jocassee Dam, the following process was used by Professor Briaud:

- A cross section of the dam was drawn, see Figure 4.2.
- An erosion category was chosen for each material within the dam based on the specified values of the median particle size, D_{50} (see Table 4.1); since the drawings specified that the D_{50} was the minimum allowed, this selection is conservative.
- Three erosion levels were placed across the dam as shown on the Figure 4.2 at levels AA, BB, and CC.
- For each level, a weighted average of the erosion category was determined according to the length of material exposed to the flow for that level:

$$EC = \frac{\sum_{i=1}^{n} L_i EC_i}{\sum_{i=1}^{n} L_i}$$

- Where EC is the average erosion category, L_i is the length of material i exposed to water, and EC_i is the erosion category for material i (low = 4, medium = 3 and high = 2).
- Section AA gave an EC value of 3.93, section BB gave 4.08, and section CC gave 4.11.
- Therefore, the overall average erosion category for Jocassee Dam is clearly 4 or low erodibility.

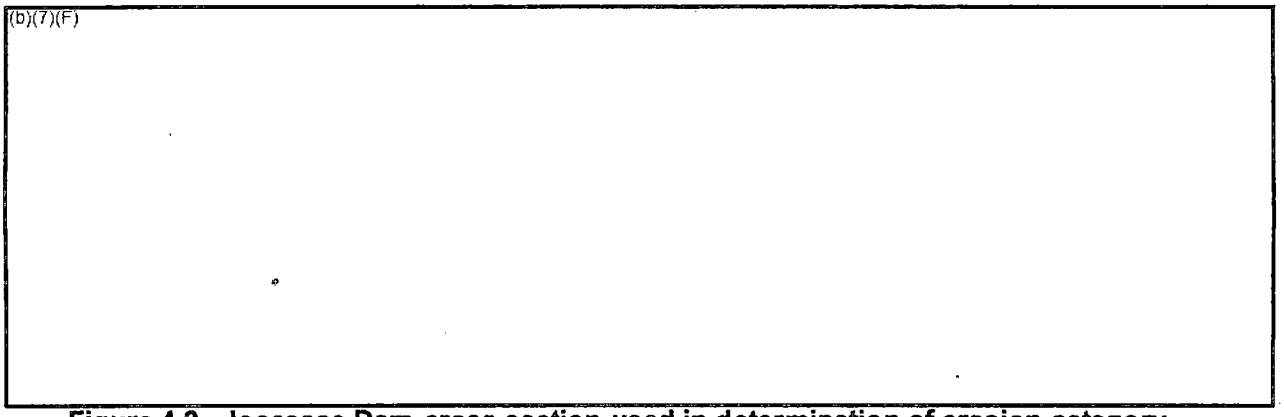

Figure 4.2. Jocassee Dam cross section used in determination of erosion category

~~Security sensitive information. Withheld from public disclosure under 10 CFR 2.390 (d)(1)~~

Table 4.1. Jocassee Materials Evaluation by Briaud

Material (Figure 4.2)	Description	Estimated critical velocity (m/s)	Erosion Category
Rock fill	(b)(7)(F)		
Impervious core			
Random fill			
Filters			

The above conservative analysis by Professor Briaud clearly shows that the erosion category of the Jocassee Dam is low or Category IV, for erosion rates based on velocity or shear stress as shown on Figures 4.1a and 4b, respectively.

A similar evaluation was conducted by Professor Briaud for the Teton Dam since this dam was used by Xu and Zhang (2009) as an illustration and evaluation of their original regression equations. In addition, an application of the revised Xu and Zhang regression equations to the Teton Dam failure is reported in Section 6.5. Professor Briaud showed that the erosion category of the Teton Dam is at the boundary between medium and high or Category III/II, for erosion rates based on velocity or shear stress as shown on Figures 4.1a and 4b, respectively.

The high resistance to erosion (low erodibility) of compacted rockfill has recently been affirmed by the experience of flooding and water passage through a rockfill embankment in the February 2014 flooding at the Tokwe-Mukosi Dam in Zimbabwe. The Dam is a Concrete Faced Rockfill Dam (CFRD) and experienced an extreme flood during construction prior to placement of the concrete face. It successfully passed extreme floodwaters through the compacted rockfill embankment with only local raveling and maintained stability. See Appendices C.1 and C.2 for a description and photos.

5.0 ORIGINAL XU AND ZHANG REGRESSION EQUATIONS

In our February 2013 report (Ehasz and Bowles 2013) it was concluded that the HRR (Duke 2013) breach hydrograph for the Jocassee Dam is a realistic but conservative breach hydrograph that has good defendability based on the following:

1) the validity of the Xu and Zhang (2009) method;
2) the conservative nature of the median breach parameter estimates;
3) a piping failure mode initiating in the (b)(7)(F)
4) the deposition of rockfill immediately below the dam;
5) the low erosion category of the rockfill material; and
6) the various characteristics of a modern dam that were included in the design and construction of the Jocassee Dam.

The original Xu and Zhang regression methodology and its previous implementation to Jocassee Dam are described in Appendix B. This appendix provides background for Section 6 where we address the questions raised by the FERC and the NRC. It also provides background for Section 7 where we describe the implementation of a revised version of the Xu and Zhang equations in a sensitivity analysis, which provides support for the breach hydrograph submitted in the Hydrologic Reevaluation Report (HRR) to the NRC by Duke on March 12, 2013 (Duke 2013).

Section B.2 summarizes the breach parameters and control variables in the Xu and Zhang (2009) regression equations. Section B.3 discusses the case histories that were used to develop these equations and Section B.4 summarizes the regression equations, including their confidence limits. The implementation of the original Xu and Zhang (2009) methodology for the Jocassee Dam is described in Section B.5 and details of the use of the failure time estimate in the HEC-RAS model are discussed in Section B.6.

6.0 REVIEW AND REVISION OF XU AND ZHANG REGRESSION EQUATIONS

6.1 Approach to Review and Revision

The FERC and NRC questions about the use of the Xu and Zhang (2009) methodology are summarized in Section 2.2 and are repeated here:

1) **Precedence** - where has use of the Xu and Zhang (2009) methodology been accepted?
2) **Chinese case histories** – about 43% of the dam failure case histories on which the Xu and Zhang (2009) methodology is based are for Chinese dams for which little information is available in the US.
3) **Representation of case histories for rockfill and other low erodibility dams** - the data set of dams used by Xu and Zhang (2009)to develop the regression equations has only three dams that are considered large (i.e. > 15 meters high) embankment dams with low erodibility and both of these dams are all outside of the US.
4) **Use of the Briaud erosion categories** – how were the erosion categories developed by Briaud (2008) applied in developing the Xu and Zhang (2009) methodology and are they applicable to dam breach?
5) **Breach time definition** – the definition of time to failure used by Xu and Zhang (2009) includes at least part of the breach initiation phase in addition to the breach formation process unlike other regression methods that include only the breach formation process.

To respond to these questions raised by the regulatory agencies we arranged for the primary author of the Xu and Zhang (2009) technical paper to meet with us in the Denver Offices of URS during the period November 7 – 10, 2013. Those in attendance were Dr. Yao Xu of the China Institute of Water Resources and Hydropower Research, Dr. David Bowles with RAC Engineers & Economists and Utah State University, Professor Jean-Louis Briaud with Texas A&M University, Joseph Ehasz with URS, and Adam Johnson from Duke Energy. On the morning of Friday November 8, Dr. Xu and Professor Briaud independently met with Tony Wahl, Bruce Feinberg and Dan Osmun of the Bureau of Reclamation (Reclamation) at Reclamation's Hydraulics Laboratory in the Federal Center near Denver. This meeting was in response to Tony Wahl's request to meet with Dr. Xu during his visit to the US to discuss his questions regarding the Xu and Zhang (2009) methodology.

The four-day working session was divided into two parts: first discussions of the agency questions and second a detailed case-by-case review of the 75 case histories that were used to develop the original Xu and Zhang (2009) regression equations. The ultimate objective was to make appropriate changes to the Xu and Zhang (2009) case histories data set to address the agency questions and any other issues identified during our review so that Dr. Xu could develop revised regression equations.

A summary of our discussions with Dr. Xu and Professor Briaud for each of the questions raised by the FERC and NRC and for some additional issues that were identified during these discussions is presented in Section 6.2. Specifically, these additional issues, which are discussed in Section 6.2.6 – 6.2.8, were as follows:

1) Erosion category assigned to dams with corewalls and concrete-faced rockfill dams
2) Differences in values of breach parameters and control variable in other sources, especially Froehlich (1995a and b and 2008) and Wahl (1998)
3) Inconsistencies between peak breach flows and breach development times

The changes made to the data set of case histories are summarized in Section 6.3 and detailed in Appendix D. The revised regression equations are presented in Section 6.4 and their test implementation for Teton Dam is discussed in Section 6.5. Their implementation for Jocassee Dam as a sensitivity study to evaluate the HRR hydrograph is presented in Section 7.

6.2 Summary of Review Findings

6.2.1 Precedence

In the U.S. dam safety community the acceptance of new methodologies often comes through adoption by the major government dam owners and regulatory agencies. These agencies include the US Army Corps of Engineers (USACE) and the Bureau of Reclamation as major government dam owners and the FERC as the federal regulator for hydropower dams. As with any new methodology it takes time for it to become accepted into practice and for precedence to be established. From this perspective the Xu and Zhang (2009) methodology is still quite new.

In the case of the Xu and Zhang (2009) methodology, the questions raised by the FERC and the NRC must be addressed as part of the process if this methodology is to become more widely accepted. Addressing these questions is the purpose of this section of the report.

The inclusion of erodibility in the Xu and Zhang (2009) regression methodology is widely recognized as a significant advantage over other breach parameter estimation regression analysis methodologies. In fact Xu and Zhang (2009) demonstrated that erodibility is the single most important control variable in predicting all five breach parameters. Such a significant advantage justifies a careful evaluation of the Xu and Zhang (2009) methodology to see if it can be more rapidly put to use in the profession.

Three uses of the Xu and Zhang (2009) methodology have been identified, as follows:

1) In developing a simplified risk assessment procedure for small reservoirs for the equivalent of the dam safety regulator[2] in England and Wales [the Environment Agency and the Department for Environment, Food and Rural Affairs (Defra)], HR Wallingford (2014) evaluated the Xu and Zhang (2009) methodology for estimating peak breach flows. In their comparative study they concluded that the Froehlich (1995a) and Xu and Zhang (2009) approaches both yield "conservative" estimates of peak breach flow for highly erodible embankment dams and that the physically-based HR BREACH model (Mohamed 2002) and the simplified AREBA model (HR Wallingford 2012) provide more realistic estimates.

2) The Xu and Zhang (2009) methodology is included in the breach parameter methodologies that are available in the USACE HEC-RAS computer model, which is widely used in the US for dam breach modeling. It was also included in a discussion of "Hydraulic modeling aspects that are unique to performing a dam break analysis" by Brunner (2011), who is the USACE Hydrologic Engineering Center (HEC) technical lead for the HEC-RAS model. In both cases a caution is given that "*the data Xu and Zhang used in the development of the equation for breach development time includes more of the initial erosion period and post erosion period than what is generally used in HEC-RAS for the critical breach development time*" (Brunner 2011). In addition it is stated that "*... because of this fact, the Xu and Zhang equation for breach development time should not be used in HEC-RAS*" (Brunner 2011). However, in a Personal Communication (December 2013) with Dr. Brunner he agreed that it was reasonable to iteratively change the breach progression relationship and the values orifice and weir coefficients in the manner described in Section B.6 for Jocassee Dam when using failure time estimates based on Xu and Zhang (2009). He also expressed interest in replacing the original Xu and Zhang (2009) regression relationships in HEC-RAS with the revised relationships that are described Section 6.4.

3) We understand from Dr. Xu that the Xu and Zhang (2009) methodology is being applied by government agencies in China.

6.2.2 Chinese Case Histories

About 43% or 32 of the 75 dam failure case histories on which the Xu and Zhang (2009) methodology is based are for Chinese dams. None of these case histories are included in the Wahl (1998) data base of case histories, although that data base may be due for an update and if one is undertaken it would seem beneficial to include case histories from China.

[2] In England and Wales the Environment Agency is responsible for enforcement of reservoir safety requirements for specific reservoirs "in the interest of safety" that are determined by Panel Engineers who are appointed by the Secretary for State. Defra has a policy role for development of reservoir safety legislation and guidance.

In discussing the quality of data for the Chinese case histories, Dr. Xu stated that he felt that the available information was similar in quality to what he had examined in his research for case histories from the US and some other countries. In at least two cases detailed failure investigations reports have been prepared for the Banqiao and Shimantan Dam failures. Dr. Xu referenced a report by Ru and Niu (2001), which contains information on many Chinese dam breaches. This report is readily available outside of China. He also had access to a detailed database on dam failure case histories, but this is not available outside China. However, Dr. Xu made extensive reference to this data base during our detailed evaluation of the case histories that were used as a basis for developing the Xu and Zhang (2009) regression methodology (see Section 6.3).

Dr. Xu also described a screening process that he performed before using the case history data from China and other countries in his regression analysis. Any case histories where significant concerns existed about the quality of the available data were omitted. It should be noted that the Chinese data used by Xu include some more recent dam breaches than used by others, such as Froehlich (1995 and 2008).

We also enquired about the quality of construction for the Chinese case history dams. Dr. Xu indicated that dams designed and constructed before 1977 were not up to modern standards, and that modern construction methods and equipment were not used. Dams constructed since 1977 can be considered to meet modern standards. The significance for the Chinese case histories is first that there are more of them because of the poorer standards prior to 1977. Secondly, the poorer construction, and in particular the poorer compaction of Chinese embankment dams constructed prior to 1977, would be expected to result in a more erodible dam once a breach process has initiated. Unlike most other regression methods for estimating breach parameters, the Xu and Zhang (2009) approach includes the erosion category as a means of accounting for the more erodible characteristic of the Chinese dams that were constructed prior to 1977. The approach adopted by Xu and Zhang (2009) to account for the effect of poor construction in the development of their regression equations is summarized in Section 6.2.4. We also make reference to this approach in Section 6.3.2, in which we summarize the critical review that we performed of the entire Xu and Zhang (2009) data set, including all Chinese case histories.

In summary, Dr. Xu demonstrated the overall validity of his evaluation of the case history data from all sources, including China, and that good backup information exists, although for some Chinese case histories access to this information is restricted. For the Chinese case histories this conclusion is based on the detailed information that Dr. Xu provided from the data sources of failure analyses and records, which he accessed during the detailed review that we conducted with him over a four-day period. Our detailed evaluation of all case histories is summarized in Section 6.3 and notes for specific case histories are presented in Appendix D. In addition, based on our detailed review (see Section 6.3), we found that in a majority of the cases a valid assessment of the case histories was performed by Xu and Zhang (2009) as the

basis for the values assigned to the control variables and breach parameters that were used in the regression analysis. The exceptions, which resulted in our making some adjustments to the assigned values, are discussed in Section 6.3 and documented in Appendix D. The revised values were used in the revised regression analysis that is presented in Section 6.4 and used in a sensitivity analysis on the HRR breach hydrograph that is presented in Section 7.

6.2.3 Representation of Case Histories for Rockfill and Low Erodibility Dams

The small number of case histories for rockfill dams that are classified in the low erosion category is a reality that is likely due to the intrinsic safety of rockfill dams in general. Another limitation is the lack of case histories of the failure for large (high) dams with a reservoir capacity similar to Lake Jocassee. This can be clearly seen in Figures B.1a and b. However, when volume is plotted logarithmically in Figure B.1b, which corresponds to its representation in the multiplicative regression equations, the extrapolation from the range of case histories to Lake Jocassee for the reservoir volume above the breach invert can be seen to be relatively less significant.

These limitations apply to all breach parameter regression methodologies. However, Xu and Zhang (2009) offset these limitations to some extent by including case histories from China for the Danghe and Gouhou large rockfill dams. In addition, their inclusion of the Briaud (2008) erosion categories as a control variable was another innovation that was intended to account for the important effects that differences in the erodibility of materials in embankment dams have on breach parameters. Still regression equations are limited in their ability to explain all the variability that exists in the available case history data. In contrast physically-based approaches are less limited than regression equations because they introduce a representation of the physics of the erosion, instability and hydraulics phenomena that determine breach processes,. However, these approaches must be used in an appropriate manner that accounts for their own limitations and the resulting uncertainties in predictions when used to develop breach hydrographs.

6.2.4 Use of the Briaud Erosion Categories

We asked Dr. Xu what information he used as the basis for the assignment of erosion categories to the case histories used in developing his regression equations. He described two-step process. In his first step the soil type within the dam was used to assign a range of erosion categories as low erodibility (LE) to medium erodibility (ME) for rockfill and clay and ME to high erodibility (HE) for silt and sand. The second step was to evaluate the construction quality, particularly compaction effort, based mostly on the period of construction to determine which end of the range of erosion categories to assign. For example, the period 1950 to 1976 in China would be characterized by low compaction using human powered tampers, and after about 1977 in China high compaction would be achieved using machine rollers. Other useful

pieces of information such as dam cross-sectional geometry, materials and slope surface protection were used as supplementary information for assigning the dam erosion categories. Professor Briaud's independent review confirmed the appropriateness of using his erosion categories for dam breach parameter estimation in the Xu and Zhang (2009) methodology. His review is summarized in Section 4 and detailed in Appendix A.

The two-step approach described above is consistent with the Briaud (2008) erosion categorization approach as summarized below. The dam erosion categories high, medium or low are described by Xu and Zhang (2009) as *a relative measure based on the embankment material compositions and compaction conditions, dam cross-sectional geometry, construction time and other relevant pieces of construction information*. Briaud (2008) found that the rate of erosion can be very different for different soils that are classified in different erosion resistance categories. Specifically, rockfill and clay are often associated with medium to low erosion category while sand and silt are often associated with high to medium erosion category. Hence, material compositions are considered as a primary basis for classifying the dam erosion category. In addition, compaction conditions also play an important role in determining the dam erosion category, especially for dams constructed from fine soils. Briaud (2008) reported that the erosion resistance increases with compaction effort and that the effect is more significant for some soils with high fines contents. It was also indicated by Wan and Fell (2004) that the erosion rate index of a soil is influenced strongly by the degree of compaction. As described by Dr. Xu, the year of construction and the associated compaction methods were therefore important information for judging the compaction condition of the case history dams, and hence the assignment of dam erosion categories.

6.2.5 Breach Time Definition

As is well recognized, the predicted breach times from Xu and Zhang (2009) are significantly longer than those obtained from other methodologies such as Froehlich (1995b and 2008). Xu and Zhang (2009) based their definition of breach development time on the definition by Wahl (2004), which states that "*breach development begins when a breach has reached the point at which the volume of the reservoir is compromised and failure becomes imminent" and "ends when the breach reaches its final size.*" By 2013 Wahl (2013) revised his breach time definition to be consistent with Froehlich (1995b and 2008). The difference between the definitions of failure time used in the original Xu and Zhang (2009) methodology based on Wahl (2004) and by-others is discussed in detail in Section B.6.

We found that of the 30 case histories that were used by Xu and Zhang (2009) to establish their regression equations for breach development time, only five also appear in the Froehlich (2008) data set. Of these five, three have the same values for breach development times in both data sets but for two (Apishapa and Teton dams) the Xu and Zhang (2009) values are just over three times the Froehlich (2008) values. In our detailed review of the case history data (see Section

6.3) we addressed this inconsistency by changing these values of breach development times to match the Froehlich (1995b and 2008) definition based on available information.

In our detailed review we found that in a few cases lower erosion categories had been assigned to dam breaches that had long observed failure times when all other available information about the dam, the materials from which it was constructed, and the quality of construction pointed to a higher erosion category. In our detailed review of the case history data we changed these to a higher erosion category for developing the revised regression equations that are the sensitivity studies presented in Section 7, since in applying the regression equations one would have no basis for this type of adjustment of the erosion category.

6.2.6 Erosion Category Assigned to Dams with Corewalls and Concrete Faced Rockfill Dams

In our detailed review of the case history data, we found that the term "corewall" had been used for some dams that had a clay core but not core wall constructed of concrete, masonry or steel to distinguish them from homogenous fill dams with no clay core. This was apparently a misunderstanding about the use of terminology in English and we corrected this in assigning the dam type control variable in the data set that was used for developing the revised Xu and Zhang equations.

In some case we found dams that were assigned a low erosion category as an indirect means of accounting for the throttling effects on breach development in embankment dams with a concrete core wall or for concrete-faced rockfill dams (CFRD). While this approach has some merit, it was judged that the breach parameters for embankment dams with a concrete core wall or CFRDs would not be representative of the erosional process in low erodibility embankment dams in general, and so we excluded dams with a core wall or a concrete face from the data set that was used to develop the revised Xu and Zhang regression equations (see Section 6.4).

6.2.7 Differences in Values of Breach Parameters and Control Variable in Other Sources

All values of the control variables and breach parameters in the Xu and Zhang (2009) data set were compared with those found in other sources, including the following:

- Wahl (1998) "best reliable information"
- Froehlich (1995a and b and 2008)
- VonThun and Gillette (1990)
- Costa (1985)
- Walder and O'Conner (1997)
- MacDonald and Langridge-Monopolis (1984)

Preference was generally given to adopting values contained in the first two sources, although where available additional sources were consulted to verify or change Xu and Zhang (2009) data set values. These additional sources included Singh (1996) and various internet sources that are referenced in Appendix D. The changed values were used to develop the revised Xu and Zhang regression equations that were used for the sensitivity studies that are presented in Section 7.

6.2.8 Inconsistencies between Peak Breach Flows and Breach Development Times

An inconsistency was identified in many case histories between the peak breach flows, breach development times and the reservoir volume above the breach bottom at the time of failure. The inconsistency exists for many case histories in the Wahl (1998) data base and in the Froehlich (1995a and b and 2008) data as well as in the Xu and Zhang (2009) data. The inconsistency was identified by assuming that the breach outflow hydrograph has a general triangular shape with the base of the triangle representing the breach development time, the height the peak outflow rate, and the area of the triangle the volume of reservoir contents above the breach bottom elevation. Under this assumption an approximate breach formation time can be calculated from simple geometry as follows:

$$T = 2V_w/Q_p \qquad (6)$$

in which:

T	=	Breach development time
V_w	=	Volume of reservoir contents above breach invert at the time of failure
Q_p	=	Peak breach flow rate

On the basis that the observed values of V_w and Q_p can generally be obtained with greater accuracy than the observed value of T, we compared the values of T calculated using Equation 6 with the observed values in the case histories used by Xu and Zhang (2009) and those in Wahl (1998) and Froehlich (1995a and b and 2008) and found significant differences. To avoid changing the case history values of T in the widely accepted Wahl (1998) and Froehlich (1995a and b and 2008) data sets, we used those values to develop the revised Xu and Zhang regression equations that were used in the sensitivity studies. However, we found, not unexpectedly, that this inconsistency resurfaces when a similar comparison is made between predicted values of the breach development time and those obtained from Equation 6. We discuss this issue further in Section 7.2 and the approach that we have developed to address it.

6.3 Summary of Revisions to Case History Data Set

6.3.1 Approach

During the Denver meetings the group questioned Dr. Xu about each of the 75 case histories that were used to develop the original Xu and Zhang (2009) regression equations. All values of the control variables and the breach parameters for the case histories were discussed and reviewed and notes were recorded in a spreadsheet (see Appendix D) during the meeting and to record the results of further scrutiny following the meeting. Professor Briaud assisted in the detailed erosion category review and this resulted in changes to several case histories.

In addition, all values of the control variables and breach parameters in the Xu and Zhang (2009) data set were compared with those in other sources that are listed in Section 6.2.7 and adjusted as appropriate.

6.3.2 Summary of Xu and Zhang (2009) Data Set Revisions used in the Sensitivity Studies

A summary of the types of changes that were made were to the Xu and Zhang (2009) data set is as follows:

- Changed breach development times to the Froehlich (1995b and 2008) definition of breach development time.
- Changed the values of other variables where they were inconsistent with the Wahl (1998) and Froehlich (1995a and b and 2008) data with consideration given to other reliable information that was found in various other sources mentioned in Section 6.2.
- Changed assigned erosion categories to include the consideration that compaction associated with construction practices in the US and other developed countries (not China) improved for earthfill dams after about 1950 and for rockfill dams after about 1965. This is similar to the consideration used by Xu and Zhang (2009) for Chinese case histories before and after 1977.
- Changed to higher erosion categories cases where lower erosion categories had been assigned because of long observed failure times but where all other available information about the dam, the materials from which it was constructed, and the quality of construction pointed to a higher erosion category.
- Eliminated case histories for concrete-faced dams and dams with core walls or cut-offs (discussed below).

The above changes were made to improve the quality of the data used in the revised regression equations and to achieve consistency with the commonly-used Froehlich (1995b and 2008) definition of breach development time. In principle this definition was seen as a way to assign the duration of the breach hydrograph that is commonly developed using the HEC-RAS software; but as demonstrated in Section 7.2, it was found that another step was necessary to

estimate a breach development time that is consistent with the predicted values of peak breach flow and the reservoir volume above the breach bottom at the time of the breach. Overall the numbers of changes to US, China and other country case histories in the original Xu and Zhang (2009) data set were as follows:

- Reservoir capacity: 3 US changes
- Dam erosion categories: 10 changes comprising 4 US, 5 China and 1 Brazil
- Failure modes: 3 US changes
- Volume of water above breach invert: 5 US changes
- Depth of water above breach invert: 2 US changes
- Breach height: 2 US changes
- Breach average width: 4 US changes
- Breach side slope: 2 US changes
- Breach failure time: 9 changes comprising 6 US, 2 China and 1 Brazil

In addition to these changes, twenty out of the 75 case histories used by Xu and Zhang (2009) were eliminated for the following reasons:

- Concrete-faced dams: 5 total, 1 Argentina (Frias), 1 China (Gouhou), 3 USA (Davis Reservoir, Horse Creek, Swift)
- Dams with core walls or cut offs: 8 total, 1 China (Danghe), 1 UK (Coedty), 6 USA (Castlewood, Elk City, Lower Otay, Lynde Brook, Winston, Wilkinson Lake)
- Lack of reliable information: 6 total, 2 China (Niujiaoyu, Huqitang), 4 USA (Potato Hill Lake, Trial Lake, Upper Pond, Otter Lake)
- Not representative due a large volume reservoir with a small height dam that resulted in a long breach development time and a very wide breach: 1 USA (Hatfield)

The concrete-faced dams and dams with core walls were removed because their breach characteristics would not be representative of the erosional process for breaching of embankment dams in general. Specifically the concrete membrane would be expected to resist breach development and to have a throttling effect on breach development. Xu and Zhang (2009) assigned a low erosion category as an indirect means of accounting for these effects of a core wall or concrete face but this was judged to bias the data set.

Given more time it is possible that additional information may have been obtained for some cases that were eliminated due to a lack of reliable information. Also it is possible that some accepted US and other developed country case histories, which were not included by Xu and Zhang (2009), could have been added to the dat a set.

Lastly, and despite the scrutiny imposed on the data from China during our meetings, the Chinese case histories were omitted from the data set that was used to develop the revised Xu and Zhang equations used in the sensitivity studies. This conservative step was taken to increase confidence in the revised Xu and Zhang regression equations by avoiding the potential criticism that we had only limited and indirect access to the original references for the Chinese case histories. However, this step further reduced the total number of case histories from 55 to 27.

The numbers of case histories that were used to estimate the revised best exact and best simplified equations, respectively, are as listed below:

- Breach depth (H_b): 23 and 23
- Breach top width (B_t): 21 and 24
- Average breach width (B_{ave}): 22 and 24
- Peak outflow rate (Q_p): 16 and 19
- Breach development time or failure time (T_f): 14 and 14

These are significantly fewer than for the original Xu and Zhang (2009). However, as can be seen from Figures 6.1a and b, they cover the same range as the original data set. Figures 6.1a and b are similar to Figures B.1a and b. Figures 6.1a and b show the depth of water above breach invert, H_w, and volume of water at the breach time, V_w, on arithmetic-arithmetic and arithmetic-log axes, respectively, for the 75 case histories in the original Xu and Zhang (2009) data set and the 55 case histories in the revised data set. The 27 US or other country data remaining after the Chinese data are omitted can also be identified in these figures.

The revised data set include three low erosion category case histories, 11 medium erosion categories and 13 high erosion categories. It includes seven overtopping failures and 20 seepage-erosion failures.

6.4 Revised Regression Equations for use in the Sensitivity Study

Dr. Xu personally developed revised regression equations for the best exact prediction using all five control variables. He also developed the best simplified prediction equations as those that gave the highest R^2_{adj} as obtained through a stepwise regression procedure (see Section B.4).

The revised Xu and Zhang regression equations were developed using the revised case history data as described in Section 6.3. As explained in Section 6.3.2, the Chinese case histories were excluded from the revised regression equations that we used in the sensitivity study to evaluate the appropriateness of the HRR breach hydrograph.

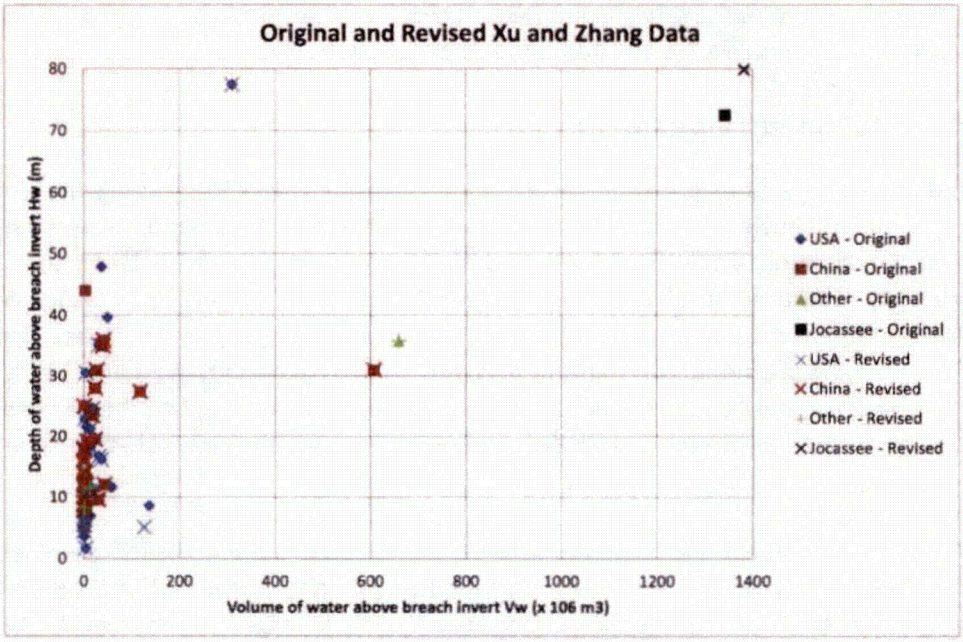

a) Arithmetic-arithmetic scales

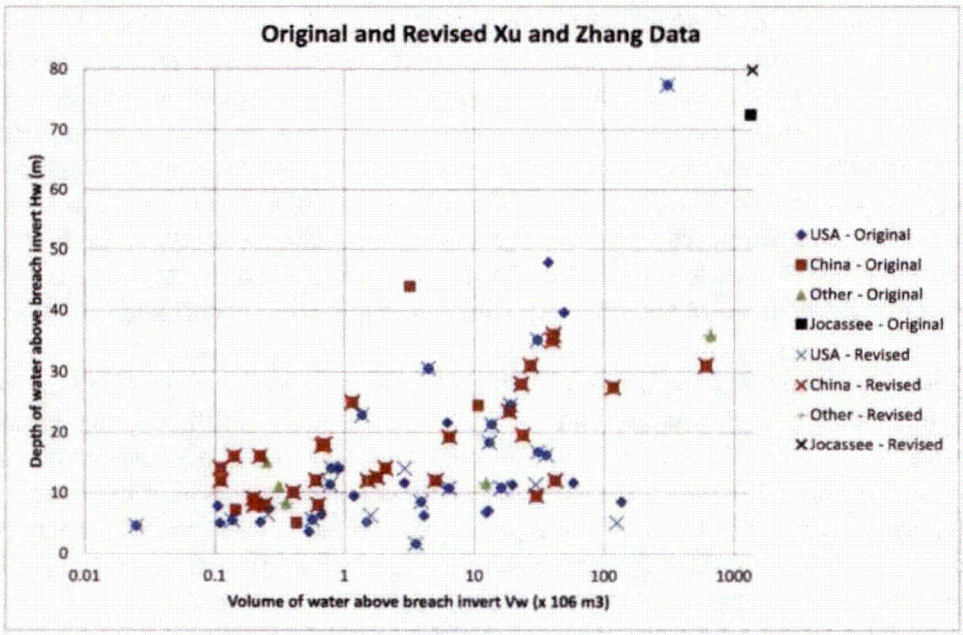

b) Arithmetic-logarithmic scales

Figure 6.1. Depth of water above breach invert vs. volume of water at the breach time for the original and revised Xu and Zhang case histories.

The coefficients for the revised regression equations are presented in Tables 6.1 and 6.2 for the best exact and best simplified prediction equations, respectively.

6.5 Application to Teton Dam Failure

The revised Xu and Zhang equations were applied to the Teton Dam using the same control variable values as shown in Table 10 of the Xu and Zhang (2009) paper. We selected Teton Dam for this evaluation since, like the hypothetical failure for Jocassee Dam, the Teton Dam failed by piping, whereas the other dam evaluated by Xu and Zhang (2009), Banqiao Dam, was an overtopping failure. Since the evaluation of the erosion category by Professor Briaud, which is summarized in Section 4.2 (see Figures 4.1a and b), indicated that the Teton Dam lies on the boundary between the high and medium erodibility categories, we applied the revised equations for the high and medium erosion categories and then averaged the two sets of median predicted values.

Tables 6.3 and 6.4 contain the observed and predicted values of the breach parameters for the original Xu and Zhang (2009) and the revised Xu and Zhang described in Section 6.4 for the best exact and best simplified equations, respectively. Two values of observed breach time are shown, 4 hours for the original Xu and Zhang (2009) definition of breach formation time and 1.25 hours for the definition of breach formation time that is used in the revised Xu and Zhang equations based on the Froehlich (1995b and 2008) definition. In addition to displaying the median predicted values, the percent differences between the observed and predicted median values are presented. The lowest percent differences for the original Xu and Zhang (2009) or the revised Xu and Zhang equations are indicated in red. For the best exact equations (Table 6.3) the revised approach yields smaller percent differences than the original equations for three out of five breach parameters. For the best simplified equations (Table 6.4) the revised approach yields smaller percent differences than the original equations for four out of five breach parameters. Therefore, for Teton Dam, the revised equation predictions have smaller percent differences with the observed values than the original Xu and Zhang (2009) predictions.

The revised regression equations were also evaluated for the Teton Dam based on a mean breach time estimate that was obtained from the uncertainty distribution on predicted peak outflow and the volume of water released through the breach. The basis for this estimate is discussed in Section 7.2 in which the mean estimate is distinguished from the median estimate, which results directly from the multiplicative regression equations for all breach parameters except breach depth. The resulting estimates are provided at the bottom of Tables 6.3 and 6.4 for the best exact and best simplified equations, respectively. In both cases they significantly overestimate the observed breach time. However, these estimates may be reasonable for a reservoir with the stored volume that Teton had at the time of its failure and that the observed breach time was shorter than predicted by the regression equations because of an unusual failure mechanism that has been documented by the Teton Dam owner, the Bureau of

Table 6.1. Summary of the five revised Xu and Zhang best exact regression equations

Breach Parameter Y (or log Y)	Number of Cases	Control Variables (log: nonlinear)	b0 (or log b0)	b1	b2	b31	b32	b33	b41	b42	b51	b52	b53	R2	$S2_{y\|x}$ (or $S2_{\log y\|\log x}$)
						Dam Type					Erodibility Category				
			Intercept	Hgt	Reservoir Shape Coef.	Core Wall	CFRD	Homog Zoned	Overtop	Piping	High	Medium	Low		
Hb / Hd	23	X1,2,3,4,5	0.449	-0.023	0.001	0.134		0.138	0.178	0.271	0.222	0.186	0.041	0.375	0.016
log(Bt / Hb)	21	lnX1,2,3,4,5	0.088	0.127	0.620	0.122		-0.053	0.240	-0.328	0.246	-0.201	-0.133	0.594	0.213
log(Bave / Hb)	22	lnX1,2,3,4,5	-0.305	0.027	0.690	-0.425		0.092	0.363	-0.669	0.225	-0.378	-0.153	0.670	0.273
log(Qp / √gVw5/3)	16	lnX1,2,3,4,5	-1.528	-0.029	-1.489	-0.527		-0.409	-0.773	-0.755	-0.196	-0.509	-0.823	0.813	0.397
log(Tf / Tr)	14	lnX1,2,3,4,5	-0.883	0.017	0.715	0.47		-0.678	-1.114	0.232	-0.619	-0.442	0.178	0.646	0.902

Table 6.2. Summary of the five revised Xu and Zhang best simplified regression equations

Breach Parameter Y (or log Y)	Number of Cases	Control Variables (log: nonlinear)	b0 (or log b0)	b1	b2	b31	b32	b33	b41	b42	b51	b52	b53	$R2^{adj}$	$S2_{y\|x}$ (or $S2_{\log y\|\log x}$)
						Dam Type					Erodibility Category				
			Intercept	Hgt	Reservoir Shape Coef.	Core Wall	CFRD	Homog Zoned	Overtop	Piping	High	Medium	Low		
Hb / Hd	23	X1,4,5	0.673	-0.021					-0.006	0.089	0.297	0.26	0.117	0.133	0.013
log(Bt / Hb)	24	lnX2,4,5	-0.241		0.72				0.121	-0.363	0.23	-0.27	-0.201	0.592	0.181
log(Bave / Hb)	24	lnX2,4,5	1.577		0.871				-1.122	-1.968	-0.667	-1.346	-1.077	0.628	0.245
log(Qp / √gVw5/3)	19	lnX2,5	-2.890		-1.222						-0.55	-1.059	-1.281	0.804	0.216
log(Tf / Tr)	14	lnX2,3,5	-1.382		0.859	0.14		-0.132			-0.861	-0.53	0.009	0.085	0.538

Table 6.3. Teton Dam predictions using best exact equations

Breach Parameter	Units	Observed	Original Xu and Zhang (2009) Predcitions		Revised Xu and Zhang Predictions							
			Original - Median		High Erodibility			Medium Erodibility			Average High & Medium Erodibility	
		Value	Value	Percent Difference with Observed	Upper	Lower	Median	Upper	Lower	Median	Value	Percent Difference with Observed
Height of breach	m	87	78	-10%	87	62	113	84	58	109	85	-2%
Breach top width	m	238	198	-17%	338	122	932	208	75	573	273	15%
Average breach width	m	151	150	-1%	212	68	662	112	36	348	162	7%
Peak outflow	m^3/s	65,120	75,220	16%	77,929	16,677	364,145	56,986	12,195	266,281	67,458	4%
Breach formation time - Original Xu and Zhang	hours	4	4.1	2%								
Breach formation time - Revised Xu and Zhang	hours	1.25			0.7	0.0	9.1	0.8	0.1	10.9	1	-42%

			Mean		Mean		
Peak outflow	m^3/s	65,120	2.9		4.0	3.5	-22%
Breach formation time - Revised Xu and Zhang	hours	1.25	59,054		43,183	51,119	176%
			33.8%		33.8%		

Table 6.4. Teton Dam predictions using best simplified equations

Breach Parameter	Units	Observed	Original Xu and Zhang (2009) Predcitions		Revised Xu and Zhang Predictions							
			Original - Median		High Erodibility			Medium Erodibility			Average High & Medium Erodibility	
		Value	Value	Percent Difference with Observed	Upper	Lower	Median	Upper	Lower	Median	Value	Percent Difference with Observed
Height of breach	m	87	77	-11%	86	64	109	83	60	105	85	-3%
Breach top width	m	238	181	-24%	283	116	695	165	67	405	224	-6%
Average breach width	m	151	127	-16%	198	70	564	97	34	275	148	-2%
Peak outflow	m^3/s	65,120	55,146	-15%	84,438	31,162	228,794	50,755	18,732	137,527	67,596	4%
Breach formation time - Original Xu and Zhang	hours	4	3.2	-20%								
Breach formation time - Revised Xu and Zhang	hours	1.25			0.6	0.1	3.4	0.84	0.1	4.7	0.7	-42%

			Mean		Mean		
Peak outflow	m^3/s	65,120	74,841		44,987	59,914	-8%
Breach formation time - Revised Xu and Zhang	hours	1.25	2.3		3.8	3.1	145%
			39.9%		39.9%		

Reclamation (Osmun 2013). The failure mechanism involved the development of a large cavity piping of the core materials into the downstream rock had been unnoticed. The piping had within the dam, which formed due to the pervious nature of the foundation and the fact that moved embankment materials and continued for many days or even weeks and formed a large cavity within the core/center of the dam. Once the cavity collapsed it caused a very sudden failure with a shortened breach time, because a significant amount of material had already been eroded from within the dam, causing an enlarged and sudden opening, which is uncharacteristic of a normal erosional breaching failure. This failure mechanism is discussed in more detail in Appendix C.2.

7.0 REVISED XU AND ZHANG REGRESSION EQUATIONS SENSITIVITY STUDIES

7.1 Overview of Approach

A sensitivity study was performed to explore the effect of the revisions made to the original Xu and Zhang (2009) regression equations on the breach hydrograph for a piping failure of Jocassee Dam and compare with the HRR breach hydrograph submitted to the NRC by Duke (2013). The revised Xu and Zhang regression equations were applied to the Jocassee Dam to obtain the median estimates of the breach parameters and their confidence intervals. The revised equations were for the case in which we used the Froehlich (1995b and 2008) breach times and with all Chinese case histories omitted.

The spreadsheet that we used in our previous work to implement the original Xu and Zhang (2009) regression equations (Ehasz and Bowles 2013) was generalized such that a new set of regression coefficients for the revised equations can be input. To calculate the confidence intervals we also input the standard error of regression, the number of control variables, and the number of case histories used to develop each regression equation. The modified spreadsheet was verified against the original version in which the regression coefficients were hard wired and for the applications to the Teton and Banqiao Dams to verify that we closely matched the results published by Xu and Zhang (2009).

The breach parameter estimates obtained from the revised Xu and Zhang regression equations are presented in Section 7.2. Section 7.3 contains an example of inconsistencies between peak breach flow and breach development time for the Jocassee Dam breach hydrograph for the breach Case 2(100W) submitted to the NRC by Duke in support of the Safety Evaluation (SE) (NRC 2011). The HEC-RAS implementation by HDR of the revised Xu and Zhang regression equations breach parameter estimates to obtain a breach hydrograph for Jocassee Dam and a comparison with the HRR breach hydrograph are discussed in Section 7.4.

7.2 Revised Xu and Zhang Breach Parameter Estimates for Jocassee Dam

The resulting median and 95% confidence interval estimates (lower and upper bounds) are presented on the left side of Table 7.1 for the revised best exact equations. In addition the breach bottom elevation and average side slopes are calculated and displayed.

For comparison, Table 7.1 also displays the Froehlich (1995a and 2008) estimates of the breach parameters. Considering the widths of the confidence intervals for both methods, the two methods provide fairly similar median estimates (see Figure 7.1). In particular the median peak outflows, median breach top widths and median breach formation times are quite similar. The similarity of the median breach formation time estimates follows from changing the definition of failure time in the revised Xu and Zhang methodology to match that in Froehlich

Table 7.1. Breach parameter estimates from a) revised Xu and Zhang without Chinese case histories the Froehlich breach time definition, and b) Froehlich (1995a and 2008)

Breach Parameter	Revised Xu and Zhang Without China Froehlich Breach Times			Froehlich (1995b and 2008)		
	Upper	Lower	Median	Upper	Lower	Median
Height of breach (feet)	382	172	277	275	275	275
Breach formation time (hours)	(b)(7)(F)					
Breach top width (feet)	2,787	365	1,009	*3,384*	*587*	1,082
Average breach width (feet)	2,007	206	643	*3,192*	*395*	*889*
Peak outflow (cfs)	(b)(7)(F)					
Breach bottom elevation (feet msl)	*743*	*953*	*848*	850	850	850
Average side slopes (horiz:vert)	*2.0*	*0.9*	*1.3*	0.7	0.7	0.7
Bold = from regression Normal = input value *Italics* = calculated from other values						
Volume above breach bottom (acre-feet)			*1,119,836*			*1,117,818*
Triangular breach formation times (hours)			*10.7*			*11.2*

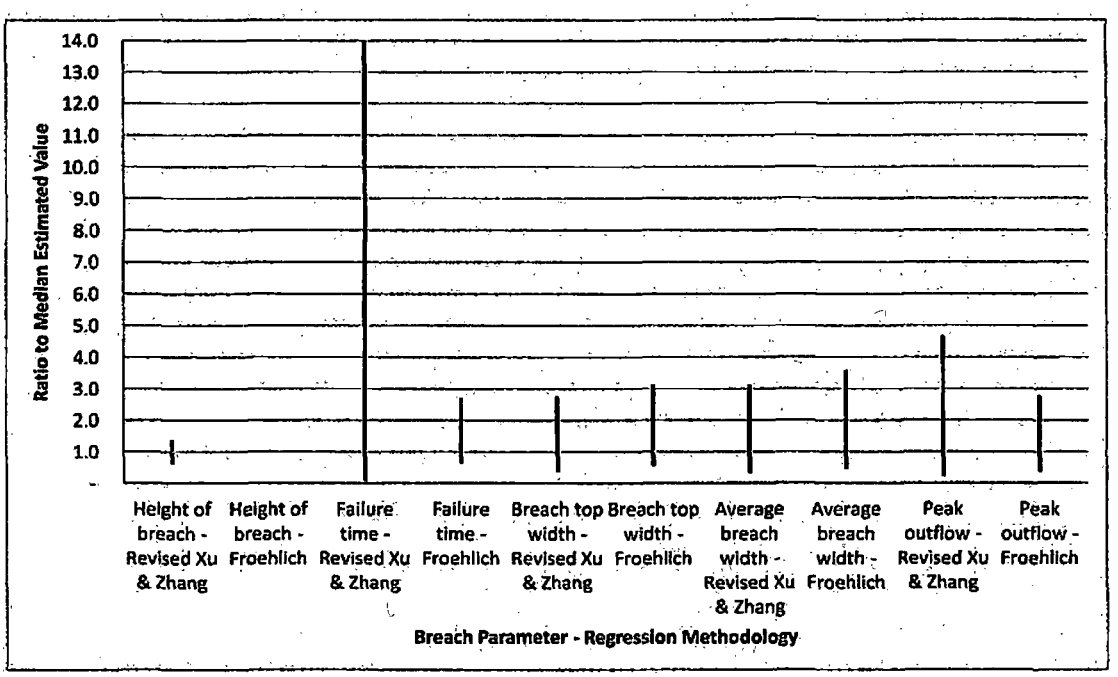

Figure 7.1. Relative width of confidence intervals for the revised Xu and Zhang and Froehlich (1995a and 2008) breach parameter estimates for Jocassee Dam expressed as a ratio to the median estimate (ratio = 1.0).

(1995b and 2008). The confidence bounds for the revised Xu and Zhang regression equations are wider than those for Froehlich (2008) due to the smaller number of case histories that remained in the revised Xu and Zhang data set. Interestingly there are other case histories with observed values of failure time that included in Froehlich (2008), but which are not included in

the original or revised Xu and Zhang data set. We could have added these but our focus was on working with those that Xu and Zhang (2009) had originally used rather than adding new cases.

The median estimate for the breach bottom elevation of 848 feet msl. (and hence an estimated height of the breach of 277 feet) predicted by the revised Xu and Zhang method is very similar to the assumed value of 850 feet msl. (and hence an estimated height of the breach of 275 feet) that we independently estimated in our application of the Froehlich (2008) method since that method does not predict this breach parameter. We based that estimate on the expectation that there would be significant deposition of material immediately below the dam that would limit the downward breach development. This position is consistent with the experimental tests on the rockfill dam breaching process by Franca and Almeida (2002), which showed that "*the deposition of the rock blocks immediately downstream of the dam has a stabilizing effect, sustaining the failure process – this is reflected mainly on the final breach depth which is about 80% of the dam height.*" In addition, many embankment dam failures case histories document that breaches less than the full dam height have occurred. However, since so few rockfill dams have failed, the experimental work of Franca and Almeida (2002) is probably the best indication of the reduced breach depth associated with a rockfill dam failure due to deposition immediately downstream of the breach.

It is noted that a breach bottom elevation of 850 feet msl. corresponds to releasing about 96% of the reservoir contents below the initial normal full pool at Elevation 1,110 feet msl. This compares with about 96.5% of the reservoir contents below Elevation 1,110 feet msl. for a breach bottom at Elevation 848 feet msl., which was predicted using the revised Xu and Zhang regression equations that was used in the sensitivity studies. For the original Xu and Zhang (2009) regression equations, which were used as the basis for the HRR breach hydrograph (Duke 2013), the predicted breach bottom elevation of 870 feet msl. corresponds releasing about 94% of the reservoir contents below Elevation 1,110 feet msl.

An additional sensitivity case is described at the end of Section 7.4 in which the breach bottom elevation was set to Elevation 800 feet msl. and all the other breach parameters were kept identical to those used for the HRR breach hydrograph (Duke 2013). Even though this run was performed in a conservative manner, it was concluded that a lower breach bottom does not significantly change the breach hydrograph.

The largest difference between estimates from the revised Xu and Zhang and Froehlich (1995b an 2008) methods is for the average breach width and as a result of that, the side slopes. The average side slope value of 0.7 was assumed in our application of the Froehlich (2008) method following a recommendation by Froehlich (2008), whereas the larger values from the revised Xu and Zhang method are predicted values. As described below in Section 7.4, where these different median values were used by HDR in the HEC-RAS model there is some effect on the breach hydrograph shape due to the different breach cross-sectional areas, but not on the peak

breach flow rate since it is determined by matching the median values for peak outflow predicted by the respective methods.

Returning to the estimated median breach formation times from the revised Xu and Zhang and the Froehlich (1995a and 2008) methodologies, we conducted a simple check on the reasonableness of these predicted times and their consistency with the predicted peak outflow rates and volume of the reservoir contents above the breach bottom elevation. The check involved assuming that the breach outflow hydrograph has a triangular shape with the base of the triangle representing the breach formation time, the height the peak outflow rate, and the area of the triangle the volume of reservoir contents above the breach bottom elevation. Under this assumption an approximate breach formation time can be calculated from simple geometry based on Equation 6, which is presented in Section 6.2.8.

The breach formation times estimated from Equation 6 are given at the bottom of Table 7.1. These times are clearly much longer than those obtained from both the revised Xu and Zhang and the Froehlich (1995a and 2008) regression methodologies. The sources of these significant inconsistencies in breach formation time estimates for Jocassee Dam are believed to include the following:

- Inconsistencies between case history estimates of observed breach times, peak outflow rates and volumes of the reservoir contents above the breach bottom elevation in the Wahl (1998), Froehlich (1995b and 2008),and Xu and Zhang (2009) data sets (see Section 6.2.8)
- The breach formation time is apparently not well represented by the regression equation methodologies for the large volume of the contents of Lake Jocassee above the breach bottom, which at the normal maximum reservoir level is about twice the volume of water for the case history with the largest reservoir breach volume (Oros Dam) and about four times the corresponding volumes for the Teton Dam breach (see Figure B.1a).

The HEC-RAS simulation model predicts a breach hydrograph with a volume equal to the reservoir contents above the breach bottom elevation. In such a simulation it would be impossible to match both the predicted values of breach formation times and peak outflow rate from either the revised Xu and Zhang or the Froehlich (1995a and 2008) regression methods because the predicted breach formation time from the regression methods is too short to release the reservoir contents. This is illustrated for the Safety Evaluation (SE) (NRC 2011) breach hydrograph for Jocassee Dam in Section 7.3.

Therefore it is clear that both regression methods underestimate the breach formation time for the large volume reservoirs such as Lake Jocassee. To address this shortcoming we developed an adjustment through following procedure, which is described below for the revised Xu and Zhang methodology with references to Figure 7.2:

(b)(7)(F)

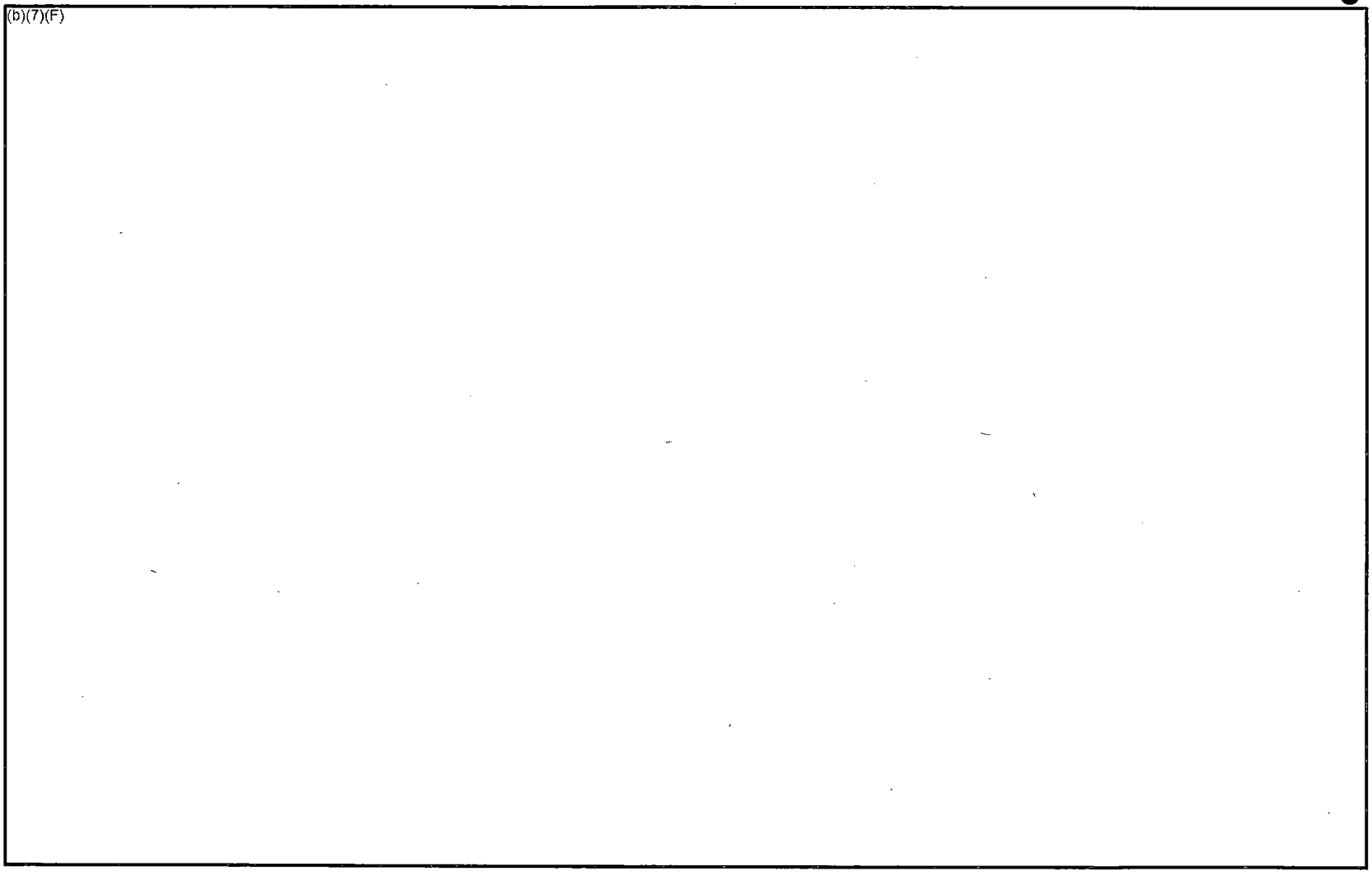

Figure 7.3. Distributions of predicted peak breach outflow rate and breach development time – Froehlich (1995a and 2008)

- The entire probability distribution representing estimation uncertainty for predicted peak breach outflow rate was developed from the 1st through the 99th percentiles using the same equation that was used to calculate the upper and lower bounds by assigning the value of the Student t statistic corresponding to each percentile (left plot in Figure 7.2).
- The distribution of predicted peak breach outflow rate (left plot in Figure 7.2) was transformed to a distribution of breach formation times (right plot in Figure 7.2) using Equation 6 based on the triangular breach hydrograph approximation applied to each percentile.
- Calculate a mean breach formation time needed to release the reservoir contents from the distribution of breach formation times (right plot in Figure 7.2). This was calculated to be (b)(7)(F) (see the blue dot-dash line on right plot in Figure 7.2), which corresponds to about the 34th percentile.
- Obtain the mean peak breach outflow rate that is consistent with the mean breach formation time needed to release the reservoir contents using the triangular breach hydrograph approximation – that is, corresponding to the 34th percentile. This was calculated to be (b)(7)(F) cfs (see blue dot-dash line on left plot in Figure 7.2).

The mean breach formation time of (b)(7)(F) was used in HEC-RAS as the time between points B and D as defined on Figure B.4 (see also Figure 7.5 in Section 7.4) together with the median estimates of the breach geometry from the revised Xu and Zhang methodology. HEC-RAS was then run to approximately match the mean peak breach outflow rate of (b)(7)(F) cfs by iteratively changing the values of the orifice and weir coefficients and the breach progression relationship as described in Section B.6.

The above adjustment procedure for addressing the shortcoming with the predicted breach formation time was also applied to the Froehlich (1995a and 2008) methodology. The resulting mean breach formation time needed to release the reservoir contents was calculated to be (b)(7)(F) (b)(7)(F) (see the green dot-dash line on right plot in Figure 7.3) and the corresponding mean peak breach outflow rate of (b)(7)(F) cfs, both of which are at about the 40th percentile on their respective probability distributions.

The adjustment described above relies on the relatively precise knowledge of the volume of the reservoir contents above the breach bottom elevation and the predicted values of the peak breach outflow rate, which of all the breach parameters have the highest R^2 values for both the revised Xu and Zhang methodology (R^2 = 81%) and the Froehlich (1995a and 2008) methodology (R^2 = 93%).

Table 7.2 contains a comparison of the breach parameter values used to develop the breach hydrographs in the Safety Evaluation (SE) (NRC 2011) (discussed in Section 7.3), the HRR (Duke 2013) (discussed in Appendix B.6) and the two sensitivity studies (discussed in Section 7.4). Table 7.3 contains the comparison of estimated Jocassee Dam peak breach

Table 7.2. Comparison of breach parameter values used in the Safety Evaluation (SE) (NRC 2011), the HRR and the sensitivity studies

Breach Parameter	January 2011 Safety Evaluation (SE) (NRC 2011) - Froehlich	3/12/2013 Hazard Reevaluation - Xu and Zhang (2009)	Sensitivity - Revised Xu and Zhang	Sensitivity - Froehlich (1995b and 2008)
Figure No. for breach hydrographs	7.4	B.5	7.5	7.6
Top Width (feet)	1,156	701	1,009	1,082
Bottom Width (feet)	425	431	277	696
Bottom Elevation (feet msl.)	800	870	848	850
Breach Formation Time (without piping phase) (hours)	(b)(7)(F)			
Peak Outflow Rate (million cfs)				
Side Slopes (horiz:vert)	Right: 1.55, Left: 0.7	Right: 0.53, Left: 0.53	Average 1.3	Average 0.7

Table 7.3. Comparison of Estimated Jocassee Dam Peak Breach Outflow Rates provided in the Safety Evaluation (SE) (NRC 2011)

Model	Peak Outflow (cfs)
McDonald & Langridge-Monopolis (1984)	(b)(7)(F)
Costa (1985)	
Evans (1986)	
SCS (1981)	
Bureau of Reclamation (1982)	
McDonald and Langridg e-Monopolis (1984)	

outflow rates from several regression methodologies that was provided in the Safety Evaluation (NRC 2011).

Table 7.4 summarizes the basis for each breach parameter estimate used in the sensitivity studies that are discussed in Section 7.4. In all cases they are the mean or the more conservative median estimate of the breach parameters. In our February 2013 report (Ehasz and Bowles 2013), we concluded that the use of median values of the breach parameter estimates for Jocassee Dam would be a conservative choice. We argued that in reality we would expect that the peak breach flow rate for Jocassee Dam to be in the range between the mean and lower bound confidence interval estimates, which is the range in which the peak breach flow rates fall for both the adjusted revised Xu and Zhang and the adjusted Froehlich (1995a and 2008) methodologies. The reasons for expecting the peak breach flow rate for Jocassee Dam to be in the range between the mean and lower bound confidence interval estimates include the fact that Jocassee Dam was designed and constructed as a modern rockfill dam such that it would be expected to be a more resistant dam to the breach process than other low erodibility dams for which failure data were used to develop the revised Xu and Zhang and Froehlich (1995a and 2008) methodologies. In addition, the uni-directional breach formation starting at the right abutment and the downstream deposition of rockfill material

Table 7.4. Summary of the basis for each breach param eter used in sensitivity studies

Breach Parameter	Basis for estimate used in sensitivity analysis		
Peak outflow, Q_p	Mean	Conservative	
Breach development time, T	Mean	Conservative	Consistent with Q_p & V
Breach depth, H_d	Mean	Conservative	
Breach top width, B_t	Median (> Mean)	Conservative	
Breach average width, B_{ave}	Median (> Mean)	Conservative	

leading to development of tailwater during breach formation also support the peak breach flow rate for Jocassee Dam to be in the range between the mean and lower bound confidence interval estimates. Mohamed (2002) demonstrated that a "side breach" results in a significantly lower peak breach flow rate and narrower breach width than a "center breach" in simulations of the Teton Dam failure.

7.3 Example of Inconsistencies between Peak Breach Flow and Breach Development Time

Figure 7.4 contains the Jocassee Dam breach hydrograph for the breach Case 2(100W) in support of the Safety Evaluation (SE) (NRC 2011) based on a HEC-RAS simulation. The Jocassee headwater hydrograph is represented by the blue line (left scale * 1000), the Jocassee tailwater hydrograph is represented by the brown line (left scale * 1,000) and the Jocassee breach discharge hydrograph is represented by the green line (right scale) at a location immediately downstream of the internal boundary in HEC-RAS model that represents the Jocassee Dam. The assumed sinusoidal form for the breach progression relationship is shown by the black line (left scale).

The peak breach flow rate for the Safety Evaluation (SE) (NRC 2011) hydrograph shown in Figure 7.4 is abou (b)(7)(F) cfs for the SE hydrograph based on using a breach formation time

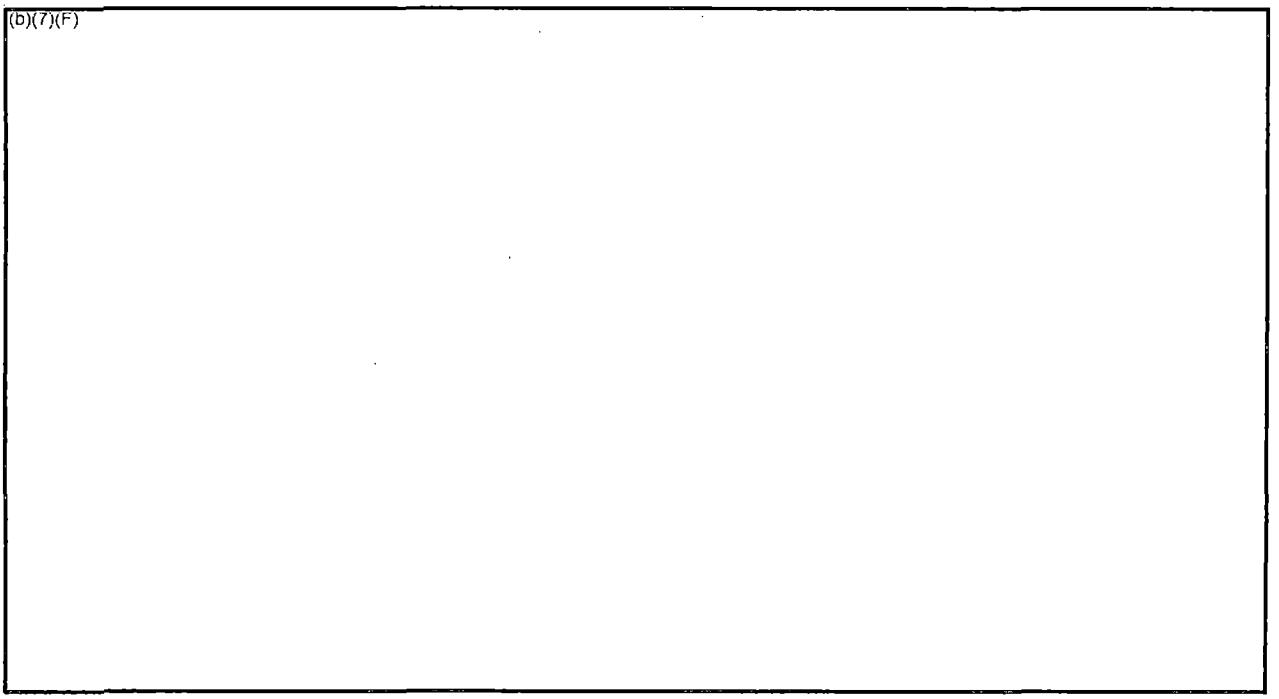

Figure 7.4. Jocassee Dam breach progression relationship and breach hydrographs based on the breach Case 2(100W) in t he Safety Evaluation (SE) (NRC 2011)

of (b)(7)(F) and median breach geometry parameter estimates based on Froehlich (1995a). The inconsistency between the peak breach flow rate and the breach development time for the SE breach hydrograph is clearly seen in Figure 7.4 because the breach progression relationship reaches 100% afte (b)(7)(F) which implies that the breach development is complete at that time. However, at this time the simulated breach flow rate is abou (b)(7)(F) cfs. The breach size certainly would not have stabilized at such a large flow rate and would be growing quite rapidly. If a more realistic and longer breach development time, consistent with emptying the reservoir contents, had been used the peak outflow rate would have been much smaller (the breach time would need to be longer thar (b)(7)(F) as in the S E hydrograph and the peak outflow rate of (b)(7)(F) cfs would decrease for a longer breach time). This type of physical inconsistency is determined by the underestimation of the breach development time that is input to HEC-RAS based on the estimate from Froehlich (1995b)[3]. The HEC-RAS model does not simulate the physical erosion and instability processes that would take place in an actual breach and therefore the model has no way to assure a consistent simulation unless a consistent set of breach parameters are input to the model. Achieving this consistency is the purpose of the adjustment that is described in Section 7.2 to account for the time required to completely empty the Jocassee reservoir and which is applied in the sensitivity analyses presented in Section 7.4.

7.4 Discussion of HEC-RAS Results

Figure 7.5 contains the breach hydrographs developed by HDR using HEC-RAS based on the breach parameters estimated from the adjusted revised Xu and Zhang regression equations with the Froehlich breach development time definition and the Chinese case histories excluded as summarized in Section 6.3.2. Figure 7.6 contains the breach hydrographs based on the breach parameters estimated from the adjusted Froehlich (1995a and 2008) regression equations. The predicted values of peak breach outflow rate and breach development time for both the revised Xu and Zhang and the Froehlich (1995b and 2008) methodologies are therefore the mean estimates obtained using the adjustment as described in Section 7.2 to account for the time required to completely empty the Jocassee reservoir (see Table 7.4). In Figures 7.5 and 7.6, the Jocassee headwater hydrograph is represented by the blue line (left scale * 1000), the Jocassee tailwater hydrograph is represented by the brown line (left scale * 1,000) and the Jocassee breach discharge hydrograph is represented by the green line (right scale) at a location immediately downstream of the internal boundary in HEC-RAS model that represents the Jocassee Dam.

The breach progression relationship, which is a required HEC-RAS input, and which was developed iteratively as described in Section 7.2, is shown by the black line (left scale). Points A, B and D are equivalent to points that are defined in Figure B.4. The final values of the orifice

[3] A similar underestimation of breach development time has been identified in Section 7.2 for Xu and Zhang (2009).

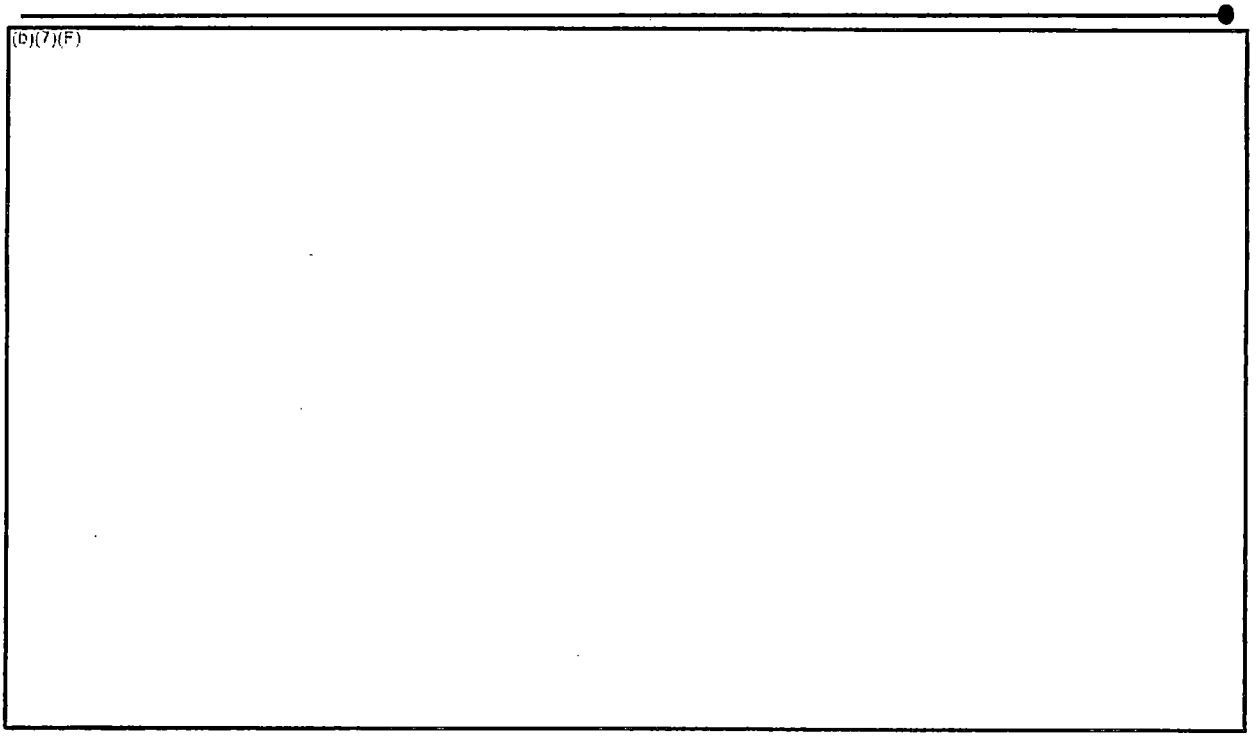

Figure 7.5. Jocassee Dam breach progression relationship and breach hydrographs – sensitivity run using revised Xu and Zhang breach parameter estimates

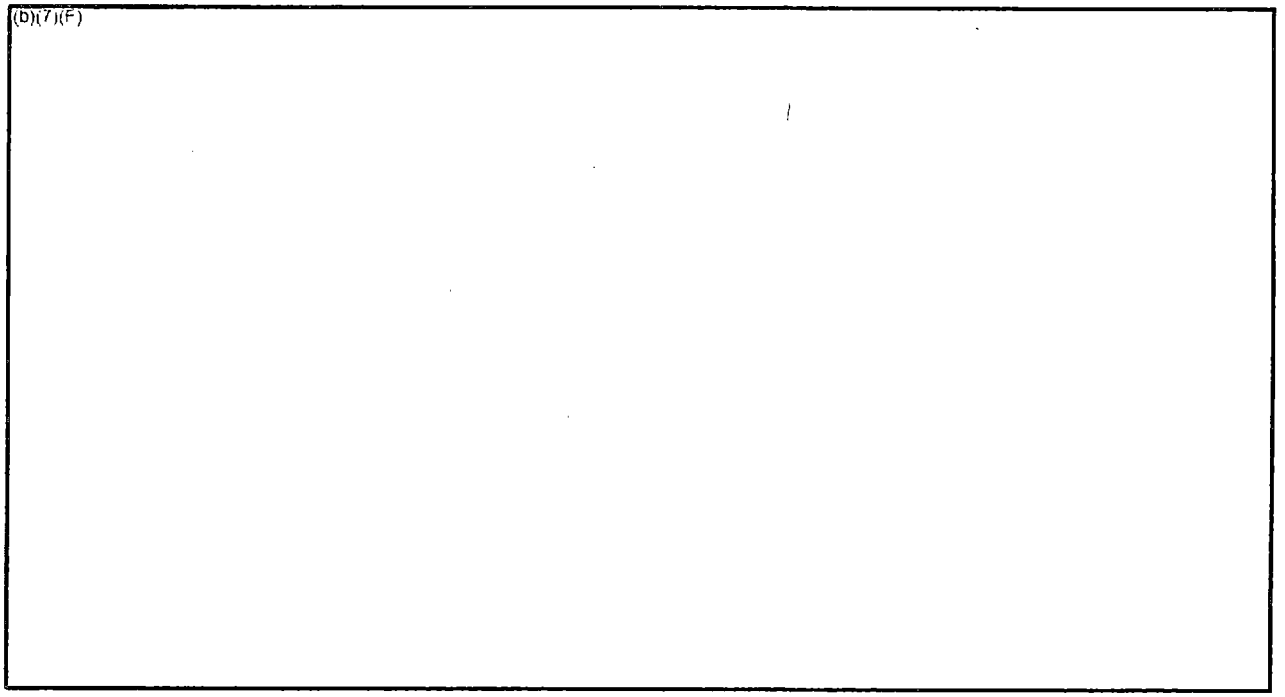

Figure 7.6. Jocassee Dam breach progression relationship and breach hydrographs – sensitivity run using Froehlich (1995b and 2008) breach parameter estimates

coefficients of 0.1 for both the adjusted revised Xu and Zhang and the adjusted Froehlich (1995a and 2008) breach parameter estimates appear to be reasonable in terms of representing a piping flow through the rockfill material. Similarly, the final values of the weir coefficients 2.2 and 2.0 for the adjusted revised Xu and Zhang and the adjusted Froehlich (1995a and 2008) breach parameter estimates, respectively, appear to be reasonable in terms of representing flow through the breach following collapse of the dam crest of the rockfill dam.

In addition, the form of the resulting breach hydrographs shown in Figures 7.5 and 7.6 also appear to be reasonable for a piping failure mode and closely match the mean peak breach flow rate estimates obtained for the adjusted revised Xu and Zhang and the adjusted Froehlich (1995a and 2008) methodologies, respectively. Point A represents the beginning of the HEC-RAS simulation of the enlargement of the pipe. The breach progression curve was adjusted to keep the flow rate to a reasonably low magnitude prior to the collapse of the pipe and the onset of overtopping that is simulated at point B on Figures 7.5 and 7.6. These points mark the end of the breach initiation phase as defined in the revised Xu and Zhang methodology, which is consistent with the definition used by Froehlich (1995b and 2008) and Wahl (2013). Point D on Figures 7.5 and 7.6 marks the end of the breach development phase. The times between points B and D in Figures 7.5 and 7.6 are approximately equal to the mean breach development time estimated using the adjustment described in Section 7.2 for both the revised Xu and Zhang and Froehlich (1995a and 2008) methodologies, respectively.

When compared with the breach hydrographs from the HRR (Duke 2013), shown in Figure B.5, we conclude that the breach hydrographs in Figures 7.5 and 7.6, which are based on the adjusted revised Xu and Zhang and the adjusted Froehlich (1995a and 2008) breach parameter estimates, respectively, provide good support for the HRR breach hydrographs (Duke 2013). In our February 2013 report (Ehasz and Bowles 2013) we concluded that the breach hydrograph in Figure B.5 is a *realistic but conservative* breach hydrograph that has good *defendablity* based on the validity of the Xu and Zhang (2009) method, the conservative nature of the median breach parameter estimates, a piping failure mode initiating in the (b)(7)(F) the deposition of rockfill immediately below the dam, the low erosion category of the rockfill material, and the various characteristics of a modern dam that were included in the design and construction of Jocassee Dam.

An additional sensitivity case was considered in which the breach bottom elevation was set to Elevation 800 feet msl, corresponding to 99.4% of the reservoir contents below the initial normal full pool at Elevation 1,110 feet msl, and all the other breach parameters were kept identical to those used for the HRR breach hydrograph (Duke 2013), including the breach progression relationship. The resulting hydrographs are presented in Figure 7.7 using the same format as used in Figures 7.4, 7.5, 7.6 and B.5. The effects of the lower breach bottom elevation can be seen by comparing the results in Figure 7.7 with those in Figure B.5 for the HRR breach hydrograph in which the breach bottom elevation was at Elevation 870 feet msl, which is the

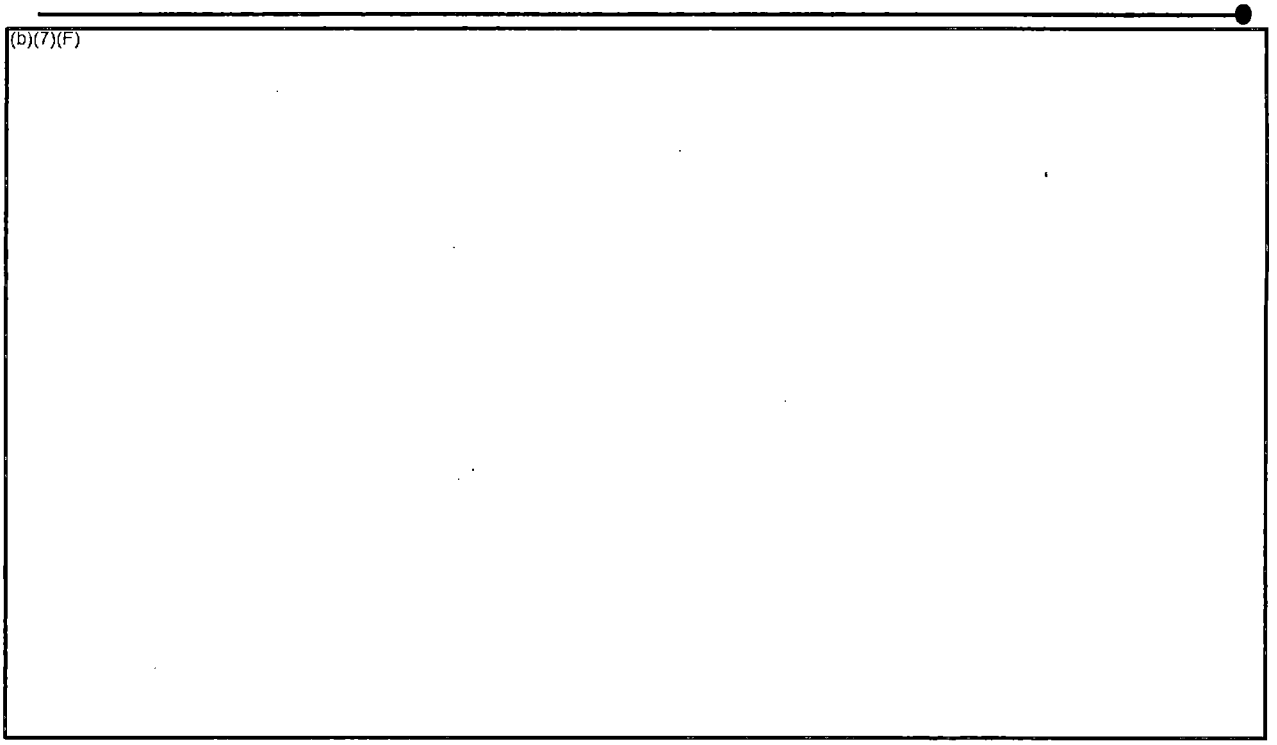

Figure 7.7. Jocassee Dam breach progression relationship and breach hydrographs – sensitivity run using breach bottom elevation of 800 feet msl. and all other breach parameters identical to those in the HRR breach hydrograph (Duke 2013) based on Xu and Zhang (2009)

estimate based on Xu and Zhang (2009), and which corresponds to 94.1% of the reservoir contents below the initial normal full pool at Elevation 1,110 feet msl. In the simulation the additional reservoir contents is released mainly on the falling limb of the hydrograph resulting in higher flows for much of the falling limb starting with a somewhat flat portion of the hydrograph following the peak flow rate. Although it is considered that a more realistic simulation of the lower breach bottom would tend to lengthen the falling limb rather than raising it, we view this simulation, in which the breach development time was constrained to match the time used in the HRR hydrograph, as a conservative case in terms of the effects on the downstream flow conditions. Therefore a more realistic simulation was not pursued and it was concluded that a lower breach bottom would not significantly change the breach hydrograph even under the conservative sensitivity case summarized above.

The discussions in Appendices C.1 and C.2 benchmark the characteristics of several recent large embankment dam failures. They also describe the properties and failure conditions as well as embankment design considerations affecting these breaches and their relevance to the Jocassee Dam.

8.0 CONCLUSIONS

8.1 Discuss Overall Conclusion

The overall conclusion of this report is that the HRR breach hydrographs (Duke 2013), which was based on the original Xu and Zhang (2009) breach parameter regression equations, is a reasonable and conservative estimate of the downstream effects of a deterministic sunny-day breach of the Jocassee Dam. This conclusion is supported by our review of the data on which the Xu and Zhang (2009) methodology is based, the confirmation of the assignment of a low erosion category to Jocassee Dam, and by comparisons with two additional breach hydrographs that are based on the Froehlich (1995a and 2008) regression equations and the revised Xu and Zhang regression equations in which the agency questions about the original Xu and Zhang (2009) methodology have been addressed. Both the revised Xu and Zhang and Froehlich (1995a and 2008) methodologies have been adjusted to allow for sufficient time to drain Lake Jocassee down to the breach bottom elevation (see Section 7.2)

The specific conclusions for this report are organized into two parts. In Section 8.2 we summarize our conclusions regarding our responses to the five agency questions. In Section 8.3 we summarize our conclusions from the review and revision of the Xu and Zhang (2009) methodology and the support that its application and an application of the adjusted Froehlich (1995b and 2008) methodology, to Jocassee Dam provide for the HRR breach hydrographs submitted to the NRC by Duke (2013).

8.2 Concluding Responses to Agency Questions

1) **Precedence:** Several uses of the Xu and Zhang (2009) methodology have been identified in addition to its application to Jocassee Dam. This new methodology seems to be following a pathway to broader acceptance in which its significant advantage over other methods by accounting for the important physical characteristic of erodibility is becoming recognized. The initial questions about the methodology are being addressed, including how to appropriately define and apply failure time estimates in dam breach modeling.
2) **Chinese case histories:** About 43% of the 75 dam failure case histories on which the Xu and Zhang (2009) methodology is based are for Chinese dams. Our review indicated that Xu and Zhang (2009) did appropriate screening and interpretation of the case history data from all sources, including China; although we identified a few improvements [see 2 in Section 8.3 below]. The quality of data for the Chinese case histories appears to be similar to that available for US case histories with more recent breaches; although access to some of this data has been limited outside of China. The poorer construction of Chinese dams built prior to 1977 would be expected to result in a more erodible dam once a breach process has initiated. This was appropriately

accounted for by assigning a higher erosion category in the Xu and Zhang (2009) methodology.

3) **Representation of case histories for rockfill and other low erodibility dams:** The small number of case histories for rockfill dams that are classified with low erodibility is a reality that is likely due to the intrinsic safety of such rockfill dams. This limitation applies to all regression methodologies. However, the inclusion of the Briaud (2008) erosion categories as a control variable in the Xu and Zhang (2009) methodology provides a way to account for the important influence of the erodibility of materials on breach parameters. Also, Xu and Zhang (2009) increased the number of case histories by including case histories from China for the Danghe and Gouhou large rockfill dams.

4) **Use of the Briaud erosion categories:** Professor Briaud's independent review confirmed the following:

   - The appropriateness of using his erosion categories in the Xu and Zhang (2009) methodology.
   - The Xu and Zhang (2009) two-step procedure for assigning low, medium or high erosion categories to case history dams is consistent with his research findings: i) an initial categorization as a range based on the soil type within the dam as low to medium erodibility for rockfill and clay and medium to high erodibility for silt and sand; and ii) an up or down adjustment in the initial range based on construction quality, particularly compaction effort, that is dependent mainly on the period of construction but also dam cross-sectional geometry and slope surface protection. In a few cases erosion categories were changed as summarized in 2 in Section 8.3 below.
   - The assignment of a low erosion category for Jocassee Dam was confirmed through a conservative analysis of the erosion rates for cross-section materials based on both velocity and shear stress.

5) **Breach time definition:** The definition of breach time used by Xu and Zhang (2009) includes both a part of the breach initiation process in addition to the breach formation process unlike other regression methods (e.g. Froehlich 1995b and 2008) that include only the latter. We found that this difference in definitions is of no concern as long as it is appropriately accounted for in using the predicted breach time in a way that is consistent with the HEC-RAS model definitions.

8.3 Concluding Support for the HRR Breach Hydrograph

1) **Agency Concerns:** Our review of the agency questions (summarized in Section 8.2) indicates support for the original application of Xu and Zhang (2009) to estimate breach parameters on which the HRR breach hydrographs are based; although some improvements to the Xu and Zhang (2009) data base were identified [see 2) below]..

2) **Revised Xu and Zhang regression equations sensitivity studies**: The revised regression equations were developed by Dr. Xu based on the following changes and improvements to the Xu and Zhang (2009) data set:

   - Changed breach development times to the commonly-used Froehlich (1995b and 2008) definition. This change was seen as a way to predict the duration of the breach hydrograph in HEC-RAS; but, as summarized in 3) below, a broader issue with inconsistent "observed" breach times was found that required another step to obtain a reasonable predicted dur ation.
   - Changed the values of other breach param eters and control variables where they were inconsistent with the Wahl (1998) and Froehlich (1995a and b and 2008) data sets with consideration given to reliable information from other sources.
   - Changed some assigned erosion categories to include the consideration that compaction associated with construction practices in the US and other developed countries (not China) improved for earthfill dams after about 1950 and for rockfill dams after about 1965.
   - Changed to a higher erosion category where a lower category had been assigned because of long observed failure times but where all other available information pointed to the higher erosion category.
   - Embankment dams with a core wall or concrete-faced dams that had been assigned to the low erosion category as a means of accounting for the throttling effects of these features on breach development were omitted from the revised data set because their breach parameters would not be representative of low erodibility embankment dams in general.
   - All Chinese case histories were omitted from the revised data set to avoid the potential criticism that we only had indirect access to the original references for these case histories.

3) **Inconsistencies between peak breach flows and breach development times:** An inconsistency was identified for many case histories in the Wahl (1998), Froehlich (1995a and b and 2008), and Xu and Zhang (2009) data sets. Specifically, the "observed" breach development time is too short to discharge the reservoir contents above the breach bottom and match the "observed" peak breach flow rate. This inconsistency can be clearly seen in the Jocassee Dam breach hydrograph submitted to the NRC by Duke in support of the Safety Evaluation (SE) Report (NRC 2011) (Figure 7.4) that is based on using a breach formation time of (b)(7)(F) and median breach geometry parameter estimates based on Froehlich (1995a). The breach progression relationship reaches 100% after (b)(7)(F) which implies that the breach development is complete at that time. However, the simulated breach flow rate is about (b)(7)(F) cfs at (b)(7)(F) and therefore the breach size certainly would be growing quite rapidly. A more realistic simulation would require a longer breach development time that would produce a smaller peak breach outflow rate. To address this shortcoming an adjustment was

developed to obtain an estimate of the mean peak breach flow rate that is consistent with the mean breach formation time for a triangular breach hydrograph with a volume equal to the reservoir volume above the breach bottom (detailed in Section 6.2.8). This adjustment was also applied to the Froehlich (1995a and 2008) methodology to overcome the same shortcoming [see 5) below]. The adjustment relies on the relatively precise knowledge of the volume of the reservoir contents above the breach bottom elevation and the predicted values of the peak breach outflow rate, which of all the breach parameters have the highest R^2 values for both the revised Xu and Zhang methodology (R^2 = 81%) and the Froehlich (1995a and 2008) methodology (R^2 = 93%).

4) **Application of Revised Xu and Zhang regression equations to Teton Dam:** The revised best exact and best simplified Xu and Zhang equations were applied to the Teton Dam. The median predicted values for the high and medium erodibility categories were averaged, based on an evaluation by Professor Briaud that Teton Dam erodibility is on the boundary between the high and medium erosion categories. The percent differences between the observed and predicted breach parameters were smaller for most breach parameters compared with those obtained using the original Xu and Zhang (2009) equations. An attempt to evaluate the adjustment procedure for accounting for the inconsistency in predicted breach time summarized in 3) above was found to be problematic because the observed breach time for the Teton Dam is uncharacteristically short due to an unusually sudden breach mechanism caused by the large internal void, which has been documented by the Bureau of Reclamation cause evaluation (Osmun 2013).

5) **Sensitivity of the Jocassee HRR Breach Hydrograph based on Adjusted Revised Xu and Zhang Equations and Adjusted Froehlich (1995a and 2008):** Considering the widths of the confidence intervals for both methods, both methods provide fairly similar median and mean estimates. Specifically with the adjusted revised best exact Xu and Zhang methodology, which uses the same breach formation time definition as Froehlich (1995b and 2008), and the adjusted Froehlich (1995b and 2008) methodology the mean breach formation time estimates are (b)(7)(F) and (b)(7)(F) respectively. By iteratively changing the orifice and weir coefficients and the breach progression relationships HEC-RAS was run to approximately match the mean peak breach flow rate estimates of (b)(7)(F) cfs and (b)(7)(F) cfs, for the two methodologies respectively. The resulting breach hydrographs obtained by HDR for a deterministic piping failure of Jocassee Dam are similar to the HRR breach hydrograph (Duke 2013). It is therefore concluded that the use of the adjusted revised Xu and Zhang and the adjusted Froehlich (1995a and 2008) provide additional support for the conclusion in our February 2013 report (Ehasz and Bowles 2013) that the HRR breach hydrographs are *realistic but conservative* breach hydrographs that have good *defendablity* based on the validity of the Xu and Zhang (2009) method, the conservative nature of the median breach parameter estimates, a piping failure mode initiating in the (b)(7)(F) resulting in a breach developing in a single direction towards the center of the dam, the deposition of rockfill immediately below the dam, the low erosion category of the rockfill material, the

various characteristics of a modern dam that were included in the design and construction of Jocassee Dam and the time required to drain Lake Jocassee to the breach bottom elevation.

6) **Sensitivity of the Jocassee HRR Breach Hydrograph to a Lower Breach Bottom Elevation**: A sensitivity run was performed with the breach bottom elevation set to Elevation 800 feet msl. instead of Elevation 870 feet msl., but with all the other breach parameters unchanged from the HRR breach hydrograph (Duke 2013). Even though this run was performed in a conservative manner, it was concluded that a lower breach bottom would not significantly change the breach hydrograph.

9.0 REFERENCES

Bureau of Reclamation. 1982. Guidelines for defining inundated areas downstream from Bureau of Reclamation dams. Reclamation Planning Instruction Rep. No. 82-11, U.S. Dept. of the Interior, Bureau of Reclamation, Denver.

Bureau of Reclamation. 1988. Downstream hazard classification guidelines. ACER Tech. Memorandum Rep. No. 11, U.S. Dept. of the Interior, Bureau of Reclamation, Denver.

Briaud, J. L. 2008. Case Histories in Soil and Rock Erosion: Woodrow Wilson Bridge, Brazos River Meander, Normandy Cliffs, and New Orleans Levees. Journal of Geotechnical and Geoenvironmental Engineering, 134(10):1425–1447.

Briaud, J. L. 2013. Jocassee Dam. Report to URS. October 22. (Appendix A of this report)

Brunner, G.W. 2011. Hydraulic Model Development for Dam Break Studies. Hydrologic Engineering Center, U.S. Army Corps of Engineers. March.

Costa, J.E. 1985. Floods from Dam Failures. U.S Geological Survey Open File Report 85-560, Denver, Colorado. 54p.

Duke Energy Company. 2013. Hydrologic Reevaluation Report submitted to the NRC on March 12, 2013.

Ehasz, J.L. and D.S. Bowles. 2013. Jocassee and Keowee Dams Breach Parameter Review. Report for Duke Energy by URS Civil Construction & Mining and RAC Engineers & Economists. February.

Evans, S. G. 1986. 'The maximum discharge of outburst floods caused by the breaching of man-made and natural dams. Canadian Geotechnical Journal, 23(4):385–387.

Fell, R., Wan, C.F., Cyganiewicz, J. and Foster, M. 2003. Time for Development of Internal Erosion and Piping in Embankment Dams. Journal of Geotechnical and Geoenvironmental Engineering, 129(4):307–314.

Franca, M.J. and A.B. Almeida. 2002. Experimental tests on rockfill dam breaching process. Proc. Intern. Symp. on Hydraulic and Hydrological Aspects of Reliability and Safety Assessment of Hydraulic Structures, St. Petersburg, Russia.

Froehlich, D.C. 1995a. Embankment dam breach parameters revisited. Proc., Water Resources Engineering, 1995 ASCE Conf. on Water Resources Engineering, ASCE, NY, 887–891.

Froehlich, D.C. 1995b. Peak outflow from breached embankment dam. J. Water Resour. Plann. Manage., 121(1):90–97.

Froehlich, D.C. 2008. Embankment Dam Breach Parameters and Their Uncertainties. Journal of Hydraulic Engineering, 134(12):1708-1721.

Haan, C.T. 1977. Statistical Methods in Hydrology. Iowa State University Press.

HR Wallingford. 2012. AREBA (A Rapid Embankment Breach Assessment), Breach size - rapid methods of assessment. http://www.hrwallingford.com/projects/breach-size-rapid-methods-of-assessment. Accessed January 26, 2014.

HR Wallingford. 2014. Small Reservoirs Simplified Risk Assessment Methodology: Research Modelling Report. Final report to Defra and Environment Agency Flood and Coastal Erosion Risk Management Research and Development Programme, Project FD2658. January.

MacDonald, T.C., and J. Langridge-Monopolis. 1984. Breaching characteristics of dam failures. J. Hydraul. Eng., 110(5):567–586.

Mohamed, M.A.A. 2002. Embankment breach formation and modelling methods. The Open University, England, UK. April.

Nuclear Regulatory Commission (NRC). 2011. "Staff Assessment of Duke's Response to Confirmatory Action Letter Regarding Duke's Commitments to Address External Flooding Concerns at the Oconee Nuclear Station, Units 1, 2, and 3 (ONS) (TAG Nos. ME3065, ME3066, and ME3067)". January 28.

Osum, D. 2013. Teton Dam Failure: A Review of the Technical Factors Contributing to the Failure. Presentation to the Association of Engineering Geologists. May.

Reclamation-USACE-URS-UNSW. 2008. Piping and Seepage Toolbox.

Soil Conservation Service. 1981. Simplified dam-breach routing procedure. U. S. Department of Agriculture, Technical Release 66, Washington, D.C., 25 p. plus appendix.

Singh, V.P. 1996. Dam breach modelling technology. Kluwer Academic, Boston.

Ru, N.H. and Y.G. Niu. 2001. Embankment dam - incidents and safety of large dams. Water Power Press, Beijing. [In Chinese.]

Sowers, G.F. 1987. Jocassee Main Dam Design, Construction and Performance. Report to Design Engineering Department, Duke Power Company, Charlotte, North Carolina. April.

Von Thun, J.L., and D.R. Gillette. 1990. Guidance on breach parameters. Internal Memorandum, U.S. Dept. of the Interior, Bureau of Reclamation, Denver.

Wahl, T. L. 1998. Prediction of Embankment Dam Breach Parameters - A Literature Review and Needs Assessment. Dam Safety Report No. DSO-98-004, U.S. Department of the Interior, Bureau of Reclamation, Denver, Colorado.

Wahl, T.L. 2004. Uncertainty of Predictions of Embankment Dam Breach Parameters. ASCE Journal of Hydraulic Engineering, Vol. 130, No. 5, May 1.

Wahl, T.L. 2012. Several verbal discussions with J.L. Ehasz regarding the use of the Xu and Zhang (2009) technical paper as well as verbal discussions of erodibility factors as related to rockfill dams.

Wahl, T.L. 2013. Incorporating Breach Parameter Estimation and Physically-Based Dam Breach Modeling into Probabilistic Dam Failure Analysis. Presented at the NRC Interagency Workshop on Probabilistic Flood Hazard Assessment. January 30.

Walder, J.S., and J.E. O'Connor. 1997. Methods for predicting peak discharge of floods caused by failure of natural and constructed earth dams. Water Resour. Res., 33(10):2337–2348.

Wan, C.F., and R. Fell. 2004. Investigation of rate of erosion of soils in embankment dams. J. Geotech. Geoenviron. Eng., 130(4):373 –380.

Xu, Y. and Zhang, L.M. 2009. Breaching Parameters for Earth and Rockfill Dams. Journal of Geotechnical and Geoenvironmental Engineering, 135(12): 1957-1970.

Xu, Y. 2010. Analysis of Dam Failures and Diagnosis of Distresses for Dam Rehabilitation. Ph.D. Thesis. The Hong Kong University of Science and Technology. January.

Appendices

Jocassee Dam

Validation of HRR Breach Hydrograph for Jocassee Dam

Appendix A

Briaud's Report

JOCASSEE DAM

17 January 2014

Report to URS

Prepared by: Professor Jean-Louis BRIAUD, PhD., PE

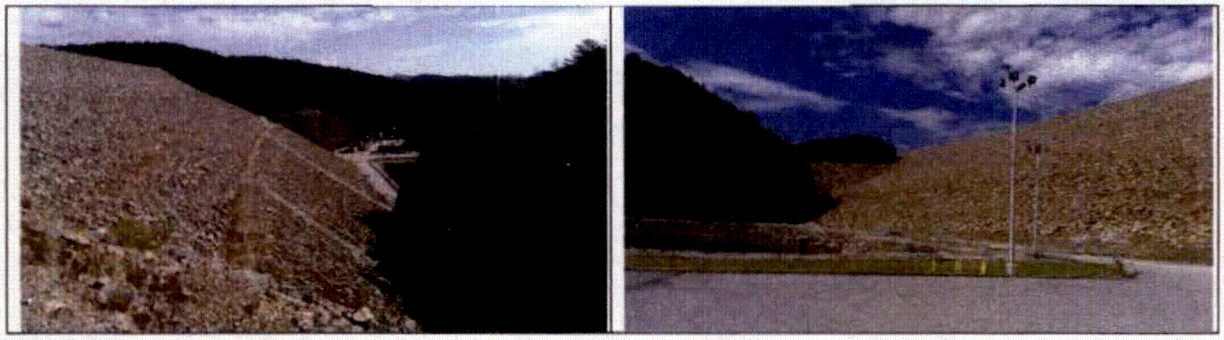

Fig. 1 – Jocassee Dam

1. MEETING LOGISTICS

A meeting took place at the Jocassee Dam in South Carolina on 3 and 4 October 2013. The purpose of the meeting was to evaluate the erosion characteristics of the Jocassee Dam, which forms a large storage reservoir 12 miles upstream of Duke Energy's Oconee Nuclear Power Plant Complex near Salem, South Carolina.

The primary attendees were Dean Hubbard and Adam Johnson from Duke Energy; Chris Ey from HDR and Joe Ehasz from URS.

2. MEETING PURPOSE

The primary purpose of the meeting and field trip was to become familiar with the Jocassee Dam and materials and address the following questions:

- Is your (Briaud) work applicable to embankment dam erosion?
- What is your (Briaud) characterization of Jocassee dam erosion characteristics?

- Please comment on Xu and Zhang work on dam breach, and how the three erodibility classifications, used by Xu & Zhang, compare to your six classifications.

Important background details on soil erosion and rock erosion are given in the Appendix.

3. IS YOUR (BRIAUD) WORK APPICABLE TO EMBANKMENT EROSION?

The short answer is yes as long as the limitations listed below are kept in mind; the work also has significant advantages also listed below. My work (Briaud, 2008) is described in the background section of this report (Appendix). Of particular interest for Jocassee Dam are the charts shown below relating the critical velocity Vc to the mean grain size D50, the critical shear stress τc to the mean grain size D50, the erosion rate dz/dt to the velocity V, and the erosion rate dz/dt to the shear stress τ. These charts are repeated below for convenience (Fig. 31, 32, 33, 34). These charts were developed on the basis of EFA testing (Appendix Section c, Fig. 5). This apparatus reproduces the erosion process at the element level where the water is flowing parallel to the interface. The charts were developed from hundreds of EFA tests on vastly different soil types over the last 20 years. The advantages and limitations of the applicability of these charts are listed below

Limitations:

a. The soils tested over the last 20 years were soils that could be sampled in a 3 inch diameter Shelby tube or re-compacted in a 3 inch Shelby tube to match the site condition. The largest grain size that was tested was about 7 mm diameter gravel. For soils particles larger than that, the charts are based on published work by others including the US Army Corps of Engineers for example.
b. The Erosion Function Apparatus (EFA) reproduces a flow where the water is flowing parallel to the soil surface at the element level. Therefore using the EFA results for other flow conditions should be done with caution and with engineering judgment.

Advantages:

a. The work is characterizing the behavior of the soil at the element level so it is broadly applicable to many erosion situations, including soil and rockfill materials used in embankment dams. The measured function called the erosion function is to erosion studies what the stress strain curve is to deformation problems. It is a constitutive equation which can be used in numerical method as easily as in simple hand calculations.
b. The work is very useful in the case of fine grained soils where the erodibility is not related to the grain size.
c. The work includes the critical velocity or critical shear stress for coarse grained soils and rockfill based on an NCHRP project (Lagasse et al., 2006) which identified the USACE equation as being the best among others. This equation is Eq. 8 in the Appendix for predicting the required size given a velocity. The critical velocity charts for large rock fill blocks have this solid background and are applicable to soil materials and rockfills used in embankment dams.
d. The EFA tests which form the basis for these charts has been used to predict several erosion processes in many materials. One example is the erosion that occurs in fine grained and coarse grained soils around bridge supports as a function of time; Fig. 35

shows the precision obtained in this case. Other examples of applications include levee overtopping and meander migration in rivers.

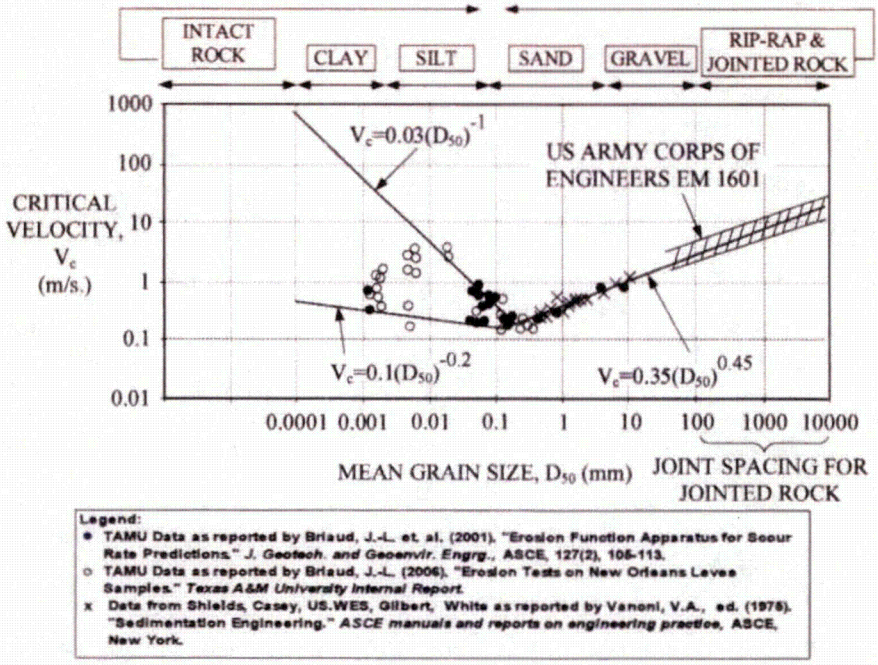

Fig. 31 – Critical velocity as a function of mean grain size (Briaud, 2013).

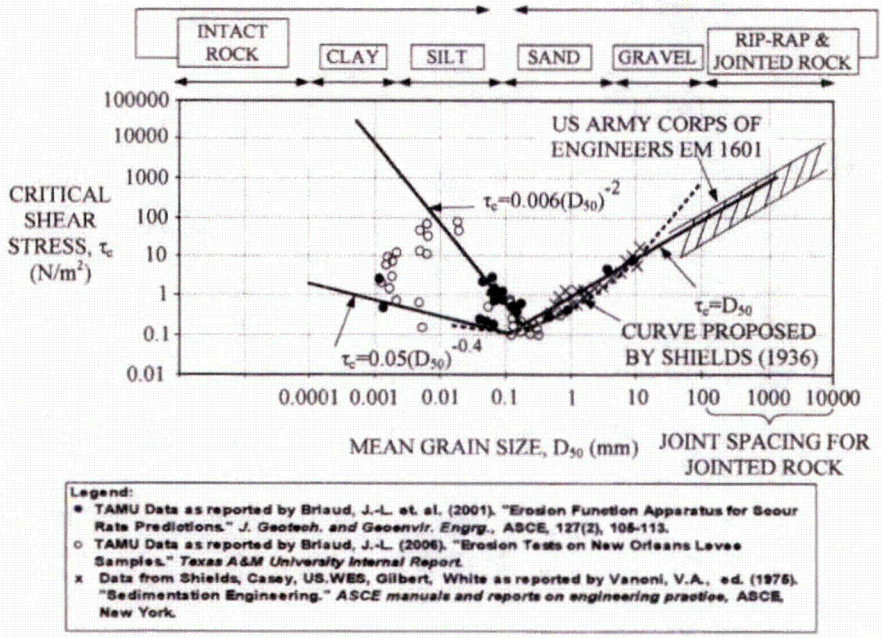

Fig. 32 – Critical shear stress as a function of mean grain size (Briaud, 2013)

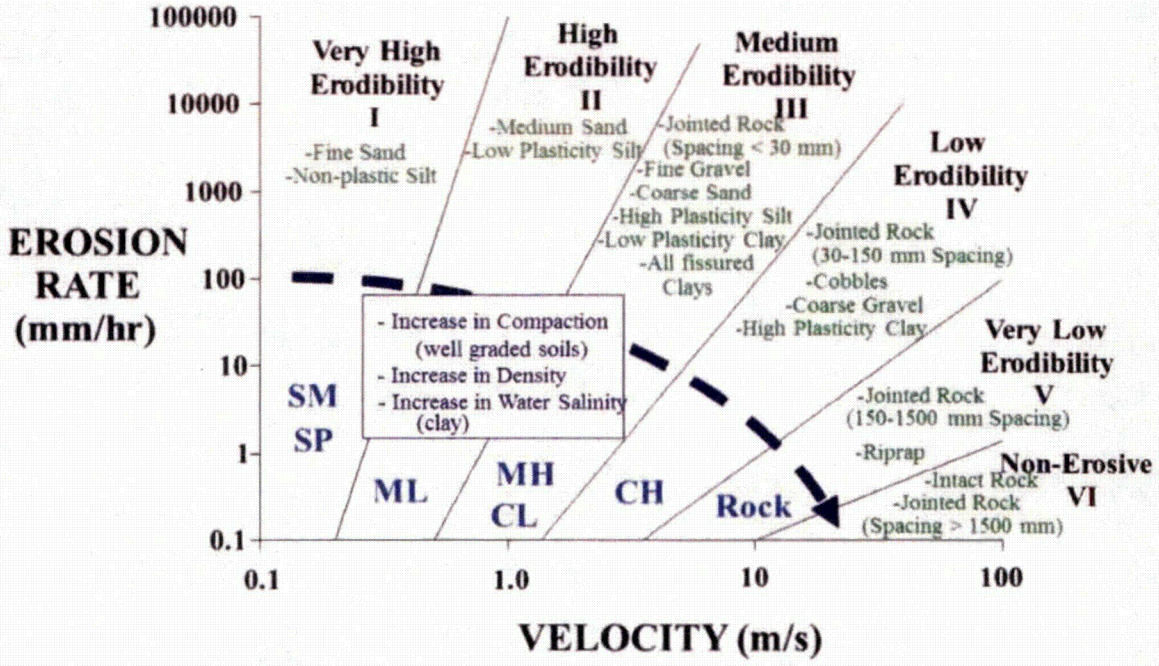

Fig. 33 – Proposed erosion categories for soils and rocks based on velocity (Briaud, 2013).

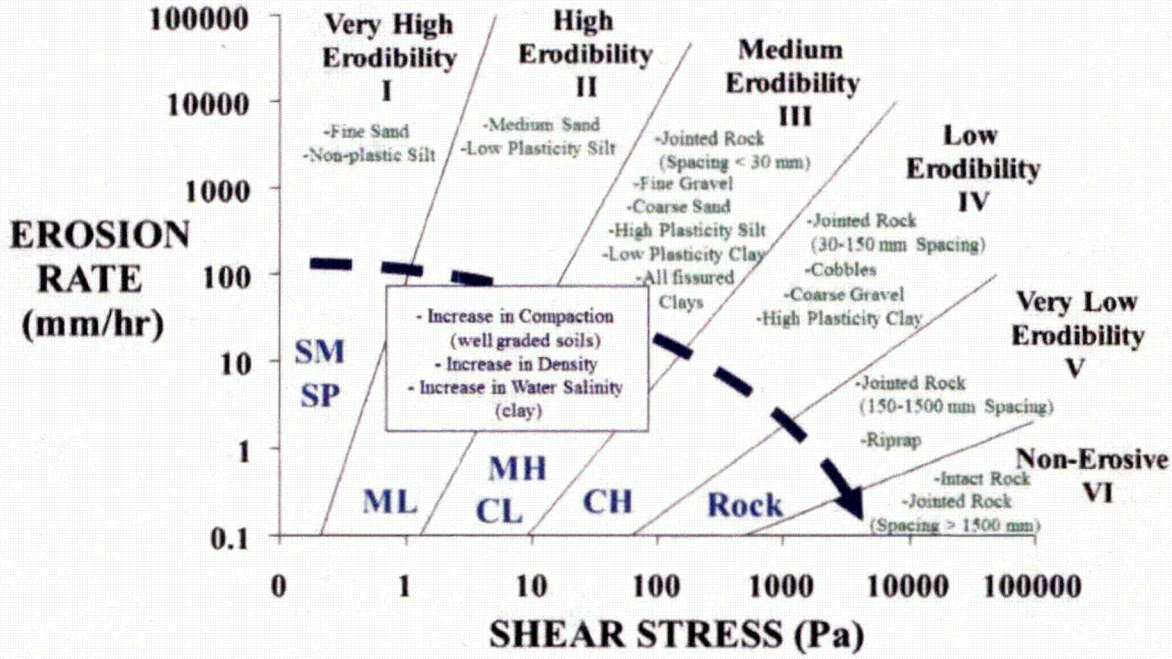

Fig. 34 – Proposed erosion categories for soils and rocks based on shear stress (Briaud, 2013).

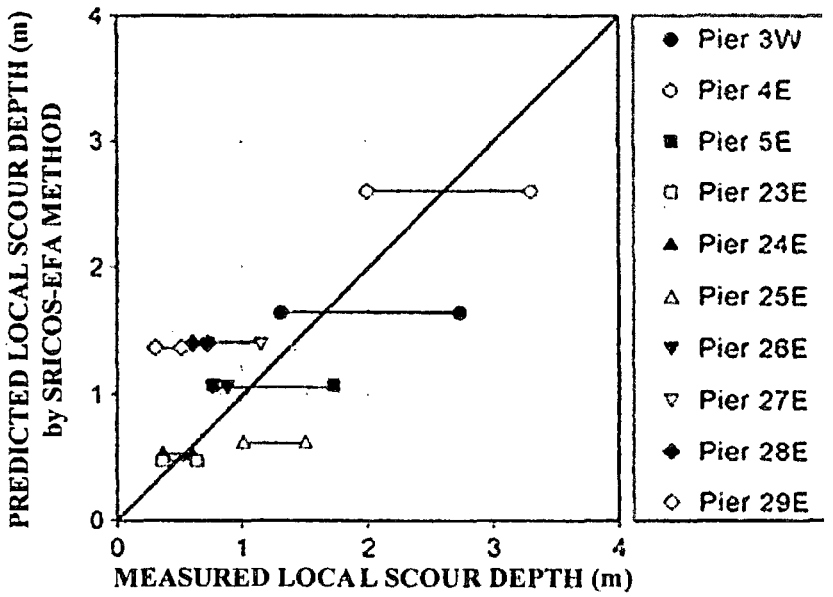

Fig.35 – Measured vs. predicted scour depth at Woodrow Wilson bridge (Briaud, 2008).

4. CHARACTERIZE JOCASSE DAM.

In order to evaluate the erosion function of the Jocassee Dam, the following process was used.

a. A cross section of the dam was drawn (Fig. 36).
b. An erosion category was chosen for each material within the dam (Table 3); since the drawings specified that the D_{50} was the minimum allowed, this selection is conservative.
c. Three erosion levels were placed across the dam as shown on Fig. 36: level AA, BB, and CC.
d. For each level, a weighted average of the erosion category was determined according to the length of material exposed to the flow for that level.

$$EC = \frac{\sum_{i=1}^{n} LiECi}{\sum_{i=1}^{n} Li}$$

Where EC is the average erosion category, Li is the length of material i exposed to water, and ECi is the erosion category for material i.

e. Section AA gave an EC value of 3.93, section BB gave 4.08, and section CC gave 4.11.
f. Therefore, the overall average erosion category for Jocassee dam is clearly 4 or low erodibility.

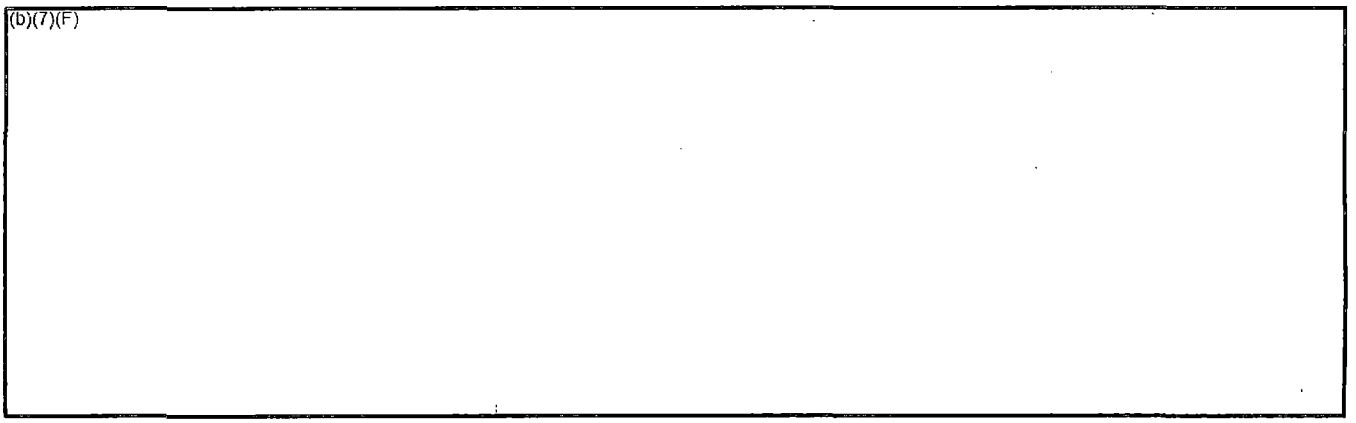

Fig. 36 – Cross section of Jocassee Dam.

Table 3 – Description of soil and rock materials in Jocassee Dam and erosion category

Material (Fig. 36)	Description	Estimated critical velocity (m/s)	Erosion Category
Rock fill	(b)(7)(F)		
Impervious core			
Random fill			
Filters			

A similar set of calculations were performed for the Teton dam. Fig. 37 shows the Teton Dam cross section and the three levels selected for calculating the weighted average erosion category for the Teton Dam. Table 4 shows the dam materials and their erosion categories. These erosion categories were estimated based upon the material description in Seed and Duncan (1981). The calculations indicate that the weighted average of the erosion category according to the length of material exposed for that level are: Section AA gave an EC value of 2.5, section BB gave 2.63, and section CC gave 2.7. The average erosion category of Teton dam is therefore estimated to be 2.6 or medium to high erodibility (Fig. 38).

If the Teton Dam failure took 4 hours for an erosion category of 2.6 (medium to high erodibility), and considering that the erosion categories are based on a log scale, it is clear that a Jocassee Dam failure which has an erosion category of 4 (low erodibility) would take much longer.

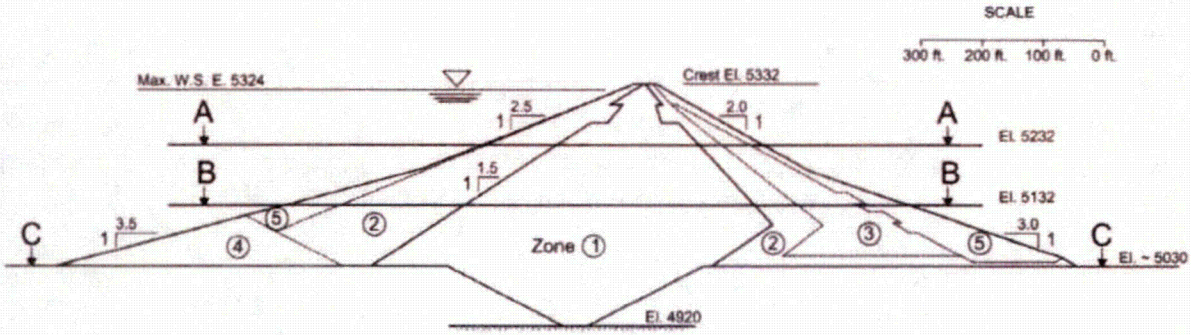

Fig. 37 – Cross section of Teton Dam.

Table 3 – Description of soil and rock materials in Teton Dam and erosion category

Material (Fig. 37)	Description	Estimated critical velocity (m/s)	Erosion Category
Zone 1 (Core)	Silt with some clay, sand, and gravel	0.2	2
Zone 2	Selected sand, gravel and cobbles	1	3.1
Zone 3	Miscellaneous fill	0.5?	2.5
Zone 4	Selected silt, sand, gravel, and cobbles	0.8	3
Zone 5	Rockfill	2	4

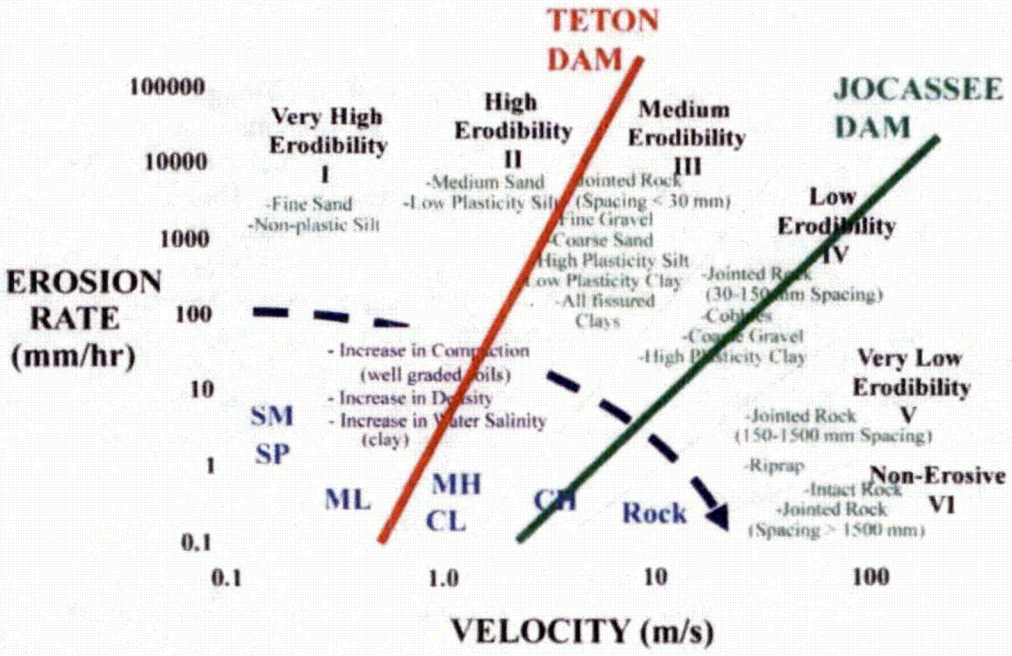

Fig. 38 – Overall erosion category for Jocassee and Teton Dams (velocity based).

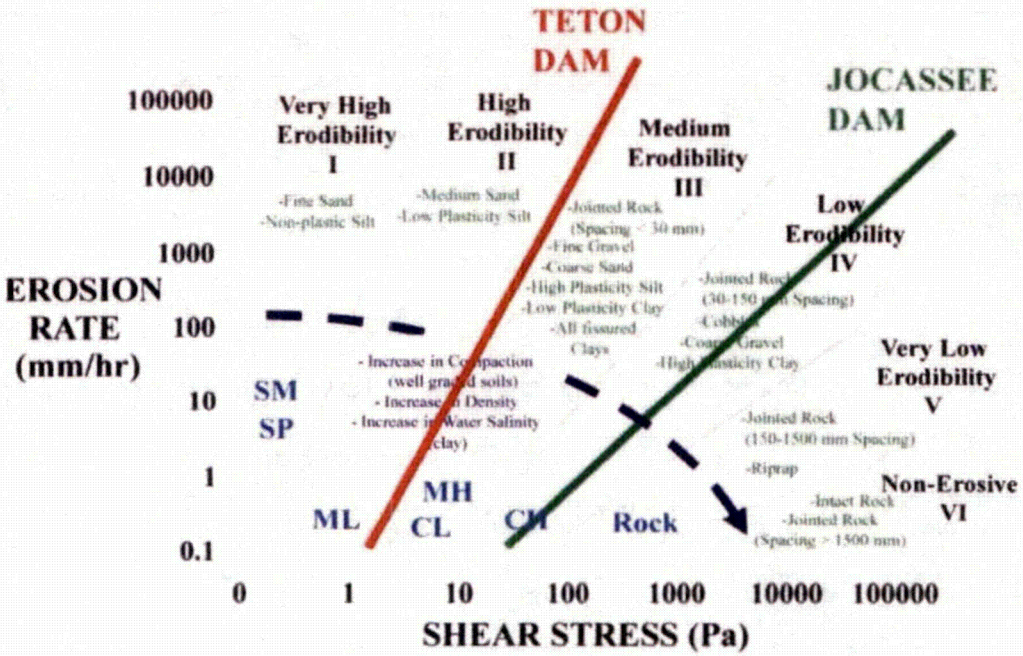

Fig. 39 – Overall erosion category for Jocassee and Teton Dams (shear stress based).

5. COMMENT ON THE CHOICE OF ERODIBILITY OF XU AND ZHANG and HOW THE THREE ERODIBILITY CLASSIFICATIONS, USED BY XU & ZHANG, COMPARE TO YOUR SIX CLASSIFICATIONS?.

The work done by Xu and Zhang is very useful as it is based on a database of observations. Since the authors point out that erodibility is the single most important factor, it is critical to understand how they defined the erodibility of the materials making up the dam. The three erodibility classifications used by Xu & Zhang (2009) refer to low, medium, and high erodibility. From their publication, it appears that these three category designations correspond to the low (category 4), medium (category 3), and high (category 2) categories proposed by Briaud (2008). This was verified with the primary author (Yao Xu) during his visit to Denver, CO in November 2013. The categorization reflects the fact that the types of materials typically used for the construction of earth dams fall into the Briaud erosion categories 2, 3, and 4 with some category 5 materials for rockfill dams. Indeed fine sands and non-plastic silts (Briaud category 1) and jointed and intact rock (Briaud category 6) are not used in earthdam engineering.

6. CONCLUSIONS

- The erosion function characterizes the behavior of the soil at the element level so it is broadly applicable to many erosion situations including erosion of materials used in embankment dam construction. The erosion function is the curve which links the erosion rate to the water velocity or the hydraulic shear stress at the soil-water interface; it is to erosion studies what the stress strain curve is to deformation problems. It is a constitutive

equation which applies to the erosion mechanics of all materials including the materials used in embankment dams and can be applied in numerical methods as easily as in simple hand calculations.

- The erosion function starts at the critical velocity or critical shear stress for coarse grained soils and rock fill. The rockfill values are based on an NCHRP project which identified the USACE equation as being the best among others. This equation is Eq. 8 in the Appendix which gives the particle size corresponding to a given critical velocity. So the basis of the critical velocity charts for large rock fill blocks has this solid background and therefore applies to embankment dam materials.

- The erodibility of the Jocassee Dam materials was evaluated; see Figures 38 & 39, and the Jocassee cross-section materials are clearly and conservatively established to be "low erodibility" materials.

- The Xu and Zhang regression equations do show and consider that erodibility is the most significant factor in the development of embankment breach parameters. Thus, it is most important, in evaluating their equations, to establish how Xu and Zhang have assigned the "low, medium or high" erodibility to the various dams and data to establish their regression equations. Use of the three classifications is appropriate since they do represent the characteristics of the most commonly used materials for construction of embankment dams.

7. OPTIONS FOR FURTHER STUDY

The following options for further study can be pursued to refine the specific erodibility characteristics of the dam materials, and the time necessary to erode Jocassee dam.

a. **Numerical simulations**. The program CHEN 4D can be used to simulate the breach in 4 dimensions (x, y, z, t) together with the erosion functions of the various materials. This will give a much more precise time to total erosion than HEC-RAS which is a one dimensional solution of the problem. Professor Chen and I can team up for simulating the water flow and the soil erosion. Such dam breach simulations are possible as shown on Fig. 40 below. The results would be a movie with timed frames of the dam erosion as a function of time with associated erosion versus time curves. Note that two distinct modes of failure need to be simulated: piping erosion followed by breach as the roof of the dam embankment collapses (e.g.: Teton) and overtopping erosion and breach erosion starting at the bottom of the dam downstream face where the velocity is maximum (e.g.: Hell Hole). The first failure mode will be referred to as "piping" while the second one will be referred to as "overtopping".
b. **Calibration based on previous failures (e.g.: Teton and Hell Hole)**. The numerical simulation must first be calibrated against the failure of known dams. CHEN 4D should

be used to duplicate the erosion process vs. time for the piping failures (e.g.: Teton Dam) and for the overtopping failures (e.g.: Hell Hole).

c. **Erosion function for selected dams**. In order to directly measure the erodibility of the dam material, tube samples of the dam can be collected (e.g. Teton and Hell Hole) and run in the EFA. This would require visits to the dam sites. Samples of the finer materials can be taken by hand driving short thin wall steel tubes in the remaining part of the Teton Dam. Rockfill from Hell Hole could also be collected and tested as explained next.

d. **Erosion function for Jocassee rockfill**. In order to directly measure the critical velocity of the Jocassee Dam rockfill, flume tests can be carried out with rockfill material with a D50 matching the one from the dam. This can be done in a large laboratory flume at Texas A&M University where such a flume exists. Rockfill from the Hell Hole reconstruction site could also be tested in that fashion.

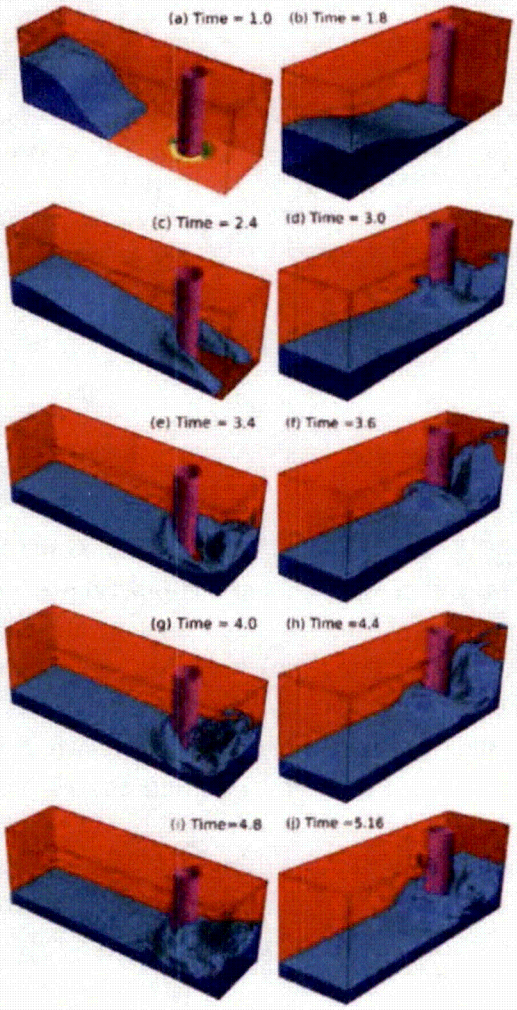

Fig. 40 – Example of advanced numerical modeling of interaction between water flow and a structure (Zhao, Chen, 2013).

REFERENCES

1. Briaud J.-L., 2008, "Case Histories in Soil and Rock Erosion: Woodrow Wilson Bridge, Brazos River Meander, Normandy Cliffs, and New Orleans Levees", The 9th Ralph B. Peck Lecture, *Journal of Geotechnical and Geoenvironmental Engineering*, Vol 134, No.10, ASCE, Reston Virginia, USA.
2. Briaud J.-L., 2013, "*Geotechnical Engineering: Unsaturated and Saturated Soils*", John Wiley and Sons Publisher, 1000 pages.
3. Lagasse P.F., Clopper P.E., Zevenbergen L.W., Ruff J.F., 2006, "Riprap Design Criteria, Recommended Specifications, and Quality Control", *NCHRP report 568*, National Cooperative Highway Research Program of the Transportation Research Board, Washington DC, USA, pp226.
4. Seed, H.B., and Duncan, J.M., (1981), "The Teton Dam Failure – A Retrospective Review", *Proceedings of 10th International Conference on Soil Mechanics and Foundation Engineering*, Stockholm, Vol. 4, pp. 219-238.
5. Xu Y., Zhang L.M., 2009, "Breaching Parameters for Earth and Rockfill Dams", *Journal of Geotechnical and Geoenvironmental Engineering*, Vol. 135, No. 12, ASCE, Reston Virginia, USA.
6. Zhao Y., Chen H.-C., (2013), "CFD Simulation of Violent Free Surface Flows by a Coupled Level-set and Volume-of-Fluid Method", *Proceedings of the 2013 ISOPE Conference*, Anchorage, Alaska, USA.

APPENDIX

BACKGROUND ON EROSION

a. The erosion phenomenon

An erosion problem always has three components: the soil or rock, the water, and the geometry of the obstacle that the water is encountering. The resistance of the soil or rock is characterized by its erodibility, the water action is quantified by its velocity, and the geometry of the obstacle by its dimensions. Fig. 3 shows a free body diagram of a soil particle, a cluster of particles, or a rock block at the bottom of a lake. The water imposes a normal stress (hydrostatic pressure) around the soil particle or rock block. The normal stress is slightly higher at the bottom than at the top since the bottom is slightly deeper in the water column. This normal stress difference creates the buoyancy force which reduces the weight of the soil particle or rock block. Fig. 4 shows the same particle, cluster of particles, or rock block at the bottom of a flowing river. Three things happen when the water starts flowing. First, a drag force and associated shear stresses develop at the interface between the soil particle or rock block and the water flowing over it. Second, the normal stress on top of the soil particle or rock block decreases because of the water flow. Indeed, as the velocity increases around the particle or the obstacle, the pressure drops to maintain conservation of energy according to Bernoulli's principle. This phenomenon is similar to the air flow on top of an airplane wing where the pressure is lower than below the wing thereby developing the uplift force necessary for the plane to fly. Third the normal stresses and shear stresses applied at the boundaries are fluctuating with time because of the turbulence in the water. These fluctuations find their roots in the appearance and disappearance of eddies, vortices, ejections, and sweeps in the flowing water; they can contribute significantly to the erosion process especially at higher velocities. In some cases they are the main reason for erosion. The contribution of turbulence fluctuations to the erosion process has been studied by several authors as reported by Briaud 2013. The combination of the mean value and the fluctuations around the mean of the drag force and uplift force can become large enough to pluck and drag the soil particle, soil particle cluster, or rock block away and generate erosion.

Note that in the case of unsaturated soils or saturated soils with water tension, the mechanical inter-particle compressive forces (f_{ci} in Fig. 3 and 4) can be significantly larger than in the case where the water is in compression. This apparent cohesion may increase the resistance to erosion at least until the flow and presence of water destroys the water tension.

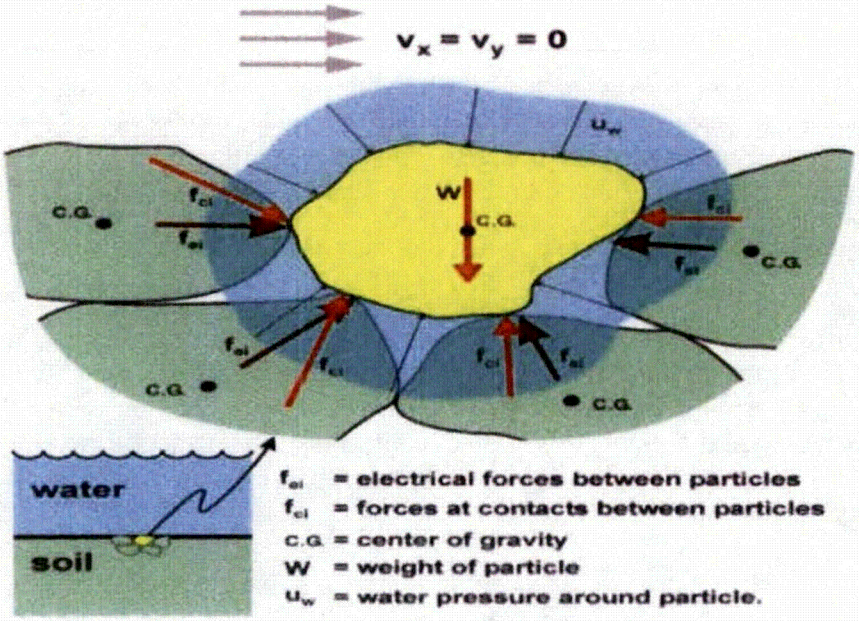

Fig. 3 – Free body diagram of soil particle or rock block for no flow (Briaud, 2013)

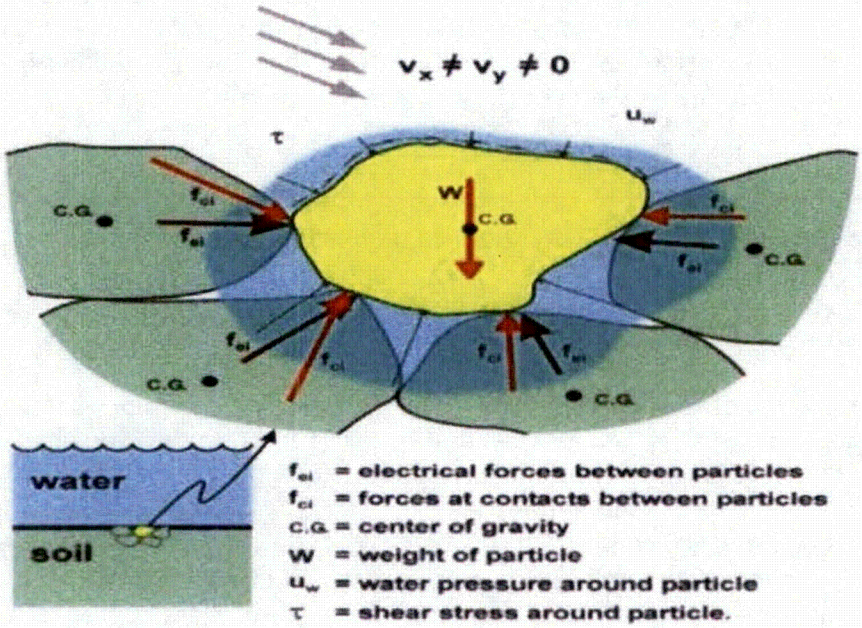

Fig. 4 – Free body diagram of soil particle or rock block when water flows (Briaud, 2013)

b. Erosion models

The erodibility of a soil or rock can be defined as the relationship between the erosion rate $\dot{z}$ and the velocity of the water v near the soil-water interface. This definition is not very satisfactory because the velocity varies in direction and intensity in the flow field. In fact, strictly speaking, the water velocity is zero at the soil/rock-water interface. A more satisfactory definition is the relationship between the erosion rate $\dot{z}$ and the shear stress τ at the soil/rock-water interface.

$$\dot{z} = f(\tau) \tag{1}$$

The erosion function described by Eq. 1 represents the constitutive law of the soil or rock for erosion problems much like a stress strain curve would represent the constitutive law of the soil or rock for a settlement problem. While a shear stress based definition is an improved definition over a velocity based definition, it is still not completely satisfactory as the shear stress is not the only stress which contributes to the erosion rate. A more complete description of the erosion function is given by Eq. 2:

$$\frac{\dot{z}}{u} = \alpha\left(\frac{\tau-\tau_c}{\rho u^2}\right)^m + \beta\left(\frac{\Delta\tau}{\rho u^2}\right)^n + \gamma\left(\frac{\Delta\sigma}{\rho u^2}\right)^p \tag{2}$$

Where $\dot{z}$ is the erosion rate (m/s), u the water velocity (m/s), τ the hydraulic shear stress, τ_c the threshold or critical shear stress below which no erosion occurs, ρ the mass density of water (kg/m^3), $\Delta\tau$ the turbulent fluctuation of the hydraulic shear stress, and $\Delta\sigma$ the turbulent fluctuation of the net uplift normal stress. All other quantities are parameters characterizing the soil being eroded. While this model is quite thorough, it is rather impractical at this time to determine the 6 parameters needed in Eq. 2 on a site specific and routine basis. Today Eq. 3 which corresponds to the first term of Eq. 2 is widely accepted.

$$\frac{\dot{z}}{u} = \alpha\left(\frac{\tau-\tau_c}{\rho u^2}\right)^m \tag{3}$$

As additional fundamental work is performed in erosion engineering, it is likely that Eq. 3 will evolve towards Eq. 2.

c. Measuring the erosion function

An apparatus was developed in the early 1990s to measure the erosion function. It is called the Erosion Function Apparatus or EFA. The principle is to go to the site where erosion is being investigated, collect samples within the depth of concern, bring them back to the laboratory and test them in the EFA. A 75 mm outside diameter sampling tube containing the sample is placed through the bottom of the conduit where water flows at a constant velocity (Fig. 5). The soil or rock is pushed out of the sampling tube only as fast as it is eroded by the water flowing over it. For each velocity, an erosion rate is measured and a shear stress is calculated using Moody's 1944 chart (Briaud 2013). Point by point the erosion function is obtained.

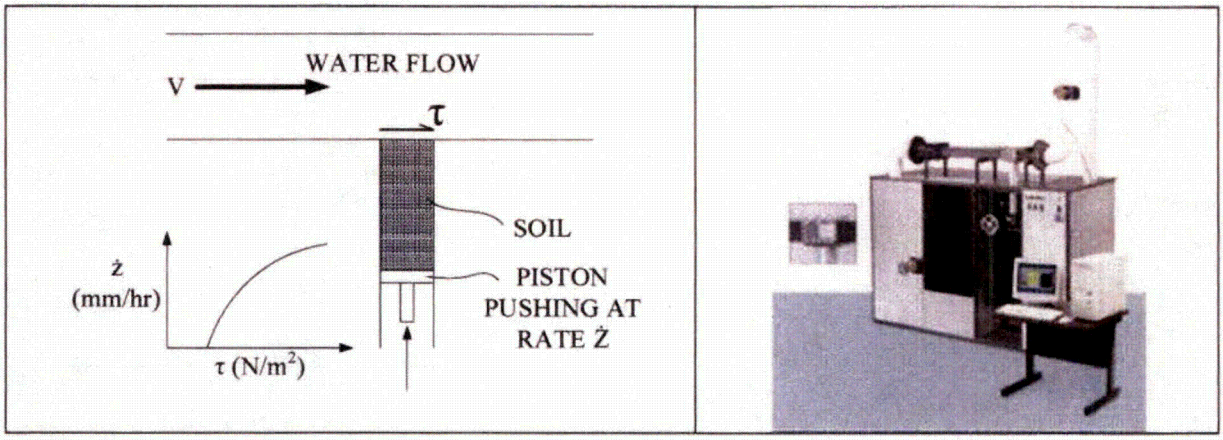

Fig. 5 – Erosion Function Apparatus to measure erodibility.

Examples of erosion functions are shown in Fig. 6 for a fine sand and Fig. 7 for a low plasticity clay. Note that for the same average velocity of 1 m/s in the EFA test conduit, the rate of erosion for the sand is about 1000 times faster than for the clay. This indicates that the rate of erosion can be very different for different soils. Other devices have been developed to evaluate how resistant earth materials are to water flow. These include the rotating cylinder to measure the erosion properties of stiff soils, the jet test to evaluate the erodibility of soils, and the hole erosion test to measure the erosion properties of stiff soils. More recently a simple and inexpensive tool for field use has been developed called the pocket erodometer. It can be performed at the site on the end of a sample and gives a first indication of the erodibility of the soil within minutes after sampling.

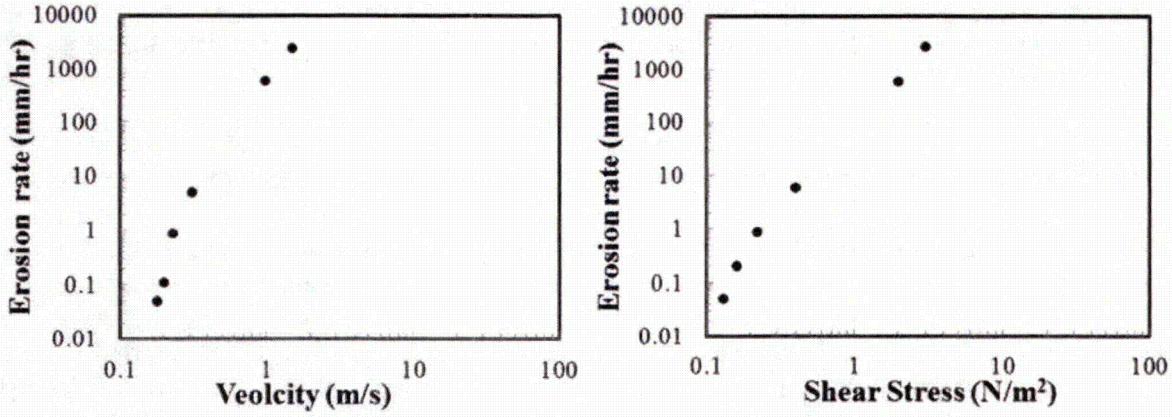

Fig. 6 – Erosion function for a fine sand as measured in the EFA.

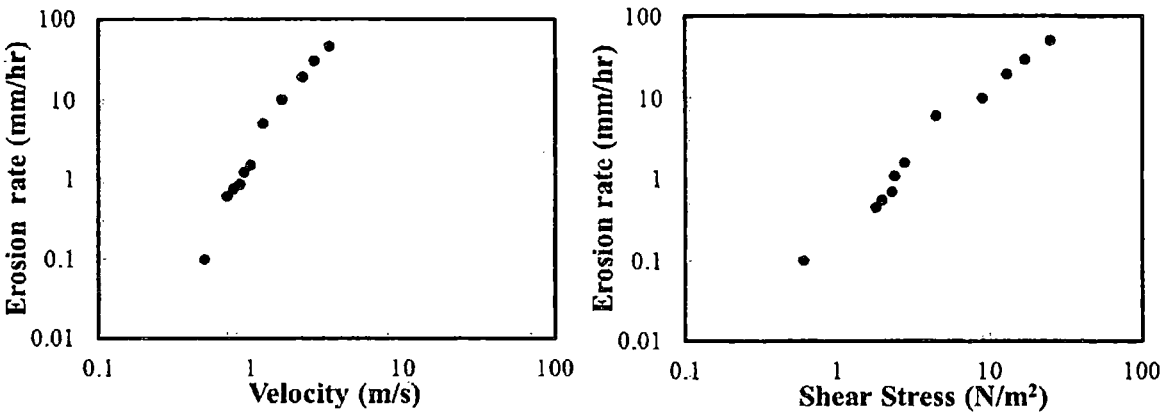

Fig. 7 – Erosion function for a low plasticity clay as measured in the EFA.

d. Soil erosion categories

Categories are used in many fields of engineering: soil classification categories, hurricane strength categories, earthquake magnitude categories. Such categories have the advantage of quoting one number to represent a more complex condition. Erosion categories are proposed (Fig. 8) in order to bring erodibility down in complexity from an erosion rate vs. shear stress function to a category number. Such a classification system can be presented in terms of velocity (Fig. 8) or shear stress (Fig. 9). The categories proposed are based on 15 years of erosion testing experience. In order to classify a soil or rock, the erosion function is plotted on the category chart and the erodibility category number for the material tested is the number for the zone in which the erosion function fits. Note that, as discussed later, using the water velocity is less representative and leads to more uncertainties than using the shear stress; indeed the velocity and the shear stress are not linked by a constant. The velocity chart has the advantage that it is easier to gage a problem in terms of velocity.

One of the most important soil parameters in erosion studies is the threshold of erosion. Below this threshold, erosion does not occur and above this threshold, erosion occurs. In terms of shear stress, this threshold is the critical shear stress τ_c and in terms of velocity, it is the critical velocity v_c. Fig. 11 shows a plot of the critical velocity as a function of the mean grain size while Fig. 12 shows the same plot for the critical shear stress. The data come from measurements in the EFA as well as measurements published in the literature. As can be seen on Fig. 11 and 12, the relationship between the critical value and the grain size has a V shape indicating that the most erodible soils are fine sands with a mean grain size in the range of 0.1 to 0.5 mm. This V shape also points out that particle size controls the erosion threshold of coarse grained soils while particle size does not correlate with the erosion threshold of fine grained soils. Shields in 1936 proposed a curve for coarse grain soils in his doctoral work which is included in Fig. 11 and 12. Shields recommendations do not include fine grain soils. Note also that Hjulstrom in 1935 proposed such a curve for both coarse grain soils and fine grain soils but his recommendations for fine grain soils turned out to be too simple.

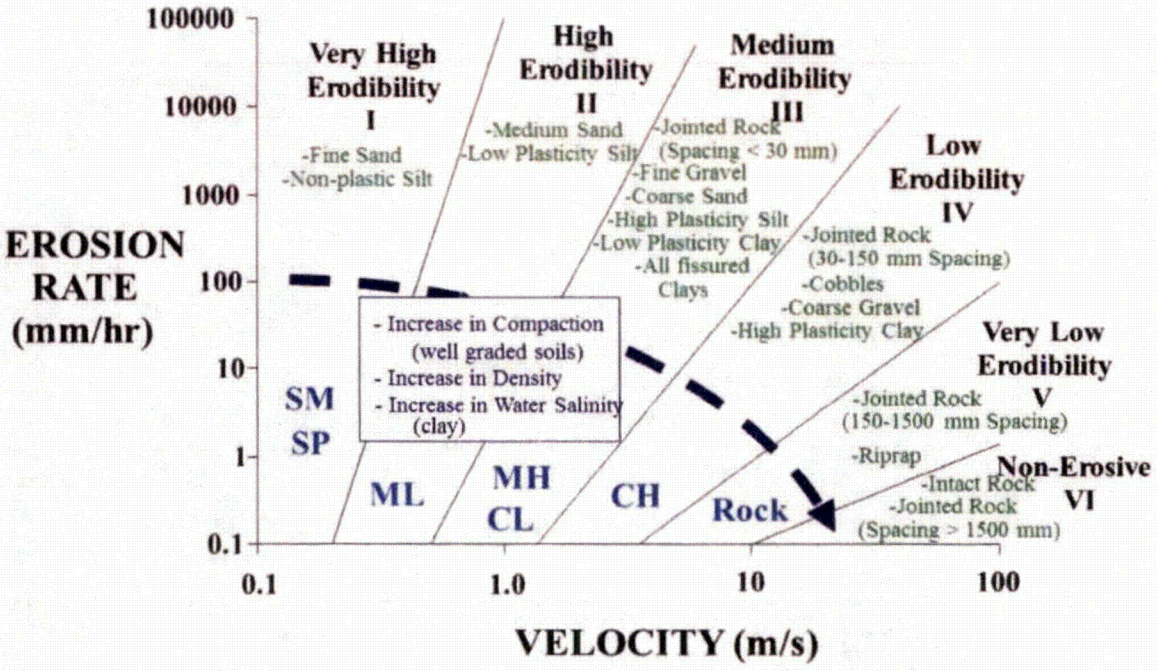

Fig. 8 – Proposed erosion categories for soils and rocks based on velocity.

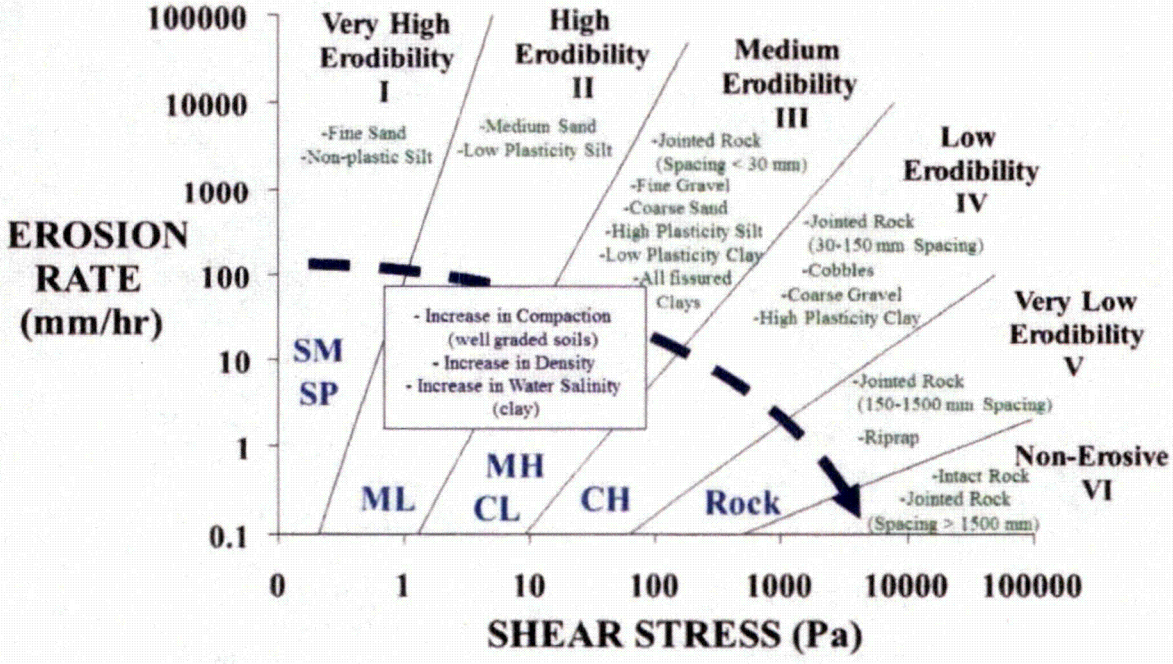

Fig. 9 – Proposed erosion categories for soils and rocks based on shear stress.

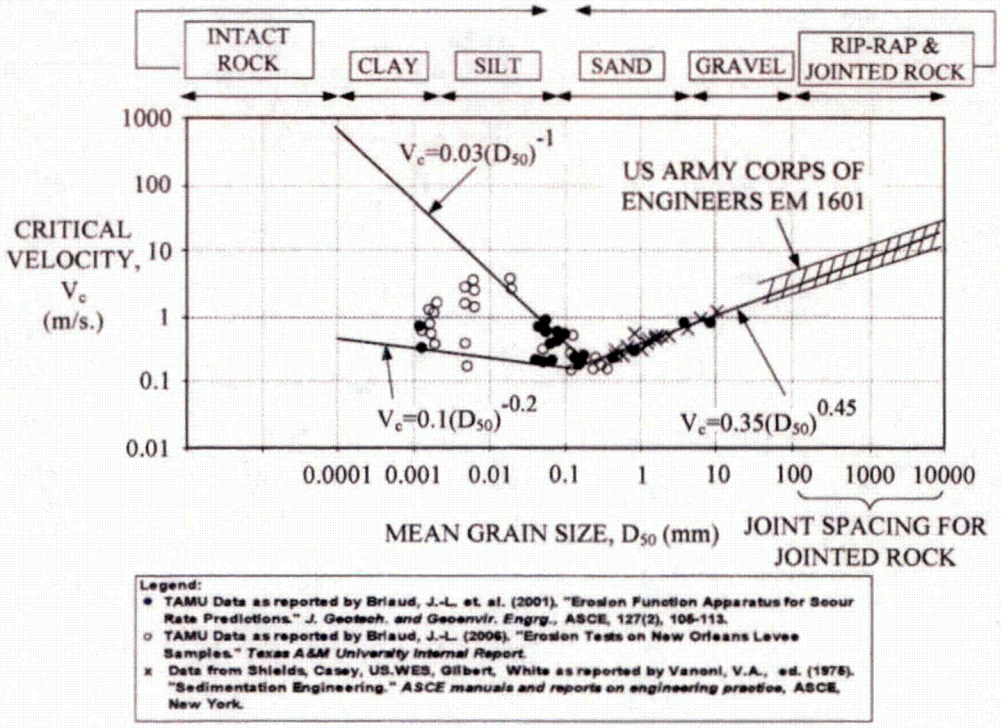

Fig. 11 – Critical velocity as a function of mean grain size.

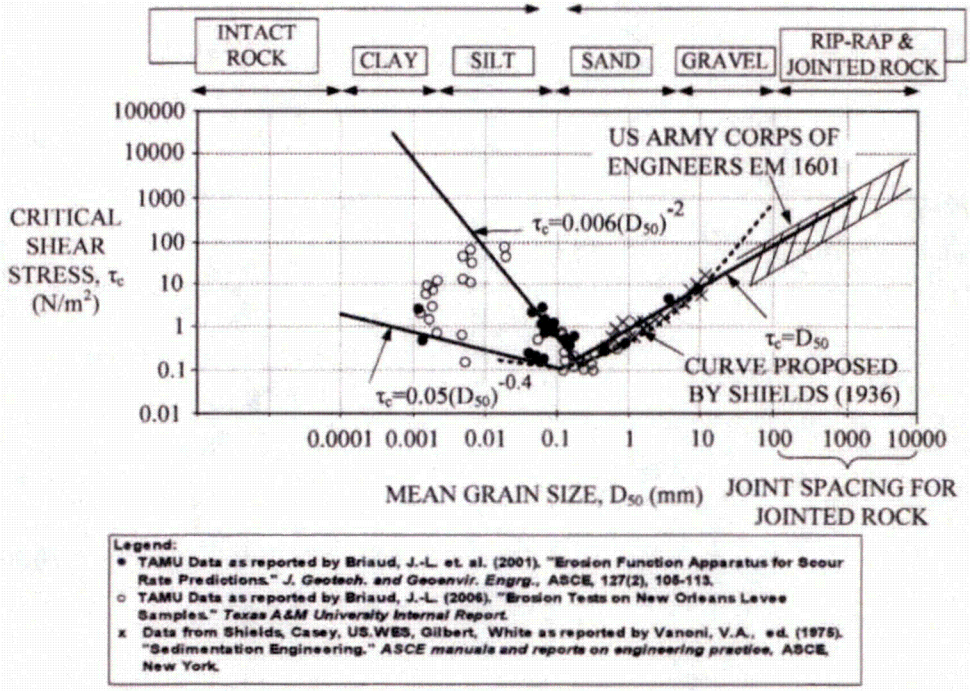

Fig. 12 – Critical shear stress as a function of mean grain size

The erodibility of soils varies significantly from one soil to the next; therefore erodibility depends on the soil properties. It depends also on the properties of the water flowing over the soil. For some soils, particularly dispersive soils, the higher the salt concentration in the water, the more erosion resistant a clay is. The properties influencing erodibility are numerous; some of them are listed in Table 1. It appears reasonable to expect that a relationship would exist between common soil properties and erodibility. But erodibility is a function not a number therefore correlations can only be made with elements of that function such as the critical shear stress or the initial slope of the erosion function. Such correlations have been attempted and failed with very low coefficients of correlation. On one hand, there should be a correlation, on the other hand, the correlation is complex and requires multiple parameters all involved in the resistance of the soil to erosion. All in all it is preferable to measure the erosion function directly in an apparatus such as the EFA.

Table 1 - Soil and water properties influencing erodibility

Soil water content Soil unit weight Soil plasticity index Soil undrained shear str. Soil void ratio Soil swell Soil mean grain size Soil percent passing #200	Soil clay minerals Soil dispersion ratio Soil cation exchange cap Soil sodium absorption rat Soil pH Soil temperature Water temperature Water salinity Water pH

e. Rock erosion

If soil erosion is not very well known, rock erosion is even less known and the engineer must exercise a great deal of engineering judgment when it comes to rock erosion. Nevertheless many engineers and researchers have contributed to the advancement of knowledge in this relatively new field.

Rock erodes through two main processes: rock substance erosion and rock mass erosion. Rock substance erosion refers to the erosion of the rock material itself while rock mass erosion refers to the removal of rock blocks from the jointed rock mass. Rock substance erosion includes three sub-mechanisms: erosion due to the hydraulic shear stress created by the water at the rock-water interface, erosion due to abrasion caused by sediments rubbing against the rock during the flow, and impact of air bubbles that pit the rock surface due to cavitation at very high velocities. Rock mass erosion includes two sub mechanisms: erosion due to slaking, and erosion due to block removal between joints. Slaking can occur when a rock, such as a high plasticity shale in an ephemeral stream, dries out and cracks during summer months; these small blocks are then removed by the next big flood. Block removal can occur if, during high turbulence events, the difference in pressure between the top and the bottom of a rock block becomes large enough to overcome the weight and side friction on the block. Brittle fracture and fatigue failure can contribute breaking the rock into smaller pieces which then are carried away by the water. Note that most of the time, rock mass erosion will be the dominant process in rock erosion with only

rare occurrences of rock substance erosion.

The critical velocity associated with rock erosion is much higher than the critical velocity associated with soil erosion in general. At the same time, the erosion rate for a given velocity is much lower for rock erosion than for soil erosion in general. Table 2 is an attempt at quantifying the critical velocity and the erosion rate of jointed rocks where the rock mass erosion may control the process. This table is preliminary in nature and should be calibrated against field behavior. The critical velocities quoted in Table 2 refer to the velocity necessary to move a particle with a size equal to the spacing between joints; as such they are likely lower bounds since they ignore any beneficial effect from the shear strength of the joints. Note that the orientation of the bedding of the rock mass is important as shown on Fig. 13. Engineering judgment must be used to increase or decrease the critical velocity when the bedding is favorable or unfavorable to the erosion resistance. In addition, it is highly recommended in all cases to measure the erosion function of the rock substance on core samples obtained from the site.

Table 2 – Rock mass erosion; this table is preliminary in nature and should be calibrated against field behavior.

Joint Spacing (mm)	Critical Velocity (m/s)	Erosion Category	Orientation of joints
<30	0.5-1.35	Category III Medium	Not applicable
30-150	1.35-3.5	Category IV Low	Evaluation needed
150 – 1500	3.5-10	Category V Very Low	Evaluation needed
>1500	>10	Category VI Non-Erosive	Not applicable

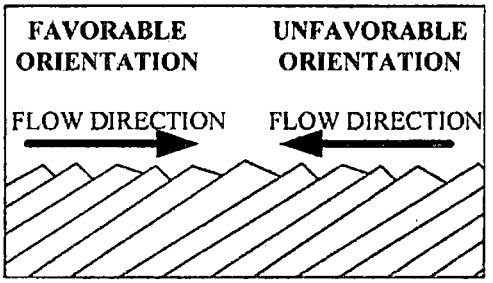

Fig. 13 – Effect of joint orientation on erosion resistance.

Examples of rock erosion rates can be collected from geology. For example, the Niagara Falls started about 12000 years ago on the shores of Lake Erie and have eroded back primarily through undercutting of the falls rock face to half way between Lake Erie and Lake Ontario. This represents 11 km and an average rate of 0.1 mm/hr, through sandstones, shales and limestones sedimentary rocks. Another example is the Grand Canyon where the Colorado River has

generated 1600 m of vertical erosion through complex rock layers over an estimated 10 million years for an average rate of 0.00002 mm/hr as the Colorado Plateau was up-heaving. These rates appear negligible at first glance yet neglecting them would be neglecting the Grand Canyon or the retreat of Niagara Falls. The lesson is clear: it is not only the rate of erosion which is important but also the length of time over which that rate is being applied.

f. Water velocity

Fig. 14 shows the profile of water velocity as a function of flow depth. The water velocity is largest near the top of the water column and zero at the bottom. This has been measured repeatedly in hydraulic engineering. By comparison, the shear stress is highest at the bottom and near zero at the top of the water column. The relationship between the shear stress and the velocity can be established as follows. Because water is a Newtonian fluid, there is a linear relationship between the shear stress τ and the shear strain rate $d\gamma/dt$.

$$\tau = \mu\left(\frac{d\gamma}{dt}\right) \tag{4}$$

Where μ is the dynamic viscosity of the water (10^{-3} Pa.s at 20°C). This viscosity is different from the kinematic viscosity ν of water (10^{-6} m^2/s at 20°C) defined as $\nu = \mu/\rho$ where ρ is the mass density of water (1000 kg/m^3). Since, as shown on Fig. 14, γ is du/dz, then $d\gamma/dt$ is dv/dz where v and u are the water velocity called shear velocity and horizontal displacement in the horizontal direction at a depth z respectively. Then the shear stress τ at depth z is given by:

$$\tau = \mu\left(\frac{dv}{dz}\right) \tag{5}$$

Therefore the shear stress is proportional to the gradient of the shear velocity profile with flow depth and the shear stress at the soil/rock-water interface is the slope of the profile at the interface. If the slope of the water velocity profile at the water-soil or water-rock interface (interface shear stress) is kept constant and if the water depth is varied, then it can be shown that the mean depth velocity will vary as well. This implies that there is no constant ratio between mean depth velocity and interface shear stress. This is one reason why velocity alone is not as good a predictor of erosion as shear stress. As such, any erosion design tool presented in terms of velocity should be used with caution. On the other hand, velocity is much easier for the engineer to gage than shear stress, and this is why both velocity and shear stress are used in practice.

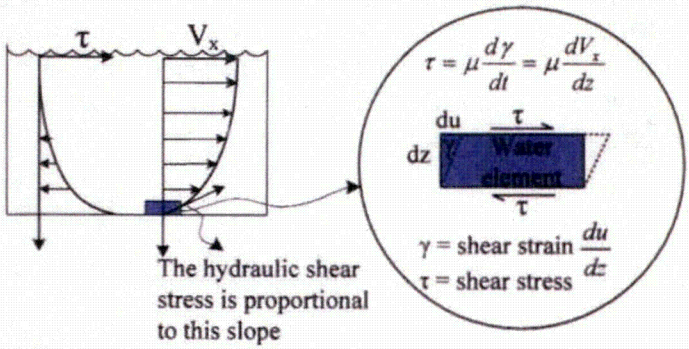

Fig. 14 – Velocity and shear stress profile versus flow depth

The magnitude of these shear stresses is very small and measured in N/m^2. They are much smaller than the shear stresses that the geotechnical engineer is used to calculate in foundation engineering for example which are in the range of kN/m^2. Fig. 15 gives examples of the range of shear stresses associated with various fields of engineering. If the undrained shear strength is a reasonable measure of the strength of a clay for foundation engineering design, the critical shear stress is the "shear strength" of the same clay for erosion studies. The difference in magnitude of the stresses and the strengths for foundation engineering and erosion is that in erosion studies one looks at the resistance of one particle, or a small cluster of particles, while in foundation engineering one looks at the resistance of the soil mass at the foundation scale.

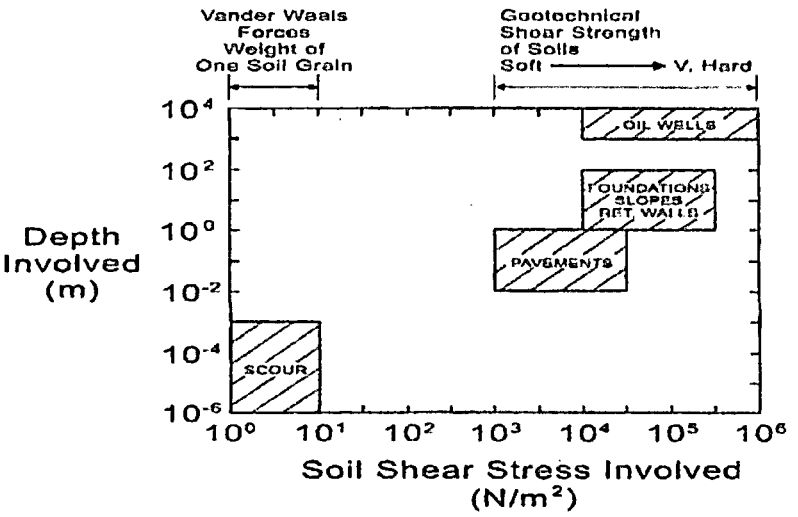

Fig. 15 – Range of shear stresses encountered in different engineering fields.

The water does not flow at a constant velocity in a river and the velocity history over a period of time is a necessary input to many erosion problems. This velocity history or hydrograph is not usually readily available. Often, the discharge (m^3/s) hydrograph is available and needs to be transformed into a velocity (m/s) hydrograph and a water depth (m) hydrograph. This is commonly done by using software such as HEC-RAS. An example of the results of this transformation is shown in Fig. 16. HEC-RAS solves the one-dimensional energy equation for gradually varied flow in natural or constructed channels and adds the one-dimensional momentum equation around hydraulic structures such as bridges, culverts, and weirs where the energy equation is no longer applicable.

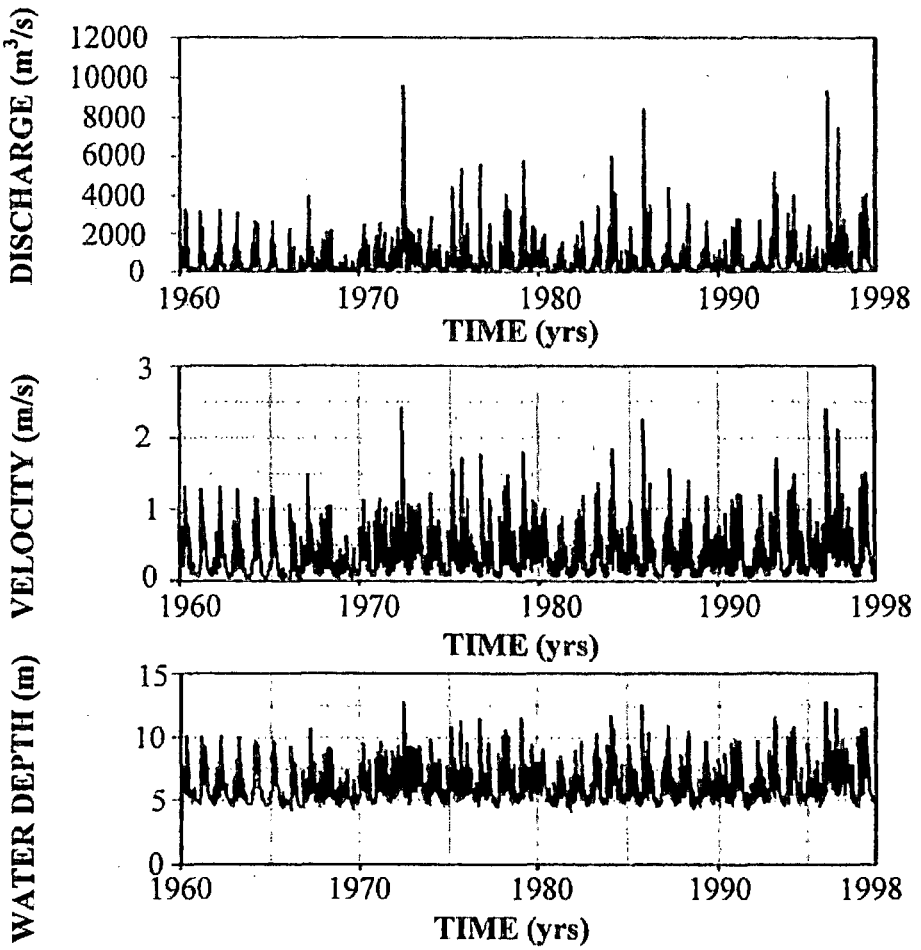

Fig. 16 – Discharge, velocity, and water depth hydrographs

The hydrograph can be used to obtain the 100 year flood or the 500 year flood. One simple graphical method consists of obtaining the yearly maximum flows from the hydrograph, ranking them in descending order of intensity, calculating for each flow the probability of exceedance as the rank divided by the total number of observations + 1, then plotting the flow versus the probability of exceedance on a semi-log paper such as the one of Fig. 17. Once the data is plotted, a linear regression is performed over say the first 20 to 30 years of data and extrapolated to the 0.01 probability of exceedance for the 100 year flood and to the 0.002 probability of exceedance for the 500 year flood. Indeed the return period is the inverse of the probability of exceedance. There are other and more refined ways of obtaining these design floods but this simple graphical method helps understand the process and the meaning of the 100 year flood: a flood which has a 1% chance of being exceeded in any one year. Fig. 17 shows the result of an analysis for the hydrograph at the Woodrow Wilson bridge. As can be seen on that figure, the 100 year flood has a discharge of 12,600 m^3/s and the 500 year flood has a value of 16,600 m^3/s.

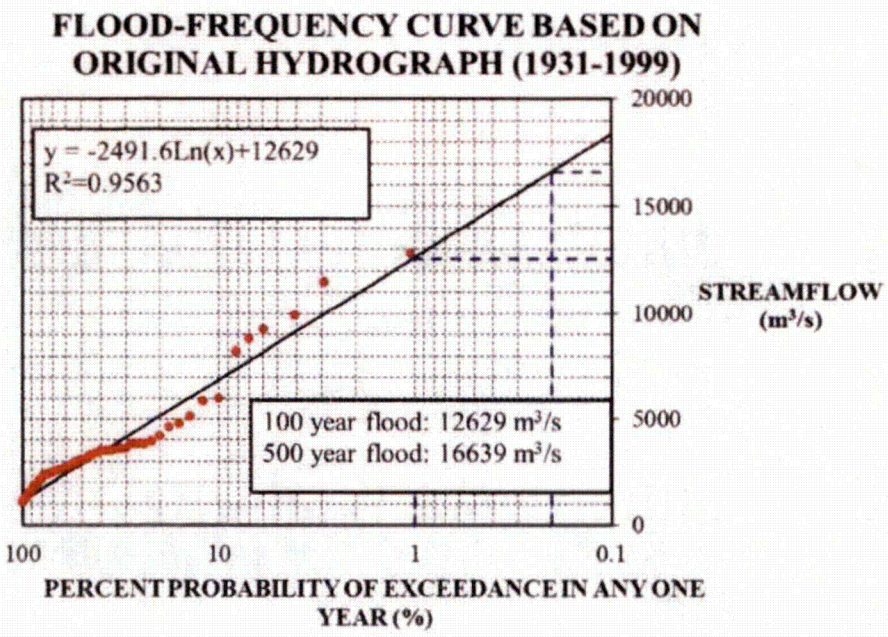

Fig. 17 – Flood frequency curve obtained from measured discharge hydrograph.

The probability of exceedance R of the design flood with a given return period T_r depends on the design life L_t of a structure.

$$R = 1 - (1 - 1/T_r)^{Lt} \quad (6)$$

If the design life of the bridge is 75 years, the probability that the flood with a return period of 100 year will be exceeded during the 75 year design life is 53% according to Eq. 6 and that probability is 14% for the 500 year flood. Only when one gets to the 10,000 year flood does the probability get to be lower than 1% (0.75%). Therefore looking at those numbers alone, it seems desirable to use the 10,000 year flood for design purposes. This flood is used in design in the Netherlands for regions of the country deemed critical. The USA uses the 100 and 500 year flood for design purposes in hydraulic engineering; this leads to probabilities of exceedance which are in the tens of percent. By comparison, the structural engineers use a probability of exceedance of about 0.1% for the design of bridge beams (LRFD target) and, judging from measured vs. predicted pile capacity data bases the geotechnical engineer uses a probability of exceedance of the order of a few percent. While these numbers can be debated, it is relatively clear that these different fields of civil engineering operate at vastly different probability of exceedance levels. Note that risk is different from the probability of exceedance as it also involves the value of the consequence. As such, the probability of exceedance target should vary with the consequence of the failure.

g. Geometry of the obstacle

The geometry of the obstacle encountered by the water influences the velocity of the water and the flow pattern including turbulence intensity. When the water approaches a pier in a river for example it has to go around the pier. In doing so it faces a restricted area and has to accelerate to maintain the flow rate. This acceleration results in a local mean depth velocity which can be 1.5

times higher than the approach mean depth velocity. If the approach velocity is lower than the critical velocity but the local velocity around the pier reaches a value higher than the critical velocity, then scour occurs around the pier. This scour type is called clear water scour that is to say scour created by water which does not carry soil particles. On the other hand, if the approach velocity and the velocity around the pier are both higher than critical, then the scour type is live bed scour. This means that the water is carrying a significant amount of soil particles. The scour depth reached under live bed scour conditions is typically less than the scour depth reached under clear water scour conditions. The reason is that during live bed scour some of the particles in suspension fall down on the river bed thereby limiting the depth of the scour hole around the pier.

Fig. 18 a and b show results of numerical simulations of erosion created by water flow in a contracted channel. The CHEN 4D computer program is the program used.

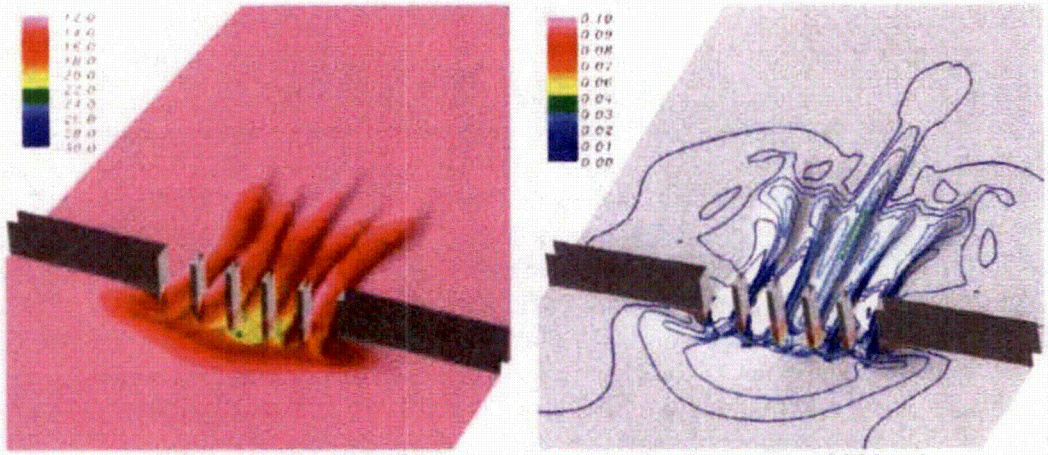

(a) Scour depth and shear stress distributions at t = 2000 min

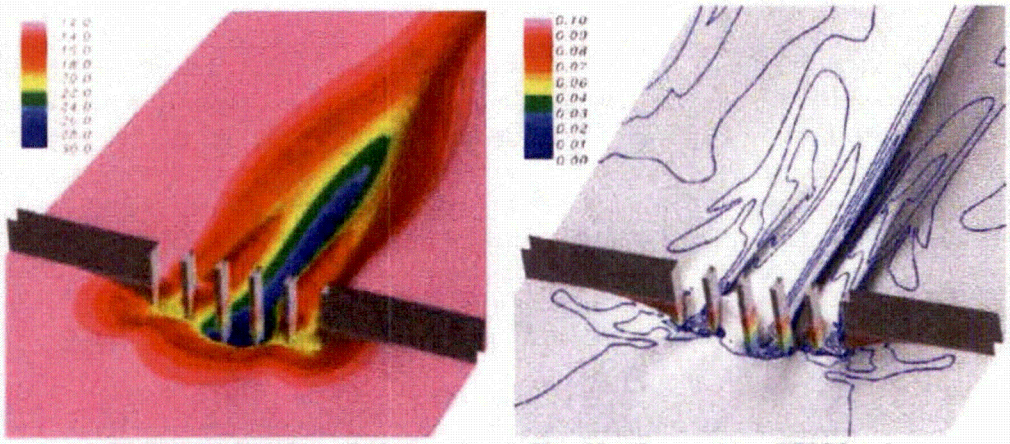

(b) Scour depth and shear stress distributions at t = 15000 min

Fig. 18 – Predicted scour hole shape and streambed shear stresses around abutments and piers: (a) t = 2000 min, (b) t = 15000 min (From Chen, 2002)

h. Background on levee overtopping

This background is given here because it is related to the topic of dam erosion. Levees are small homogeneous dams which only retain water from time to time as opposed to dams which are typically larger and retain water all the time. Nevertheless, this previous work carries some resemblance. Levees or dikes are small dams build along a river or an ocean to prevent the water from inundating the land in case of flood. The top of the levee is set at a predetermined height corresponding to the water level for a chosen design flood. This flood corresponds to a certain return period such as a 100 year flood. If the flood exceeds the design return period, water is likely to flow over the levee and generate potential erosion. One of the first observations is that if the water flows above a levee of height H, by the time the water reaches the bottom of the dry side of the levee it will have a velocity V which can be very high. One simple way to evaluate that velocity is to write conservation of energy.

$$mgH = \frac{1}{2}mV^2 \quad or \quad V = \sqrt{2gH} \tag{7}$$

For example if the levee is 5 m high, the velocity v will be approximately 10 m/s. Of course Eq. 7 does not take into account the energy lost in friction between the water and the levee surface but it does indicate that the velocity range is much higher than typically encountered in rivers where the water flows at most in the range of 3 to 4 m/s. Furthermore a distinction should be made between events such as hurricanes on one hand and river floods on the other. The major distinction is that hurricanes may overtop a levee for about 2 hours while river floods may overtop a levee for 2 days. A levee overtopping erosion chart has been developed for these two types of events and is presented in Fig. 19. It indicates which soil categories and associated erosion functions are likely to resist overtopping during a 2 hour and a 2 day overtopping. Recall that categories I to IV on the erosion chart are soils and categories V and VI are rocks. As can be seen, only the most erosion resistant soils can resists 2 hrs of overtopping without protection (Category IV) and no soil can sustain 2 days of overtopping without being totally eroded away. Armoring or vegetation satisfying strict criterions need to be used to ensure that overtopping can be sustained for longer than 2 hrs.

Vegetation can help significantly to retard erosion. This vegetation however has to satisfy the following minimum requirements. It should have a mat-like appearance, a sod-forming root system, be made of perennial grasses, have a dense consistent coverage, have a minimum height of 0.3 m during flood season. Tree roots can be considered to help reinforce the levee slope if the tree is on the levee however if the tree is toppled over by the storm, it will create a major hole in the levee. Also if the tree dies, the disappearance of the roots will leave channel for the water to seep through the levee. Overall trees on levees or near levees are not a good idea.

The following case history illustrates how the levee overtopping chart was generated.

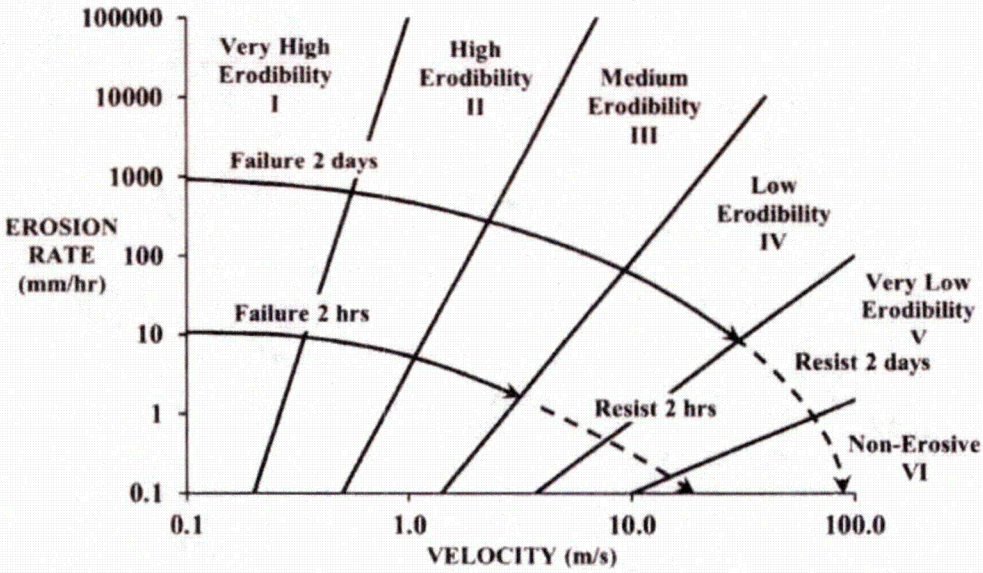

Fig. 19 – Levee overtopping chart.

i. New Orleans – Katrina hurricane levee case history

On August 29, 2005, levee overtopping and associated erosion contributed significantly to the Katrina hurricane disaster in New Orleans where some places are 6 m below the top of the levees. This case history describes the process by which overtopped levees erode and whether or not unprotected soils can resist overtopping erosion.

Soil erodibility

Thin wall steel tube samples and bag samples were obtained from the top of the levees at shallow depth (0 to 1 m). Shelby tube samples and bag samples were collected from locations S1 through S15 on Fig. 20. The bag samples were reconstituted in a Shelby tube by recompacting the soil at a low and at a high compaction effort. The soil type varied widely from loose uniform fine sand to high plasticity stiff clay. EFA tests were performed on the samples. The results of all the tests are shown on Fig. 21 and 22. One of the first observations from those figures is that the erodibility of the soils obtained from the New Orleans levees varies widely all the way from very high erodibility (Category 1) to low erodibility (Category 4). This explains in part why some of the overtopped levees failed while other overtopped levees did not.

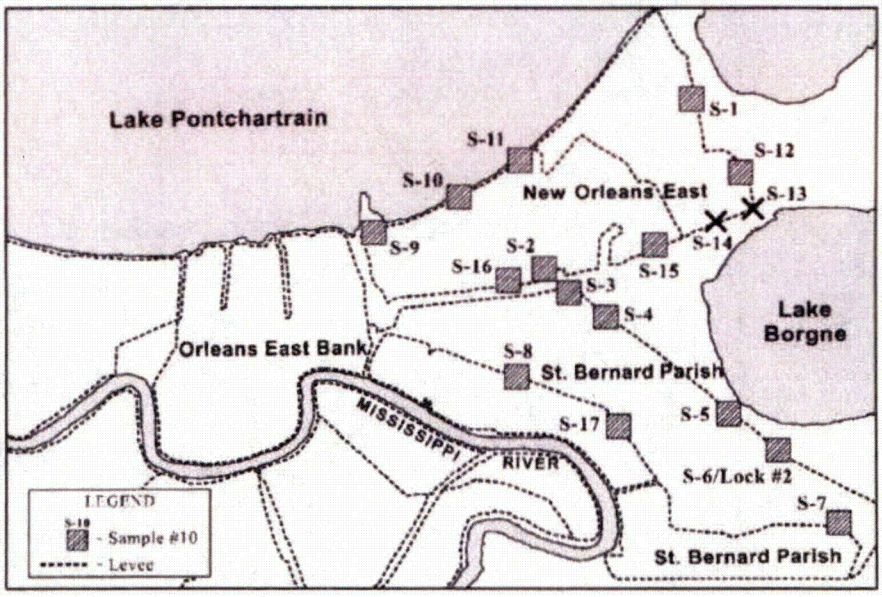

Fig. 20 – Location of shallow samples collected from the top of the levees.

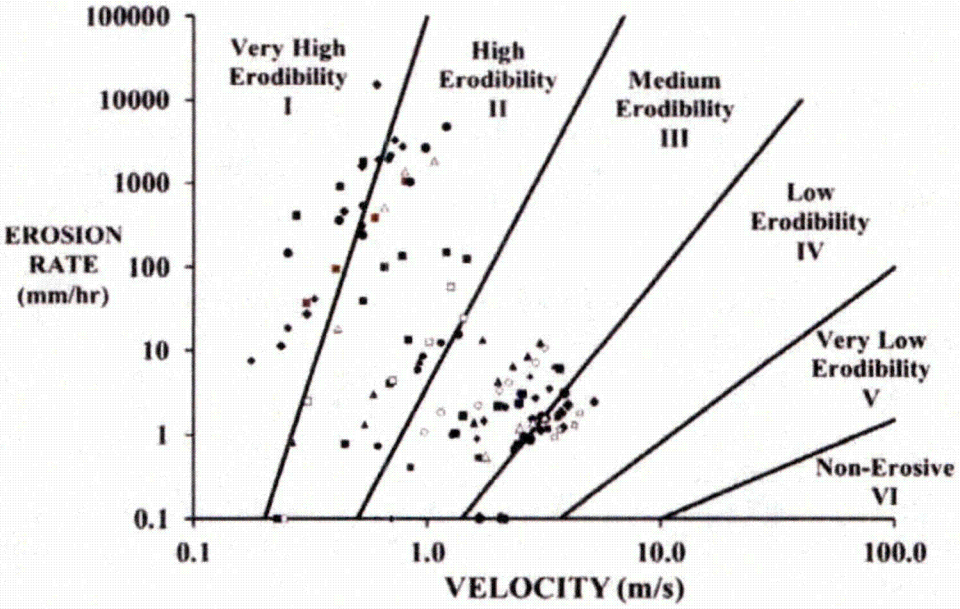

Fig. 21 – EFA test results in terms of velocity for some levee soils.

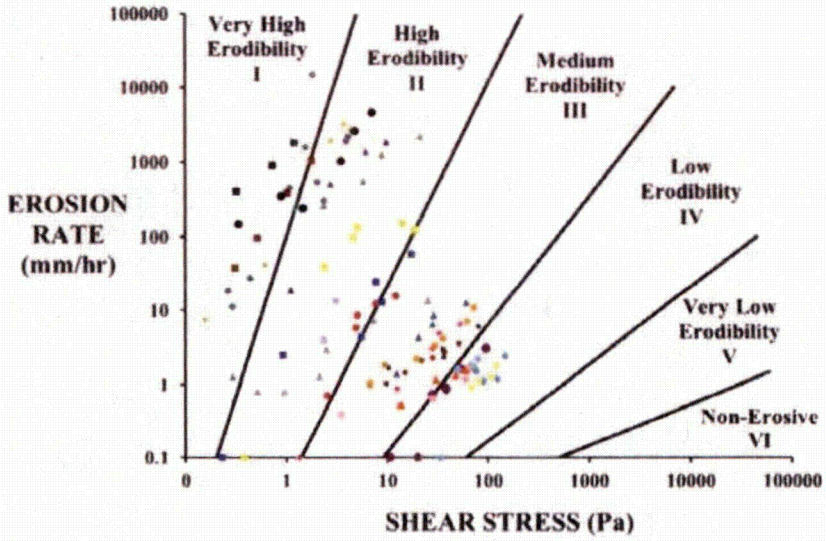

Fig. 22 – EFA test results in terms of shear stress for some levee soils.

Water velocity

Hurricanes are large rotating masses of moisture which can be 400 km in diameter. They travel relatively slowly at speeds of about 40 km/hr. Therefore a hurricane takes about 10 hr to go over a levee or a bridge. The worst part of the storm however is only a fraction of that time. The friction generated by the wind at the air-water interface drags the water into a storm surge which can reach several meters above the mean sea level and kilometers in length. The surge associated with Katrina was about 8.5 m at Bay St. Louis, 4.6 m at Lake Borgne, and 3 m at Lake Pontchartrain. The storm surge was high enough to overtop some of the levees. As discussed earlier the water velocity at the bottom of such levees can reach 10 m/s.

Geometry of the obstacle

Most levees around New Orleans are between 3 and 6 m high. They have two main shapes. The first one consists of a flat top which is some 4 m wide with side slopes at about 5 horizontal to 1 vertical. Because the width of such a levee configuration takes a lot of space, the second shape consists of the same shape as the first one at a reduce scale with a vertical wall extending on top of the levee. The problem addressed here is limited to the first shape (no wall).

Predicting levee overtopping erosion

There was overwhelming evidence that the water overtopped the levees in many places; such evidence consisted mostly of ships being trapped on top of the levees when the water receded but also of debris stuck in trees at levels higher than the top of the levees. Some levees resisted the overtopping well, some levees were completely eroded. On Fig. 23, the erodibility functions for the samples taken from levees that were overtopped and resisted well are plotted as open circles while the solid dots are for the samples of levees that were completely eroded. As can be seen, the eroded levees were made of soils in the erodibility categories 1 and 2 while the levees which resisted well were made of soils in the erodibility categories 3 and 4. This led to the levee overtopping chart shown in Fig. 19.

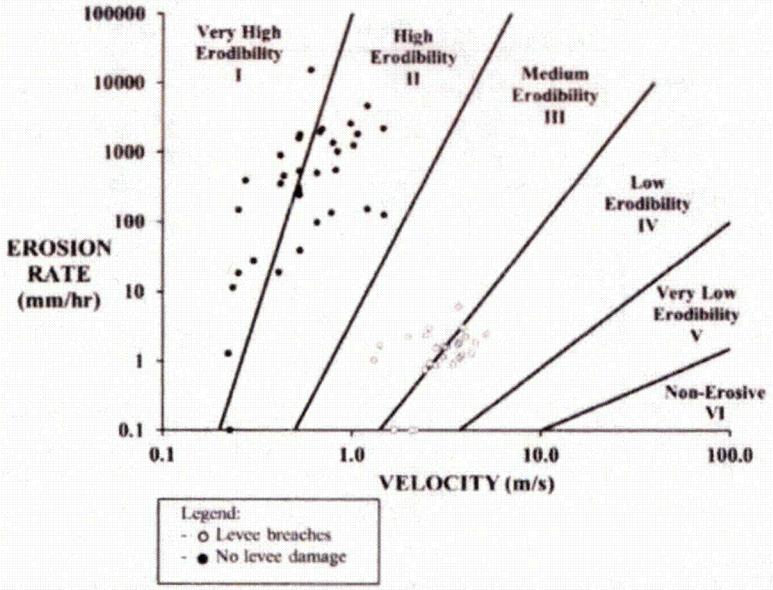

Fig. 23 – EFA test results for the soils of levees which failed and did not fail by overtopping erosion.

j. Countermeasures for erosion protection

Countermeasures for erosion protection include a number of solutions but the most prevalent is the use of rip rap (Fig. 24). Rip rap can be sized by the following USACE equation.

$$d_{30} = H_w F C_{st} C_v C_t \left(\frac{V_{des}}{\sqrt{C_{sl}(G_s - 1) g H_w}} \right)^{2.5} \quad (8)$$

Where d_{30} is the particle size of the riprap grain size distribution curve corresponding to 30% finer, H_w is the water depth, F is the factor of safety, C_{st} is the stability coefficient, C_v is the velocity distribution coefficient, C_t is the blanket thickness coefficient, V_{des} is the mean depth water velocity, C_{sl} the side slope correction factor, G_s the specific gravity of the riprap, and g the acceleration due to gravity (9.81 m/s^2). The stability coefficient C_{st} takes into account the roughness of the riprap blocks; it is 0.3 for angular rock and 0.375 for round rocks. The velocity distribution coefficient C_v takes into account the fact that water tends to accelerate on the outside of river bends; it is 1 for straight channels and inside of bends, and 1.23 in most other cases. The blanket thickness coefficient C_t is a function of the riprap gradation with a default value of 1 in the absence of additional data. The velocity V_{des} is the mean depth velocity for straight channels. For river bends it is given by:

$$V_{des} = V_{ave} \left(1.74 - 0.52 \log \frac{R_c}{W} \right) \quad (9)$$

where V_{ave} is the mean depth velocity upstream of the bend, R_c is the centerline radius of curvature of the river bend and W the river width at the water level. The side slope coefficient C_{sl} is given by.

$$C_{sl} = \sqrt{1 - \left(\frac{\sin(\theta - 14^o)}{\sin 32^o} \right)^{1.6}} \qquad (10)$$

where θ is the bank angle in degrees. The specific gravity of solids G_s is usually taken as 2.65.

It is very important to place a filter between the soil to be protected and the riprap layer. Without a filter the soil under the riprap may continue to erode through the large voids in the riprap. In the end the riprap may not move away but may simply go down significantly as the underlying soil erodes away. The filter may be a sand filter or a geosynthetic filter.

DESIGN PLAN	FIELD INSTALLATION
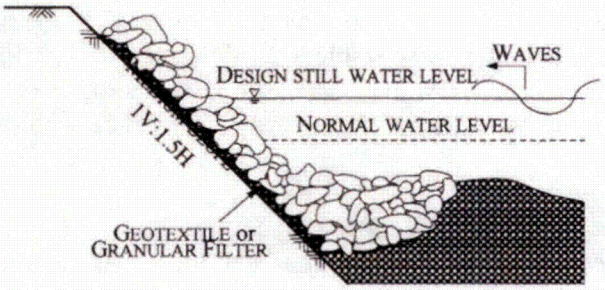	 http://www.fhwa.dot.gov/engineering/hydraulics/pubs/scanningreview1998/riprap.cfm

Fig. 24 - Riprap with geosynthetic filter Installation

Other countermeasures to prevent erosion include:

1. Flow deflectors such as spurs, jetties, dikes, guide banks,
2. Rigid armoring of the soil surface such as soil cement mixing and grouted mattresses,
3. Flexible armoring such as riprap, gabions, articulated blocks,
4. Pier geometry modification such as slender pier shape, debris deflectors,
5. Vegetation such as woody mats, root wads,
6. Fixed and portable instrumentation such as sonars, float out devices, and
7. Periodic inspection.

k. Internal erosion of earth dams

It is estimated that 46% of earth dam failures occur due to internal erosion (Fig. 25) and half of those failures occur during the first filling of the reservoir. Yet, internal erosion of earth dams remains highly based on engineering judgment and experience. While guidelines and publications exist much remains to be studied and researched in this field. For internal erosion of an earth dam to take place, the following are required

1. a seepage flow path and a source of water
2. erodible material that can be carried by the seepage flow within the flow path
3. an unprotected exit, from which the eroded material may escape
4. for a pipe to form, the material must be able to form and support the roof of the pipe.

Four different phenomena can lead to internal erosion of an earth dam (Fig. 26):

1. backward erosion
2. concentrated leak
3. suffusion
4. soil contact erosion

Backward erosion is initiated at the exit point of the seepage path when the hydraulic gradient is too high and the erosion is gradually progressing backward forming a pipe. A *concentrated leak* is internal to the soil mass, it initiates a crack or a soft zone emanating from the source of water and may or may not progress to an exit point. Erosion gradually continues and can create a pipe or a sink hole. *Suffusion* develops when the fine particles of the soil wash out or erode through the voids formed by the coarser particles. This occurs when the amount of fine particles is smaller than the void space between the coarse particles. If on the contrary, the soil has a well graded particle size distribution with sufficiently small voids, suffusion is unlikely. Soils are called internally unstable if suffusion takes place and internally stable if particles are not eroding under seepage flow. Soil *contact erosion* refers to sheet flow at interfaces between soil types. It may occur for example when water seeps down the back face of the core at the interface with the filter and then the stabilizing mass.

Earth dams deform during and after construction. This movement can be compression, extension and shear distortion. Because typical dams are made of different zones playing different roles they exhibit different deformation characteristics. This can lead to differential movement resulting in cracks or soft zones where internal erosion can be initiated. Shrinkage can also create cracks which are prone to erosion if water comes to flow through them. Fell and Fry summarized the most likely locations where internal erosion can start in an earth dam (Fig. 27).

BLACKMAN CREEK DAM	TETON DAM
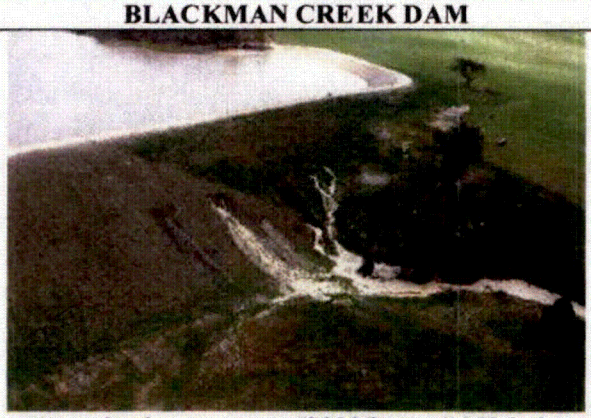 http://soer.justice.tas.gov.au/2009/image/1072/index.php	

Fig. 25 – Example of internal erosion of an earth dam.

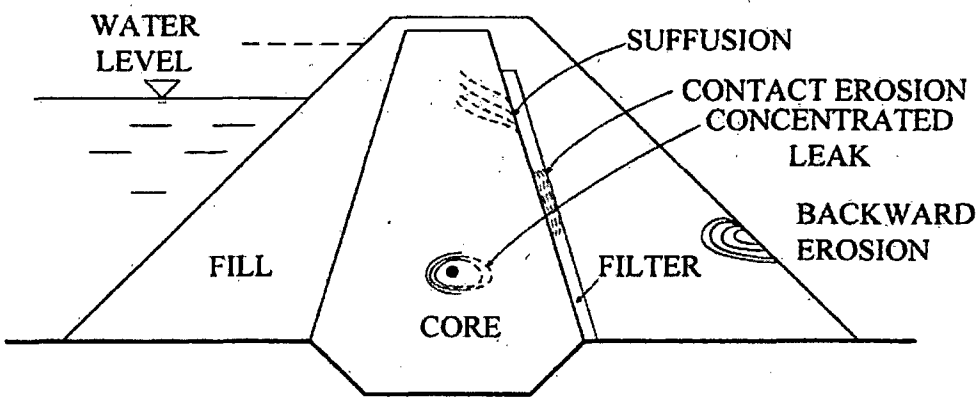

Fig. 26 – Mechanisms of internal erosion failures.

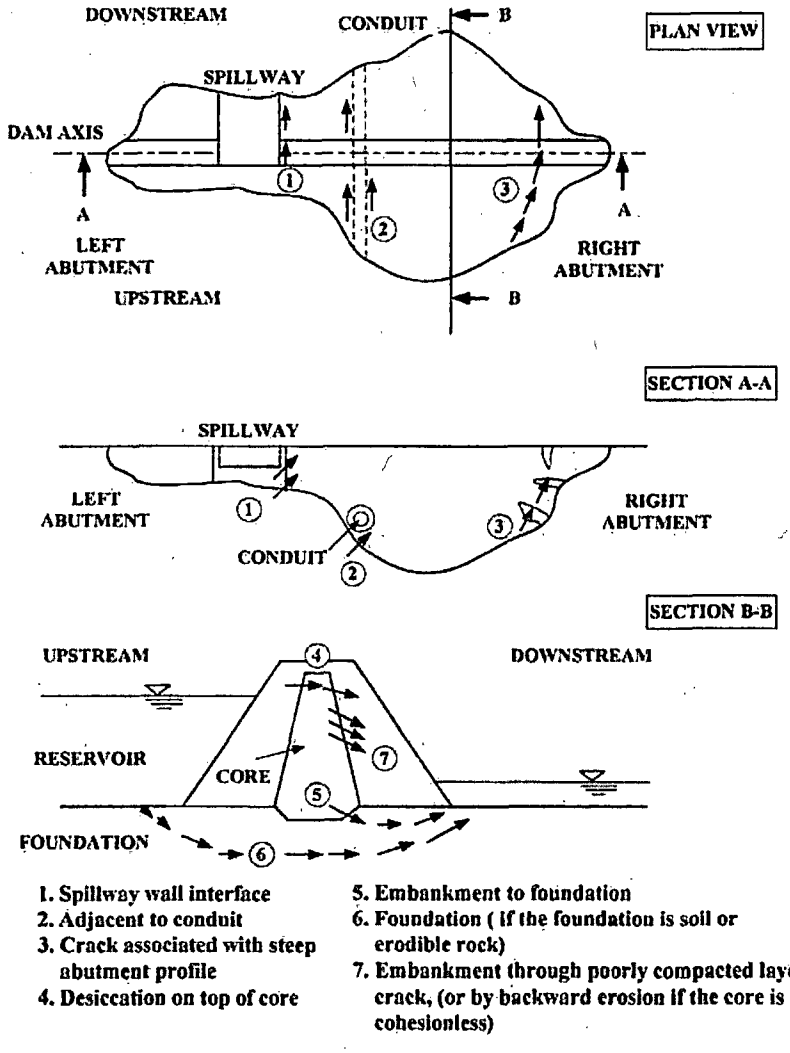

1. Spillway wall interface
2. Adjacent to conduit
3. Crack associated with steep abutment profile
4. Desiccation on top of core
5. Embankment to foundation
6. Foundation (if the foundation is soil or erodible rock)
7. Embankment through poorly compacted layer, crack, (or by backward erosion if the core is cohesionless)

Fig. 27 – Possible locations of initiation of internal erosion (After Fell, Fry, 2005).

Coarse silt and fine sand are among the most erodible soils. Therefore earth dams containing significant amounts of such materials will be more prone to internal erosion. Clays in general and high plasticity clays in particular are more resistant to erosion as long as the electrical bonds between particles are not destroyed by chemicals. It seems that some core materials of glacial origin such as glacial tills can be particularly susceptible to internal erosion. Sherard gave a range of gradation of soils which can lead to internal erosion problems (Fig. 28).

The soils which are most susceptible to suffusion are those where the volume of fines is less than the volume of the voids between coarse particles. In this case, the fines can move easily between the coarse particles and erode away to an exit face. After suffusion, such soils are devoid of fines and become very pervious clean gravel for example. Fell and Fry again indicate that gap graded soils and coarsely graded soils with a flat tail of fines (Fig. 29) are most susceptible to suffusion.

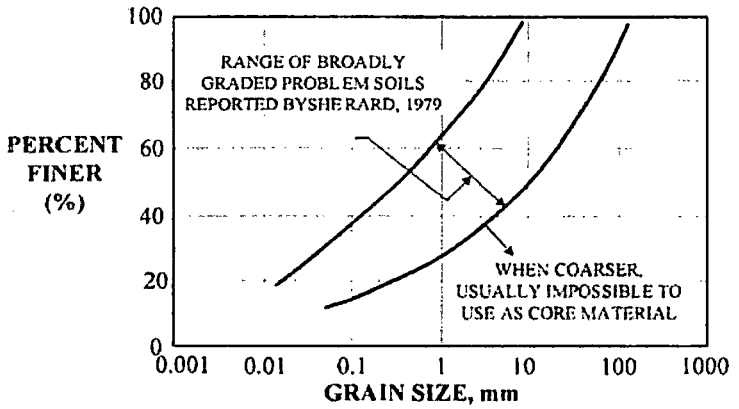

Fig. 28 – Range of problems soils for internal erosion (after Sherard, 1979).

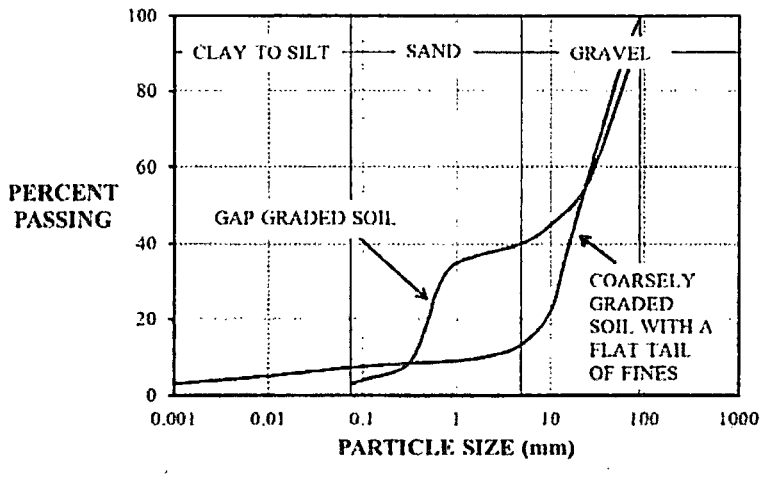

Fig. 29 – Range of problems soils for suffusion (after Fell and Fry, 2005).

One of the important criterions to evaluate erosion is to calculate the hydraulic gradient and compare it to the critical gradient. The critical gradient is given by

$$i_{cr} = \frac{\gamma_{sat} - \gamma_w}{\gamma_w} \quad (11)$$

Values of i_{cr} typically vary in the range of 0.85 to 1.2. The hydraulic gradient in dams depends on many factors including the difference in water level between the upstream and the downstream, the length of the drainage path, and the relative hydraulic conductivity of the various zones. The target maximum gradient in the flow must be kept much lower than the critical value especially in areas where internal erosion is possible. Fig. 30 shows ranges of hydraulic gradient values which are associated with initiation of internal erosion on one hand and full development of piping on the other for unfiltered exit faces. Generally speaking there is a trend towards higher porosity soils beginning to erode at lower hydraulic gradients even lower than 0.3. Yet soils with plastic fines erode at higher gradients but gap-graded soils begin to erode at lower gradients than non gap-graded soils with the same fine content. The US Army Corps of Engineers uses a lower bound value of the critical hydraulic gradient equal to 0.8 and allows a hydraulic gradient of up to 0.5 at the toe of levees provided a number of conditions are met (USACE). Another way to address the incipient motion of soil particles in internal erosion problems is to use the concept of critical velocity and charts such as Fig. 11 and 12. However these critical velocities were developed from sheet flow test and the critical velocity may be different from those initiating internal erosion.

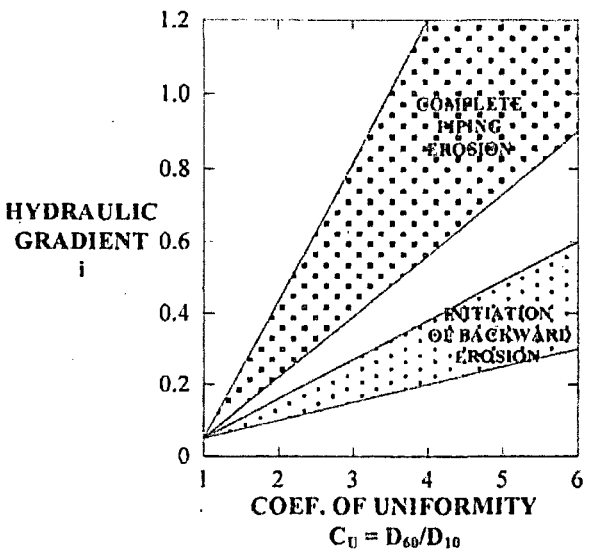

Fig. 30 – Range of hydraulic gradient values associated with internal erosion (after Perzlmaier, 2005).

Most of the time, a complete breach occurs within 12 hours of first visual detection of internal erosion and sometimes in less than 6 hours. The majority of failures occur during the first filling or within 5 years after first filling. The process of suffusion tends to develop more slowly than the back erosion and piping process.

The solution to many of the internal erosion problems is the use of quality filters. A filter is a layer of soil placed between a fine grained soil and coarse grain soil to transition the flow without having the fines of the fine grained soil erode through the voids of the coarse grained soil. The grain size distribution curve of the soil filter layer is designed to provide this transition in a gradual fine to coarse fashion.

Appendix B

Original Xu and Zhang Regression Equations and HRR Hydrograph

APPENDIX B. ORIGINAL XU AND ZHANG REGRESSION EQUATIONS

B.1 Overview

The original Xu and Zhang (2009) regression methodology and its previous implementation to the Jocassee Dam are described in this Appendix. This provides background for Section 6 where we address the questions raised by the FERC and the NRC. It also provides background for Section 7 where we describe the implementation of a revised version of the Xu and Zhang equations in a sensitivity analysis, which provides support for the breach hydrograph submitted in the Hydrologic Reevaluation Report (HRR) to the NRC by Duke on March 12, 2013 (Duke 2013).

Section B.2 summarizes the breach parameters and control variables in the Xu and Zhang (2009) regression equations. Section B.3 discusses the case histories that were used to develop these equations and Section B.4 summarizes the regression equations, including their confidence limits. The implementation of the original Xu and Zhang (2009) methodology for the Jocassee Dam is described in Section B.5 and details of the use of the failure time estimate in the HEC-RAS model are discussed in Section B.6.

B.2 Breach Parameters and Control Variables

The Xu and Zhang (2009) multiple regression equations were developed to predict the following five breach parameters (dependent variables), which are divided into two groups, breach geometry and breach hydrograph:

- Breach Geometry
  - Breach depth (H_b)
  - Breach top width (B_t)
  - Average breach width (B_{ave})
- Hydrograph
  - Peak outflow rate (Q_p)
  - Breach development time or failure time (T_f)

The predicted breach side slope, z, which is an input to HEC-RAS breach model, can be calculated from the breach depth (Hb), breach top width (Bt) and average breach width (Bave). The predicted breach bottom elevation, which is also an input to the HEC-RAS breach model, can be calculated by subtracting the breach depth from the dam crest elevation.

Unlike most previous breach parameters regression relationships, Xu and Zhang (2009) included soil erodibility as a control (independent) variable. In fact they found it to be the single most important of all the control variables that they considered in terms of its explanation of the variance in "observed" breach parameter values across the case histories on which their methodology is based.

The complete list of five control variables that they used to estimate breach parameters is as follows, including normalization for the first two variables:

- Dam height ($X_1 = H_d/H_r$, *dam height* H_d *and a reference height* H_r, *where* $H_r = 15$ *m*),
- Reservoir shape coefficient ($X_2 = V_w^{1/3}/H_w$, *volume of water above breach invert Vw and depth of water above the breach invert at the time of failure,* H_w.),
- Dam type *(with corewalls, concrete faced and homogeneous/zoned-fill)*,
- Failure mode *(overtopping and seepage erosion/piping)*,
- Dam erodibility *(high, medium and low)*.

Xu and Zhang (2009) included rockfill dams in the homogeneous/zoned-fill dam type. Dam type, failure mode and dam erodibility are included in the regression analysis as virtual discrete variables that represent either the presence or absence of each of these attributes.

As mentioned above, Xu and Zhang (2009) found dam erodibility to be the most important control variable for predicting all five breach parameters. They describe dam erodibility as *a relative measure based on the embankment material compositions and compaction conditions, dam cross-sectional geometry, construction time and other relevant pieces of construction information*. The three erosion categories (low, medium or high) used in the Xu and Zhang (2009) equations refer to the technical lecture paper by Briaud (2008), whereby soils and rocks are classified into various erosion resistance categories based on erosion velocity or shear stress, as shown in Figures 4.1a and b, respectively. The appropriateness of using the Briaud erosion categories in the Xu and Zhang (2009) methodology was confirmed by Professor Briaud as detailed in Appendix A and summarized in Section 4.2.

B.3 Case Histories

The Xu and Zhang (2009) regression equations are based on an analysis that includes more recent breaches than are included in earlier relationships, such as Froehlich (1995a and b). It also includes data from China that has not been previously used in breach regression equations. Data from a total of 75 earth and rockfill dam failure cases was used to develop the original multiple regression equations, although for each breach parameter the number of case histories that were used to estimate the best exact and best simplified equations, respectively are as listed below:

- Breach depth (H_b): 66 and 71
- Breach top width (B_t): 54 and 61
- Average breach width (B_{ave}): 45 and 53
- Peak outflow rate (Q_p): 34 and 39
- Breach development time or failure time (T_f): 28 and 30

38 (51%) of the 75 case histories are for US dams, 32 (43%) are from China and 5 (7%) are from other countries. 7% (5) of the 75 case histories are for dams that were classified as dams with core walls, 5% (4) were classified as concrete-faced dams and the remainder were classified as composite-fill dams. 61% (46) of the case history dams failed by overtopping and 39% (29) by seepage-erosion failure modes. 40% (30) of the case history dams were classified as high erodibility, 51% (38) as medium erodibility and 9% (7) as low erodibility.

Figures B.1a and b show the depth of water above breach invert, Hw, and volume of water at the breach time, Vw, for the 75 case histories on arithmetic-arithmetic and arithmetic-logarithmic axes, respectively. Across the 75 case histories the depth of water above breach invert, Hw, ranges from 1.7 to 77 m (5.5 – 254 feet) compared with a predicted value of 72.5 m (238 feet) for the Jocassee Dam using the original Xu and Zhang (2009) methodology. The dam heights, Hd, range between 3.2 and 93 m (10 – 305 feet) compared with 117.3 m (385 feet) for the Jocassee Dam. The volume of water at the breach time varied between 0.025 to 660.0 m^3 x 106 (5.5 - 535,000 acre-feet) compared with a predicted value of 1.34 x 10^6 m^3 (1,088,208 acre-feet) for the Jocassee Dam using the original Xu and Zhang (2009) methodology.

B.4 Regression Equations and Confidence Intervals

Xu and Zhang (2009) developed two types of multiple regression equations for estimating the five breach parameters:

- Best exact prediction equations - based only on failure cases where all five control variables were available
- Best simplified prediction equations – includes some additional failure cases where not all five control variables were available

Best exact prediction regression equation for breach depth is in the following additive (linear) form:

$$Y_i = b_0 + b_1X_1 + b_2X_2 + (b_{31}X_{31} + b_{32}X_{32} + b_{33}X_{33}) + (b_{41}X_{41} + b_{42}X_{42}) + (b_{51}X_{51} + b_{52}X_{52} + b_{53}X_{53}) \quad (1)$$

in which:

Y_i	=	the first (i.e. i = 1) breach parameter or dependent variable, i.e. normalized breach depth as defined in Figure B.2
$X_{i,j}$	=	the control variables as defined in Figure B.2
$b_{i,j}$	=	the regression coefficients corresponding to the control variables

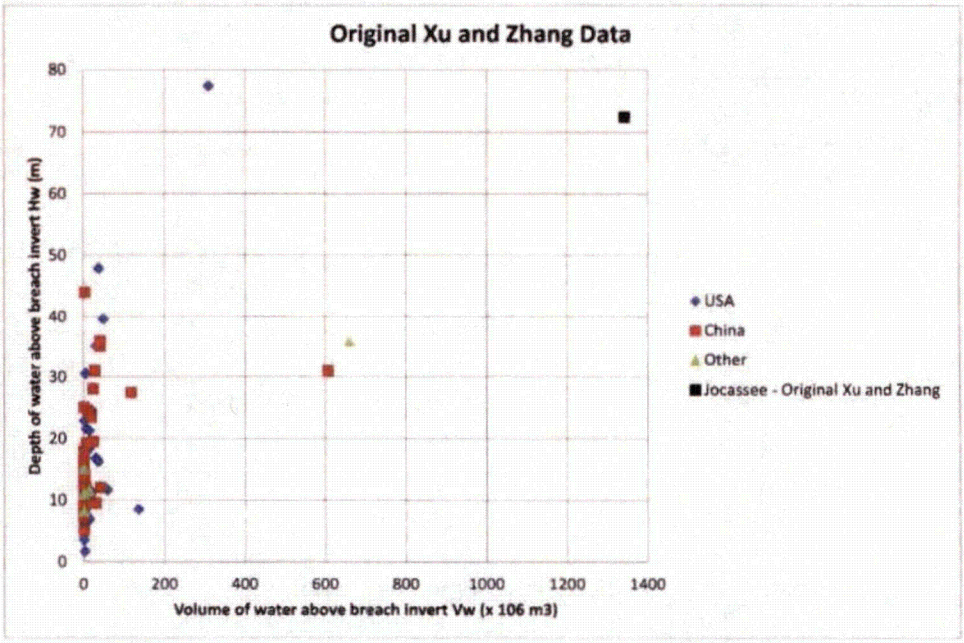

a) Arithmetic-arithmetic scales

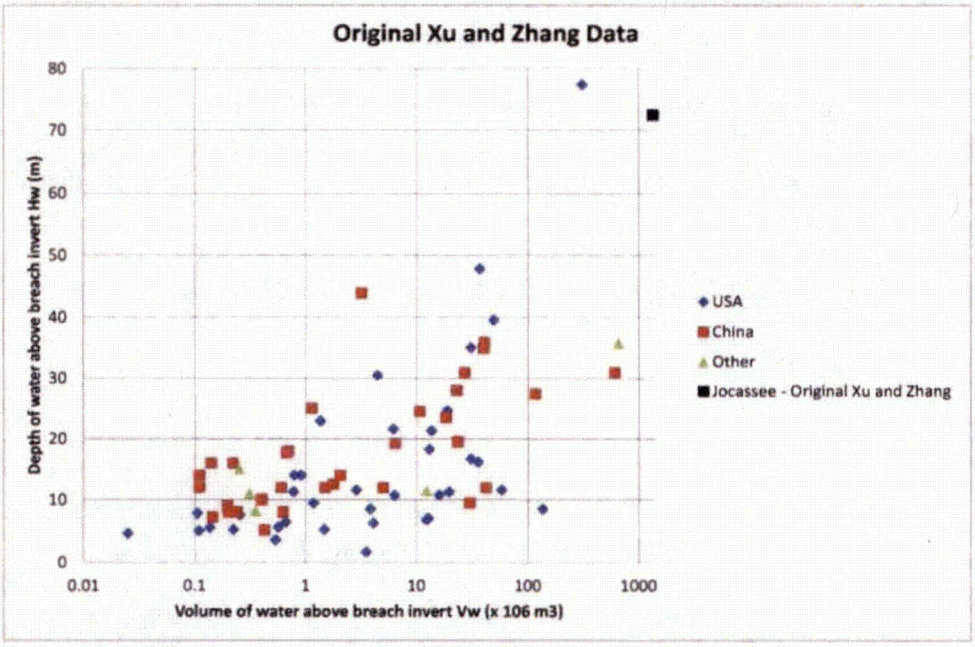

b) Arithmetic-logarithmic scales

Figure B.1. Depth of water above breach invert vs. volume of water at the breach time for the original Xu and Zhang (2009) case histories.

Breaching Parameters		Control Variables			
Breach depth	$Y_1 = H_b/H_d$	Dam height	$X_1 = H_d/H_r$		
Breach top width	$Y_2 = B_t/H_b$	Reservoir shape coefficient	$X_2 = V_w^{1/3}/H_w$		
Average breach width	$Y_3 = B_{ave}/H_b$	Dam type	X_{31}	X_{32}	X_{33}
Peak outflow rate	$Y_4 = Q_p/\sqrt{gV_w^{5/3}}$	with corewalls	$1^a(e^b)$	0(1)	0(1)
Failure time	$Y_5 = T_f/T_r$	concrete faced	0(1)	$1(e)$	0(1)
		homogeneous/zoned fill	0(1)	0(1)	$1(e)$
		Failure mode	X_{41}	X_{42}	
		overtopping	$1(e)$	0(1)	
		seepage erosion/piping	0(1)	$1(e)$	
		Dam erodibility	X_{52}	X_{52}	X_{53}
		high	$1(e)$	0(1)	0(1)
		medium	0(1)	$1(e)$	0(1)
		low	0(1)	0(1)	$1(e)$

Note: [a] Values for additive regression analy sis
[b] Values for multiplicative regression analysis
$H_r = 15\ m$; $T_r = 1\ hour$

Figure B.2. Summary of the five breach parameters and five control variables in the Xu and Zhang (2009) regression equations

For the other four breach parameters, the following multiplicative (non-linear) form of regression equation was used in which all five control variables were included for the best exact prediction equations but a subset of these variables were included for the best simplified prediction equations, as described below:

$$Y_i = b_0 X_1^{b1} X_2^{b2} (X_{31}^{b31} X_{32}^{b32} X_{33}^{b33})(X_{41}^{b41} X_{42}^{b42})(X_{51}^{b51} X_{52}^{b52} X_{53}^{b53}) \quad (2)$$

$$= 10^{Z_i} \quad (3)$$

in which:

Y_i = the second through fifth (i.e. i = 2, 3, 4 and 5) breach parameters or dependent variables as defined in Figure B.2

Z_i = untransformed breach parameter in natural space

To obtain the predicted breach parameter values in natural space a log transformation must be applied to from Equation 2 , as follows:

$$Z_i = \log(Y_i)$$
$$= b_0 + b_1X_1 + b_2X_2 + (b_{31}X_{31} + b_{32}X_{32} + b_{33}X_{33}) + (b_{41}X_{41} + b_{42}X_{42}) + (b_{51}X_{51} + b_{52}X_{52} + b_{53}X_{53}) \quad (4)$$

Under the standard assumption in regression analysis that the variability in the breach parameters that is not accounted for in (i.e. explained by) the regression equations (i.e. by the variation in the values of the control variables) is distributed according to a normal or Gaussian (bell curve) probability distribution (Haan 1977). Under this assumption, the mean values predicted that are obtained using Equations 1 and 2 are also the median or 50th percentile values. However, for the multiplicative form of the regression equation in Equation 2, the effect of the log transformation shown in Equation 4 is that the variability in the breach parameters that is not accounted for in (i.e. explained by) the regression equation is distributed according to a log-normal probability distribution. After transformation, the mean value predicted in transformed log space from Equation 2, which is also the median or 50th percentile value in log space, is still the median in the natural space but it is not the mean value in the natural space due to the effect of the log transformation. Another effect of this log transformation is that the confidence intervals are asymmetric.

By design, all five control variables appear in the best exact prediction equations as shown in Figure B.2. However, for breach depth, H_b, the best exact prediction equation excludes the reservoir shape coefficient ($X_2 = V_w^{1/3}/H_w$) for two reasons. First, the reservoir shape coefficient was found to have a very small contribution to explaining the variance in predicting H_b (Xu and Zhang 2009). Second, both the volume of water above breach invert, V_w, and the depth of water above the breach invert at the time of failure, H_w (where H_w = normal maximum reservoir level of 1,110 feet msl. minus H_b) are functions of H_b and so if the reservoir shape coefficient was included as a control variable then H_b would appear on both the left and right sides of regression equation.

Best simplified prediction equations were obtained through a stepwise regression procedure in which regression equations with different combinations of the five control variables were developed for each breach parameter. This is a standard method in regression analysis (Haan 1977) with the goal of striking a balance between prediction accuracy and simplicity in the equation (i.e. fewer control variables). The equation that has the highest adjusted coefficient of determination, R^2_{adj}, is selected as the best simplified equation, where R^2_{adj} is defined as follows:

$$R^2_{adj} = \frac{(n-1)R^2 - k}{n-(k+1)} \qquad (5)$$

in which:

n	=	number case histories for which data are used in the regression analysis
R^2	=	coefficient of determination
k	=	number of control variables used in the regression analysis

The (unadjusted) coefficient of determination, R^2, is less for the selected best simplified prediction equation than for the best exact prediction equation for the same breach parameter because fewer independent or control variables are included. Hence the best exact prediction

equations have greater prediction accuracy because they explain a greater fraction of the variability between values of each breach parameter across the case histories. However, the standard error of the regression for the best simplified prediction equation, and hence the width of the confidence intervals for breach parameter estimates, is less than for the best exact prediction equation for the same breach parameter. This is because there are more degrees of freedom when fewer regression coefficients are estimated because there are fewer control variables. Another factor that may further decrease the standard error of regression, s^2, is that additional case histories may be available to use in the regression when there are fewer control variables because for some case histories estimates were not available for all five control variables as required for the best exact prediction equations.

The Xu and Zhang (2009) best exact and best simplified prediction equations for all five breach parameters are presented in terms of the estimated values of their regression coefficients (b_i's) in Tables B.1 and B.2, respectively. These tables also include the standard error of the regression, which can be used to calculate confidence intervals for breach parameter estimates in addition to median predictions that are obtained directly from the regression equations.

Xu and Zhang (2009) conducted a comparison with two breach prediction methods (Bureau of Reclamation 1982 and 1988 and Froehlich 1995a and b) and demonstrated that their method provides a lower bias and standard error on predictions than these other methods. They admit that since this comparison used data on which their model is based it may have had an advantage over other models included in the comparison, but they nevertheless claim that the comparison is fair.

Xu and Zhang (2009) included two applications of their equations to actual dam breaches for Banqiao and Teton dams. Banqiao Dam was an overtopping failure and Teton Dam was a piping failure. The predictions are compared with the observed values of the breach parameters for both the best exact and the best simplified models in Tables 7 and 8 of their paper, respectively. They also include lower and upper bound estimates based on a 95% confidence interval. The theoretical meaning of this confidence interval is that there is a 95% chance that the true values of the breach parameters are contained in the range between the lower and upper bound values. The lower and upper bound values for an additive (linear) regression model for breach depth are equally spaced on either side of the median estimate and this can be seen, within the limits of round off in the estimates, as shown in Tables 7 and 8 of the Xu and Zhang (2009) paper. However, the spacing between the median estimates and the lower and upper bounds for the remaining four breach parameters is very asymmetric due to the multiplicative (non-linear) form of the regression models for these parameters as explained above. Specifically there are approximately two to three and a half fold differences between the median and lower bound estimates compared with between the upper bound and median estimates for these breach parameters. Clearly the widths of the 95% confidence intervals are large for all breach parameters. We return to the topic of the confidence intervals on the Xu and Zhang (2009) breach parameter estimates in Section B.5 where we discuss how they apply specifically to the Jocassee Dam breach parameter estimates that are the focus of this report.

Table B.1. Summary of the five Xu and Zhang (2009) best exact regression equations

Breach Parameter Y (or log Y)	Number of Cases	Control Variables (log: nonlinear)	b0 (or log b0)	b1	b2	b31	b32	b33	b41	b42	b51	b52	b53	R2	$S2_{Y\|X}$ (or $S2_{\log Y\|\log X}$)
						Dam Type					Erodibility Category				
			Intercept	Hgt	Reservoir Shape Coef.	Core Wall	CFRD	Homog Zoned	Overtop	Piping	High	Medium	Low		
Hb / Hd	66	X1,2,3,4,5	0.453	-0.025	0.000	0.145	0.176	0.132	0.218	0.236	0.254	0.168	0.031	0.350	0.012
log(Bt / Hb)	54	lnX1,2,3,4,5	0.060	0.092	0.508	0.061	0.088	-0.089	0.299	-0.239	0.411	-0.062	-0.289	0.620	0.169
log(Bave / Hb)	45	lnX1,2,3,4,5	-0.240	0.133	0.652	-0.041	0.026	-0.226	0.149	-0.389	0.291	-0.140	-0.391	0.648	0.184
log(Qp / √gVw5/3)	34	lnX1,2,3,4,5	-1.744	0.199	-1.274	-0.503	-0.591	-0.649	-0.705	-1.039	-0.007	-0.375	-1.362	0.800	0.365
log(Tf / Tr)	28	lnX1,2,3,4,5	-1.190	0.707	1.228	-0.327	-0.674	-0.189	-0.579	-0.611	-1.205	-0.564	0.579	0.793	0.365

Table B.2. Summary of the five revised Xu and Zhang (2009) best simplified regression equations

Breach Parameter Y (or log Y)	Number of Cases	Control Variables (log: nonlinear)	b0 (or log b0)	b1	b2	b31	b32	b33	b41	b42	b51	b52	b53	$R2^{adj}$	$S2_{Y\|X}$ (or $S2_{\log Y\|\log X}$)
						Dam Type					Erodibility Category				
			Intercept	Hgt	Reservoir Shape Coef.	Core Wall	CFRD	Homog Zoned	Overtop	Piping	High	Medium	Low		
Hb / Hd	71	X1,5	0.729	-0.025							0.343	0.257	0.129	0.314	0.011
log(Bt / Hb)	61	lnX2,4,5	-0.004		0.558				0.258	-0.262	0.377	-0.092	-0.288	0.584	0.159
log(Bave / Hb)	53	lnX2,4,5	1.713		0.739				-1.207	-1.747	-0.613	-1.073	-1.268	0.669	0.173
log(Qp / √gVw5/3)	39	lnX2,4,5	-2.020		-1.276				-0.788	-1.232	-0.089	-0.498	-1.433	0.777	0.304
log(Tf / Tr)	30	lnX1,2,5	-1.893	0.654	1.246						-1.375	-0.828	0.310	0.727	0.288

B.5 Implementation for Jocassee Dam – Xu and Zhang Breach Parameter Estimates

As described in our February 2013 report (Ehasz and Bowles 2013), we applied the Xu and Zhang (2009) regression equations to the Jocassee Dam to obtain the estimates of the breach parameters for a sunny-day piping failure. We also estimated the confidence intervals for the estimated breach parameters. These were calculated using the values of the standard errors of regression published by Xu and Zhang (2009) in Tables B.1 and B.2 and the equations for the confidence intervals for a multiple regression that can be found in many textbooks (e.g. Haan 1977). To verify our spreadsheet for applying the Xu and Zhang (2009) regression equations we first reproduced, within a small round-off error, the median and confidence interval estimates that are presented in the Xu and Zhang (2009) paper for Teton and Banqiao dams. We also closely matched estimates made independently by HDR for the Jocassee Dam as shown in our February 2013 report (Ehasz and Bowles 2013).

Values representing the Jocassee Dam were assigned to the five control (independent) variables in the Xu and Zhang (2009) regression equations as follows:

- Dam height, H_d = 385 feet.
- Reservoir shape coefficient, $V_w^{1/3}/H_w$, in which V_w is the *volume of water above breach invert* based on the stage-capacity relationship for Lake Jocassee evaluated between the normal maximum reservoir level of 1,110 feet msl. and the elevation of the breach invert [i.e. crest elevation of 1,125 feet msl. minus breach depth H_b and the depth of water above the breach invert at the time of failure, Hw (i.e. normal maximum reservoir level of 1,110 feet msl. minus breach depth)]. Both V_w and H_w are calculated using the predicted values of breach depth obtained from Xu and Zhang (2009). The Lake Jocassee elevation-area-storage volume was obtained from Jocassee DWG No. J-17.
- Dam type selected as homogeneous/zoned-fill, which is the dam type that includes rockfill dams in the Xu and Zhang (2009) methodology.
- Failure mode selected as seepage erosion/piping,
- Dam erodibility assigned as the low erosion category.

The low erosion category was assigned based on the characterization of the Jocassee Dam summarized in Section 3.1 and the descriptions of the erosion categories from Briaud (2008) contained in Figures 4.1a and b. The Jocassee Dam is designed and constructed as a modern dam with very dense (b)(7)(F) core zone. The assignment of the low erosion category for Jocassee Dam for application of the Xu and Zhang (2009) methodology was subsequently confirmed by Professor Briaud as detailed in Appendix A and summarized in Section 4.3.

Table B.3 shows the input values and the breach parameter estimates from our application of the original Xu and Zhang (2009) methodology to the Jocassee Dam. Separate breach parameter estimates are included for the best exact and best simplified prediction regression

Table B.3. Breach parameters estimates from Xu and Zhang (2009) application to Jocassee Dam.

Breach Parameter	Erosion Category	Best Exact Prediction			Best Simplified Prediction		
		Median	95% Confidence Interval		Median	95% Confidence Interval	
			Lower	Upper		Lower	Upper
Height of breach, Hb ft.	Low	253	168	337	255	176	334
Failure time, Tf hrs.	Low	(b)(7)(F)					
Breach top width, Bt ft.	Low	701	306	1,606	666	299	1,485
Average breach width, Bave ft.	Low	566	246	1,306	515	223	1,193
Peak outflow, Qp ft3/sec.	Low	(b)(7)(F)					

equations. A more detailed version of Table B.3, which includes the values calculated for all regression parameters and references the regression equation numbers for the equations that we used from the Xu and Zhang (2009) paper, is contained in Appendix B of our February 2013 report (Ehasz and Bowles 2013).

From Table B.3 it can be seen that using the low erodibility category in the best exact prediction equations, the median failure time is estimated to be abou(b)(7)(F) the median breach top width about 700 feet, the median average breach width about 570 feet, the median (or mean) breach depth about 250 feet, and the median peak discharge unde(b)(7)(F) cfs. Estimates based on the best simplified prediction equations are smaller for all parameters except the breach depth.

The 95% confidence interval estimates for each breach parameter are shown in Table B.3 as lower and upper bound estimates that define the confidence interval both below and above the median estimates. Similar to the examples for Banqiao and Teton dams, which we discuss in Section B.4, the asymmetry in the confidence intervals can be seen for all breach parameters except breach depth, which is symmetrical because of the additive form of the regression equations for breach depth as explained in Section B.4. The symmetry in breach parameter estimates for breach depth and the asymmetry in estimates for failure time, breach top width, and average breach width can be seen in Figures B.3a and b. In these figures the confidence intervals for breach parameter estimates for Jocassee Dam are plotted as a ratio to the median estimate for the Xu and Zhang (2009) best exact and best simplified prediction equations, respectively. The asymmetry in the confidence intervals for failure time, breach top width, and average breach width can be seen by the longer lines above the median estimate (plotted at a ratio = 1.0 shown by the blue dashed line) than b elow the median estimate.

In Table B.3 we have placed boxes around the values of the breach parameters that we recommended in our February 2013 report (Ehasz and Bowles 2013) as being most applicable to the Jocassee Dam. These were used in developing the HRR breach hydrograph submitted to the NRC by Duke (2013). They are median estimates based on the low erosion category.

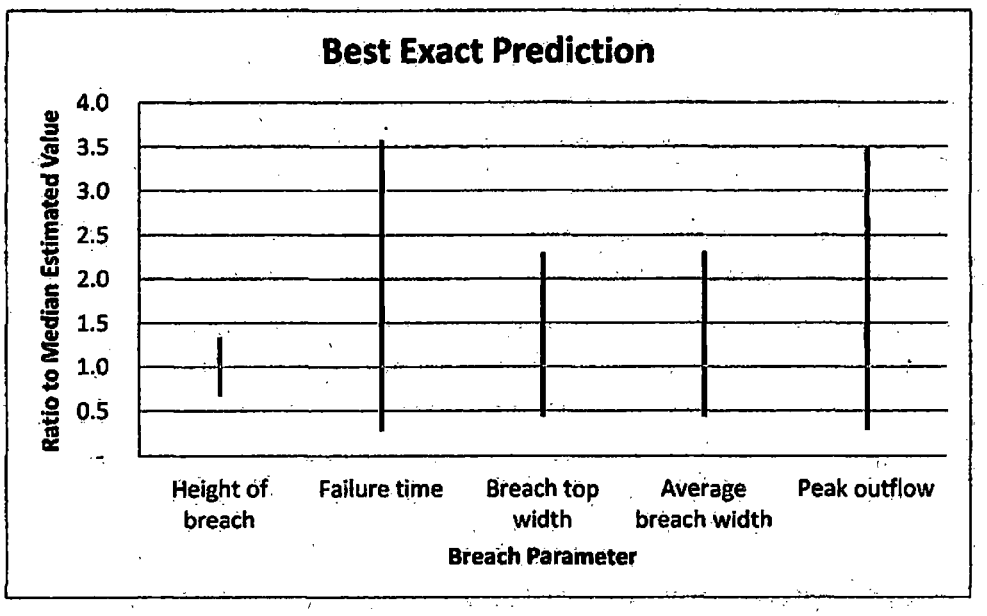

a) Best exact predictions

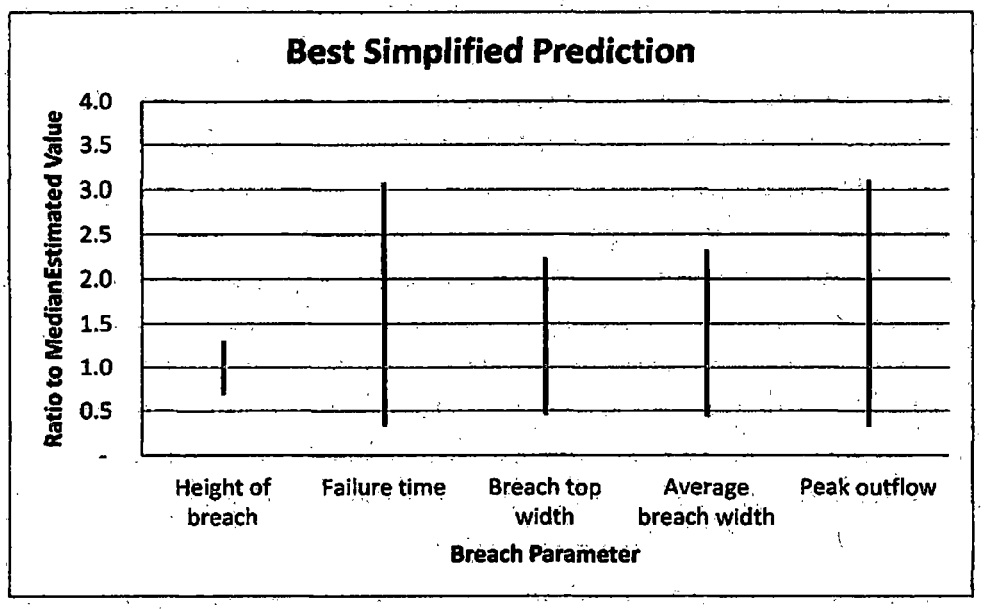

b) Best simplified predictions

Figure B.3. Relative width of confidence intervals for the original Xu and Zhang (2009) breach parameter estimates for Jocassee Dam expressed as a ratio to the median estimate (ratio = 1.0).

The basis for using low erosion category is explained above in this section. The basis for using median estimates is discussed below.

The Xu and Zhang (2009) median and confidence interval breach parameter estimates have the following bases:

- **Median estimate**: Predicted values from applying a regression equation whose coefficients have been estimated to minimize the sum of the squares of the differences between the predicted values associated with the regression equation and the observed values. All predicted values, except for breach depth, must be transformed using a log transformation to their natural space as shown in Equation 4. The resulting regression equation represents or "explains" the fraction, R^2, of the variability in the observed breach parameter values in the data set of historical dam breaches in terms of the variation in the observed values of the control variables that were used to derive the regression equation in the space in which the regression analysis was performed (i.e. natural space for breach depth and log transformed space for all four other breach parameters). Thus a regression equation that perfectly fits the observed breach parameter values would have an R^2 value equal to 100%.
- **Lower and upper bound estimates** (Confidence interval): Based on the variability between observed breach parameter values in the data set of historical dam breaches that is not represented or "unexplained" by a regression equation. This unexplained variability is the fraction, $(1 - R^2)$, of the variability in the observed breach parameter values in the data set of historical dam breaches in the space in which the regression analysis was performed (i.e. natural space for breach depth and log transformed space for all four other breach parameters).

Graphically one can picture the unexplained variability in breach parameter estimates as being a scatter of points representing the observed breach parameter values about the regression line. A key question is, "Where would one expect Jocassee Dam to fit in the range of the scatter or unexplained variation of breach parameter values for the data set of historical dam breaches used by Xu and Zhang (2009)?" Based on the fact that the Jocassee Dam is a well designed and constructed rockfill dam, which has incorporated modern design criteria and defensive design features (see Section 3.1), the breach geometry parameter estimates are expected to be in the range between the median and lower bound estimates. Additional factors that support these ranges of geometric breach parameter estimates include the following:

- **Uni-directional breach formation**: A breach from the very unlikely failure mode of piping through the foundation in the (b)(7)(F) would start high on the (b)(7)(F) of the Jocassee Dam and can only progress downwards and laterally towards the center of the dam in contrast to developing in two directions as is the case for most historical breaches. This would be expected to reduce the width of the breach because of the greater erosional resistance of the stable (b)(7)(F) of the breach. In

addition it would be expect to slow the rate of breach development and reduce the peak breach flow rate.

- **Deposition of eroded rockfill material and development of tailwater**: The rockfill material moved by the breaching process would ravel downstream by the flow through the breach and much of this material would be deposited within a short distance downstream of the dam. This would cause a significant tailwater to develop that would reduce flow velocities through the breach thus inhibiting both downward erosion and lateral development of the breach with the result that a narrower and shallower breach would be formed, taking a longer time to form, and resulting in a lower peak breach flow rate.

The combination of all these considerations provides strong evidence that the use of median values of breach geometry parameter estimates for the Jocassee Dam would be a conservative choice. Therefore we would expect that realistic breach geometry parameter estimates for the Jocassee Dam would be in the range between the median and lower bound estimates obtained from the Xu and Zhang (2009) regression methodology.

Similar arguments to those made for breach geometry parameter estimates for the Jocassee Dam being in the range between the median and lower bound estimates can be made for failure time, except that they would support a failure time estimate between the median and the upper bound estimate. Therefore, the use of the median estimate for failure time is also considered to provide a conservative estimate of the failure time as defined by Xu and Zhang (2009).

It follows from the same reasoning as discussed above for the breach geometry parameter estimates and the failure time estimate for the Jocassee Dam, that the peak breach flow estimate would be expected to be in the range between the median and lower bound estimates obtained from the Xu and Zhang (2009) regression methodology.

Before the breach parameter estimates can be used in the HEC-RAS simulation model for the Jocassee Dam, the definition of failure time in Xu and Zhang (2009) must be fully understood so that it can be appropriately used in the model. This is addressed in the following subsection.

B.6 Implementation for Jocassee Dam – Use of Xu and Zhang (2009) Failure Time Estimate in HEC-RAS Model

It is important that the definition of failure time used by Xu and Zhang (2009) is taken into account when using failure time estimates from their methodology in the HEC-RAS breach model because this definition is different to the definition that is commonly used (e.g. Froehlich 1995b and 2008). This relates directly to the fifth question raised by the FERC and NRC (see Section 2). In this subsection we explain how the Xu and Zhang (2009) failure time definition differs from the definition used by others (e.g. Froehlich 1995b and 2008) and how that was taken into account in the HEC-RAS breach model for the Jocassee Dam.

For the purpose of this discussion, Figure B.4 is adapted from the Xu and Zhang (2009) paper. It illustrates, for a seepage/erosion/piping failure mode, the distinction between the breach initiation and breach development phases of the breaching process. Outflow during the breach initiation phase is small, and in the case of a piping failure it is the flow through a developing pipe or seepage channel. As commonly defined the time for the breach development phase is the time that the embankment would take to washout after the internal erosion process (piping) advances far enough to form a cavern within the downstream shell of the dam leading to a collapse of a portion of the downstream shell that exposes the core and results in a partial and progressive collapse of the core, exposing it to overtopping. The overtopping would then washout the embankment.

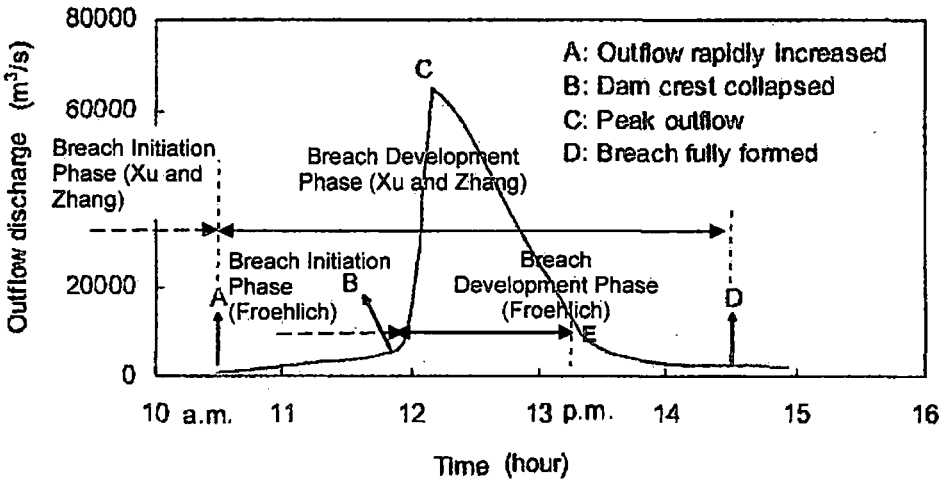

Figure B.4. Definition of breach phases in Xu and Zhang (2009) compared with Froehlich (1995b and 2008) illustrated for failure of Teton Dam [Adapted from Xu and Zhang (2009)].

Figure B.4 shows the example of the breach outflow hydrograph for the piping failure of the Teton Dam in 1976. Xu and Zhang (2009) were based on breach development time as defined by Wahl 2004 which states "*breach development begins when a breach has reached the point at which the volume of the reservoir is compromised and failure becomes imminent. During the breach development phase, outflow from the dam increases rapidly. The breach development time ends when the breach reaches its final size.*" According to the Xu and Zhang (2009) definition, the time of 10:30 a.m. is a critical point where failure becomes imminent and this time separates the breach initiation phase (ending at point A) from the breach development phase (between points A and D). After 10:30 a.m. (point A) the rates of discharge and erosion of embankment materials from the pipe outflow increased more rapidly. After the collapse of the dam crest at about 11:55 a.m. (point B), the breach developed rapidly due to overtopping of the collapsed dam crest and soon a peak discharge at about 12:15 p.m. (point C). According to Xu and Zhang (2009) the failure time associated with the breach development process, T_f, was approximately 4 hours starting at about 10:30 a.m. (point A) and ending at about 2:30 p.m. (point D).Many authors, including Fell et al (2003), point out that it has not been possible to identify the starting time for internal erosion associated with piping, and so it has not been

possible to estimate breach initiation phase times for historical dam breaches. As indicated in Figure B.4, it is the breach development time, T_f, between points A and D that is the predicted "failure time" in the Xu and Zhang (2009) method. However, this definition of failure time differs to that used by others, such as Froehlich (1995b and 2008) and Wahl (2013), in which breach development time[4] is defined as the period of higher outflow between points B and E in Figure B.4, or about 1.25 hours[5]. Specifically, the more commonly-used definitions of breach development time are as follows:

- *the time from the beginning of rapid growth of a breach to the time when significant lateral erosion has stopped* (Froehlich 1995b)
- *the needed time from initiation of a breach until it has reached its maximum size* (Froehlich 2008)
- the time from when the *active erosion front reaches upstream face of dam* to when the *breach has enlarged to its maximum size* (Wahl 2013)

From Figure B.4 it is clear that the Xu and Zhang (2009) definition of breach development time is a longer period of time (points A – D) than the more commonly-used definition (points B – E). The importance is not so much that there are differences between the way that failure time is defined in Xu and Zhang (2009) compared with other methods, but rather that the way that failure time is applied in a breach model (e.g. HEC-RAS) should be consistent with the definition that underlies its estimation. Achieving this consistency is discussed next for the application to the Jocassee Dam.

To achieve a compatible implementation of the Xu and Zhang (2009) breach parameter estimates in HEC-RAS, the Xu and Zhang (2009) median breach failure time (between points A and D) and median breach geometry estimates were input to the HEC-RAS model. The Xu and Zhang (2009) median peak breach flow rate estimate was then closely matched by iteratively changing the orifice coefficient to a final value of 0.1, the breach weir coefficient to a final value of 2.0, and the rate of breach progression relationship between points A and D to the final curve shown in Figure B.5.

Figure B.5 contains the breach hydrographs obtained by HDR for a piping failure of Jocassee Dam using the Xu and Zhang (2009) breach parameter estimates presented in Section B.5. Specifically, this figure includes hydrographs for the Jocassee headwater hydrograph represented by the blue line (left scale * 1,000), the Jocassee tailwater hydrograph represented by the brown line (left scale * 1,000), and the Jocassee breach discharge hydrograph is represented by the green line (right scale) at a location immediately downstream of the internal boundary in HEC-RAS model that represents the Jocassee Dam. The breach progression relationship, which is a required HEC-RAS input, and which was developed iteratively as

[4] In this report the terms *breach development time* and *breach formation time* are used interchangeably.
[5] It is noted that, if the breach development time is estimated using a triangular hydrograph based on the peak flow rate and volume of water released from the reservoir using Equation 6 (see Section 6.2.8), then the estimated breach development time is 2.5 hours, which corresponds to the time between points B and D on Figure B.4.

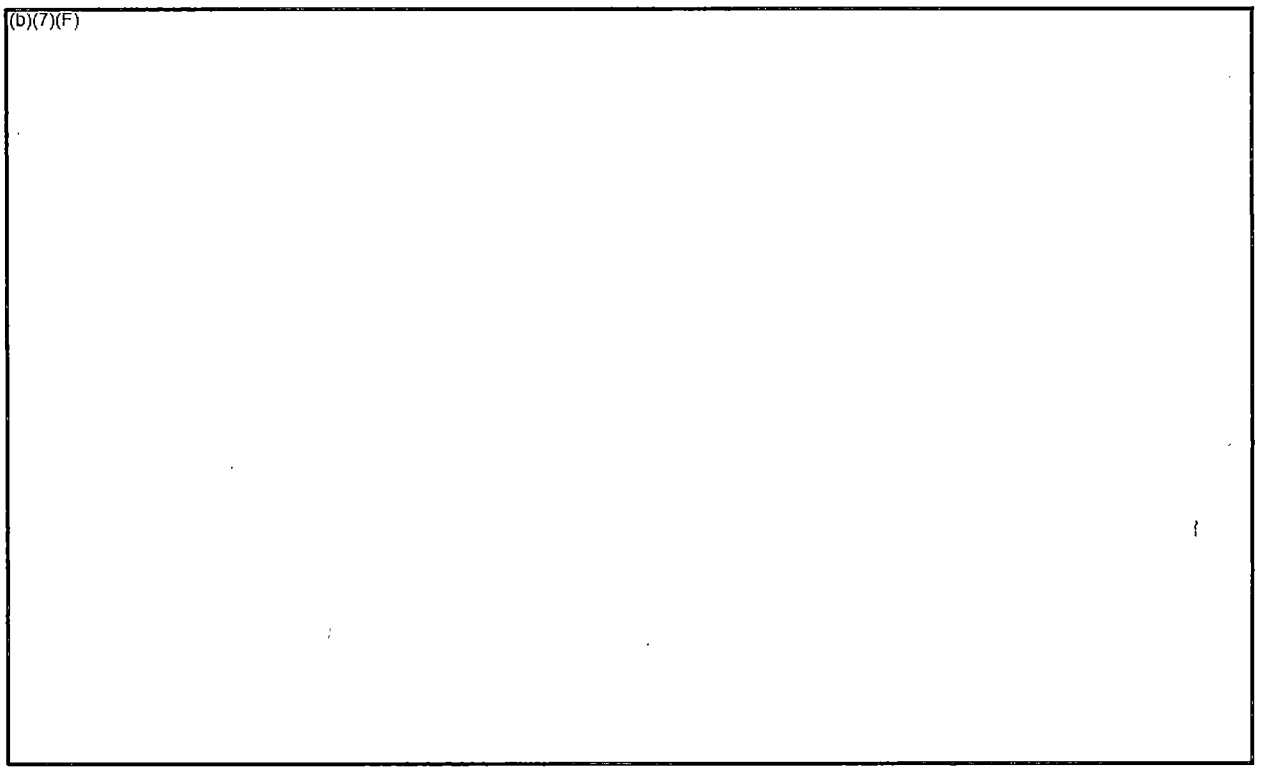

Figure B.5. Jocassee Dam breach progression relationship and breach hydrographs from the HRR (Duke 2013)

described in the previous paragraph, is shown by the black line (left scale). Points A, B and D are equivalent to points that are defined in Figure B.4.

The final values of the orifice and weir coefficients of 0.1 and 2.7, respectively, appear to be reasonable in terms of representing flow through the rockfill material and flow through the breach following collapse of the dam crest of the rockfill dam, respectively. In addition the form of the resulting breach hydrograph also appears to be reasonable for a piping failure mode and they closely match the Xu and Zhang (2009) median peak breach flow rate estimate. Point A represents the beginning of the failure time as defined by Xu and Zhang (2009) and is the beginning of the HEC-RAS modeling of the enlargement of the pipe. The breach progression curve was adjusted to keep the flow rate to a reasonably low magnitude prior to the collapse of the pipe and the onset of overtopping that is simulated at point B on Figure B.5. This point marks the end of the breach initiation phase as defined by Froehlich (1995b and 2008). Point D on Figure B.5 marks the end of the breach development phase as defined by Xu and Zhang (2009). The time between points B and D is longer than that estimated by other breach parameters estimation methodologies, but as is discussed in Section 6.5, the longer time is reasonable given the volume of the reservoir contents that must be released while simulating a peak breach flow rate that is consistent with the median predicted value.

In our February 2013 report (Ehasz and Bowles 2013) we concluded that the breach hydrograph in Figure B.5 is a *realistic but conservative* breach hydrograph, which has good

defendablity based on the validity of the Xu and Zhang (2009) method, the conservative nature of the median breach parameter estimates, a piping failure mode initiating in the (b)(7)(F) the deposition of rockfill immediately below the dam, the low erosion category of the rockfill material, and the various characteristics of a modern dam that were included in the design and construction of Jocassee Dam.

Appendix C

Bench Marking / Comparative Analysis

Appendix C.1

Benchmarking Rockfill Dams and Failures

BENCHMARKING/COMPARATIVE ANALYSIS

This Section presents the characteristics of several large embankment dams and describes the properties and failure conditions and their relevance to the J ocassee Dam

Benchmarking Rockfill Dams and Failures

Some of the large embankment dams that have failed over the past 50 years are summarized in the table at the end of this Appendix C.1. Although none of these dams are directly relevant to the potential breaching of the Jocassee Dam, as given by the characteristics of each dam and as compared to the modern design and character of Jocassee, they are the most closely related examples on record.

Oros Dam - Brazil 1960

- 116 feet high failed by overtopping during constr uction
- Cross-section contained very little rockfill – just outer zones
- Contained mostly sandy shell and sandy lean clay core
- 12 hours to initiate breach and 6.5 to 12 hours to breach and drain reservoir

Hell Hole – California, USA 1964

- 220 feet high failed by overtopping during constr uction
- Upstream sloping core with rockfill shells
- Rockfill was dumped rockfill, no compaction
- 29 hours after overtopping initi ated 20,000 cfs was passing through the rockfill
- 3 hours later the rockfill began to ravel and m ove downstream

Teton Dam – Idaho, USA 1976

- 305 feet high failed by piping during first filling
- Zoned earthfill embankment, no rockfill
- Pervious rock foundations with voids and irregular jointing
- Poor core trench design and tr eatment during constructi on
- Piping beneath and through the core for days or weeks
- Internal erosion of the core materials leaving large void within core
- Core collapsed into the large void and released the r eservoir
- Once core collapsed, failure occurred in 2.5+/- hours
- Failure was confined to right abutment where core collapsed

Taum Sauk UR Dam – Missouri, USA 2005

- 100 feet high concrete-faced rockfill dam failed by overtopping
- Rockfill was dirty, foundations were marginal and slopes were too steep (1.3H:1V)
- 10 feet high reinforced concrete parapet wall along crest
- Operated reservoir with high water levels 8 feet up the parapet wall
- Poor performance throughout life, large settlements and excessive leakage
- Overtopping of a 10 feet high parapet wall initiated slope failure and total failure
- Slope failed and released the reservoir, it was not an erosional breach
- Failure and draining of reservoir occurred in less than 1 hour

Tokwe Mukosi – Zimbabwe, 2014

- 300 feet high Concrete-Faced Rockfill Dam (CFRD) under construction
- Rockfill was compacted and slopes were 1V:1.3H
- Upstream facing was using cast-in-place curb to form upstream slope
- Upstream face was being prepared for concrete facing to be placed last
- Extreme flooding when rockfill embankment was 60% complete(200 feet)
- Water level rose to within 5 feet of existing crest
- Flood waters passed through rockfill for two weeks without failure
- Local downstream rockfill slopes raveled locally
- When flood waters receded, repairs to slopes were made and construction continued

Characteristics of Jocassee Dam (Modern Center Core Zoned Rockfill Dam) – South Carolina, USA

- 385 feet high central core zoned rockfill dam
- Protective filter and drain zones surrounding the core zone
- Densely compacted rockfill embankment with large rock outer zones and along the toe
- Widened core zone along the rock foundation contact to reduce gradients
- Grout curtain along foundation and special core material placement along the contact
- Quality control of materials and compaction
- Extensive instrumentation system and monitoring program
- 40 years of acceptable performance and continuous monitoring

A summary of some of the large embankment dams that have failed over the past 50 years

Dam	Sited	Failure Year	Dam Type	Height	Crest Length (feet)	Volume above breach (acre feet)	Erosion Category (Briaud)	Failure Mode	Breach Geometry (feet)				Peak Outflow (cfs)	Failure Time (total h)	Failure Time (piping h)	Failure Time (weir h)
									Height	Top Width	Bottom Width	Average Width				
Oros	Brazil	1960	Zoned Earth	116	2,034	535,100	ME	Overtop	118	656	426	541	340,035	8.5		8.5
Hell Hole	US	1964	Rockfill	220		24,800	LE	Piping*	185	574	219	397	259,882	50.0	44.0	6.0
Teton	US	1976	Zoned Earth	305	3,100	288,600	ME/HE	Piping	285	780	210	495	2,299,387	4.0	1.5	2.5
Taum Sauk	US	2005	Rockfill w/liner	100	6,562	4,300	ME	Overtop **	100				289,000	1.0		1.0
Tokwe-Mukosi	Zimbabwe	2014	CFRD	300	1,500	No Breach	LE	No Failure	N/A	N/A	N/A	N/A	N/A	N/A	N/A	N/A

NOTES:

*The Hell Hole failure was not a piping failure but was an overtopping of the core and flooding of the rockfill with flow through and over the rockfill until failure

**The Taum Sauk failure was caused by a dramatic ten foot overtopping of a parapet wall leading to a failure of the downstream slope and release of the reservoir.

Appendix C.2

Embankment Design Considerations Affecting Failures

EMBANKMENT DESIGN

The summary of the characteristics of other dams that have failed in recent times, as given in Appendix C.1 clearly outlines the fact that no modern rockfill dam has failed from internal erosion. Oros and Hell Hole dams were both under construction during failure and were failed by overtopping.

Oros Dam

Oros Dam was primarily a sand embankment with some rock protection along the outer shells and is therefore not relevant as a rockfill dam and should not be compared to Jocassee Dam since it is not as robust as Jocassee. Oros would be considered a medium to high erodibility embankment due to the fine materials that make up both the core zone as well as the sand materials within the shells. Due to the very wide cross-section erosion and failure took 6.5 to 12 hours.

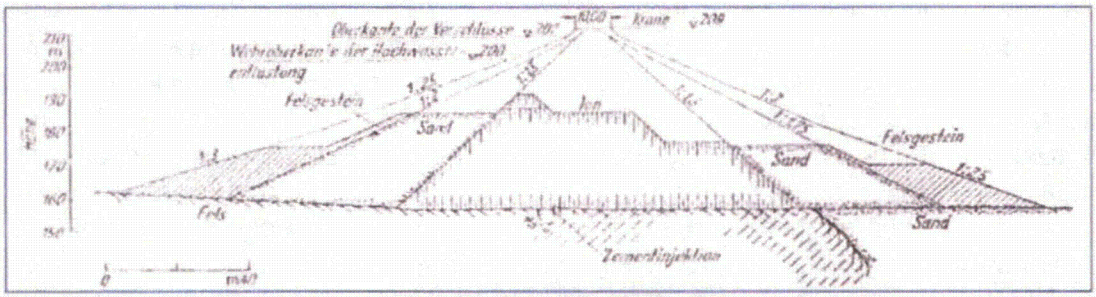

Oros Dam Cross-Section

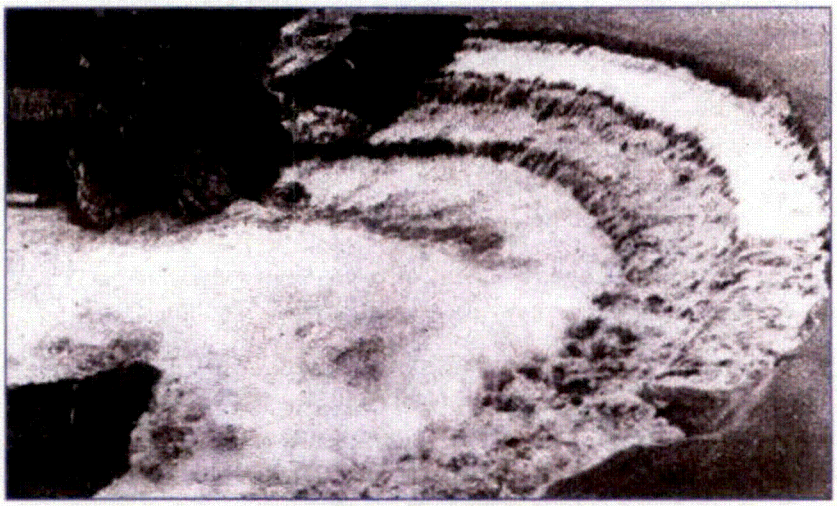

Oros Dam Overtopping

12 hours to Initiate Breach

6.5 to 12 hours to form breach and drain reservoir

Hell Hole Dam

Hell Hole was a rockfill dam, although dumped rockfill, and is the closest example from an erodibility viewpoint to Jocassee Dam. It had an upstream sloping core, and was partially constructed to a level below the adjacent downstream rockfill. The rising waters during the extreme flooding overtopped the lower level core, infiltrated the rockfill and eventually washed out the rockfill in a long and extreme process. The rockfill passed 20,000 cfs of flow for an extended time and with further rising upstream waters the rockfill began to ravel and eventually became unstable, slid downstream due to the excessive flows, formed a breach and failed.

The breaching mechanism of rockfill dams, according to the experimental tests on the rockfill dam breaching process performed at the Technical University in Lisbon, Portugal (Franca and Almeida 2002) as well as the experience and observations at Hell Hole Dam in California, is different from what is usually described for earth dam failures. The dam failure can be divided in two distinct phases: before the occurrence of the breach, and after the occurrence of the breach. In fact, until the moment when the breach develops, the downstream side of the dam experiences damage due to percolation and erosion due to overflow. The turbulent percolation flow induces slope movements, starting from the base of the flow, in an upward evolution until it reaches the surface of the rockfill. The degrading process, before the beginning of the breach, has a two-dimensional character and can be compared with typical landslide occurrences. After the initiation of the breach the flow is concentrated on the rockfill section, an eroded channel is formed in the breach direction, and the control section of the breach moves upwards. The breach cross-section evolution is due, not only to the continuous erosion induced by the flow, but also to the rock slides that occur from time to time when the equilibrium conditions are reduced. The other important facts observed in the tests and at the Hell Hole Dam failure and related to the overtopping failures of rockfill dams are the following:

- The flow over the dam induces damage on the downstream slope before initiation of the breach and influences the initial breach configuration – this damage is mostly two-dimensional sliding along the longitudinal axis of the dam;
- When the overflow discharge is enough to induce the initiation of the breach, a major and sudden slide occurs and the initi al breach appears;
- The overflow induces an initial breach width; however, the deposition of the rock blocks immediately downstream of the dam has a stabilizing effect, prolonging the failure process – this is reflected mainly in a shallower final breach depth.

Thus, a rockfill shell embankment provides more resistance to erosion, even during overtopping after the breach is initiated and thus would prolong the timing of the total breach development. Therefore, the Jocassee Dam, which is truly a rockfill dam, will provide the best resistance to erosion and be considered a low erodibility dam.

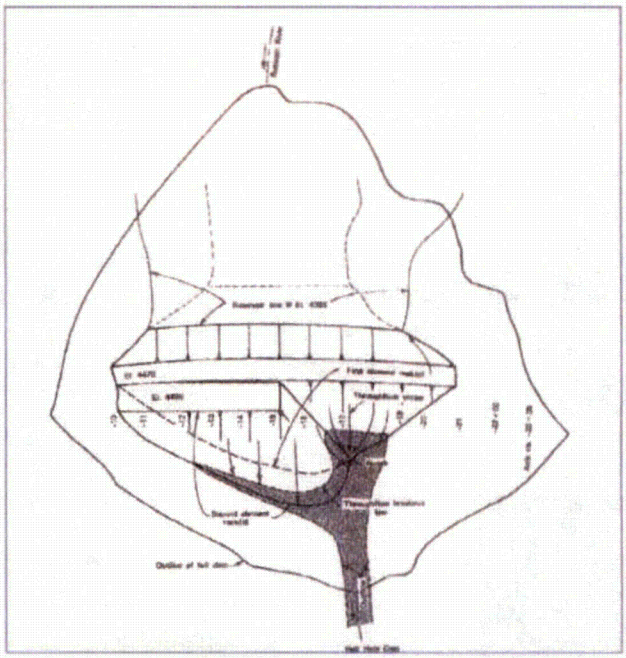

Hell Hole Dam Plan View

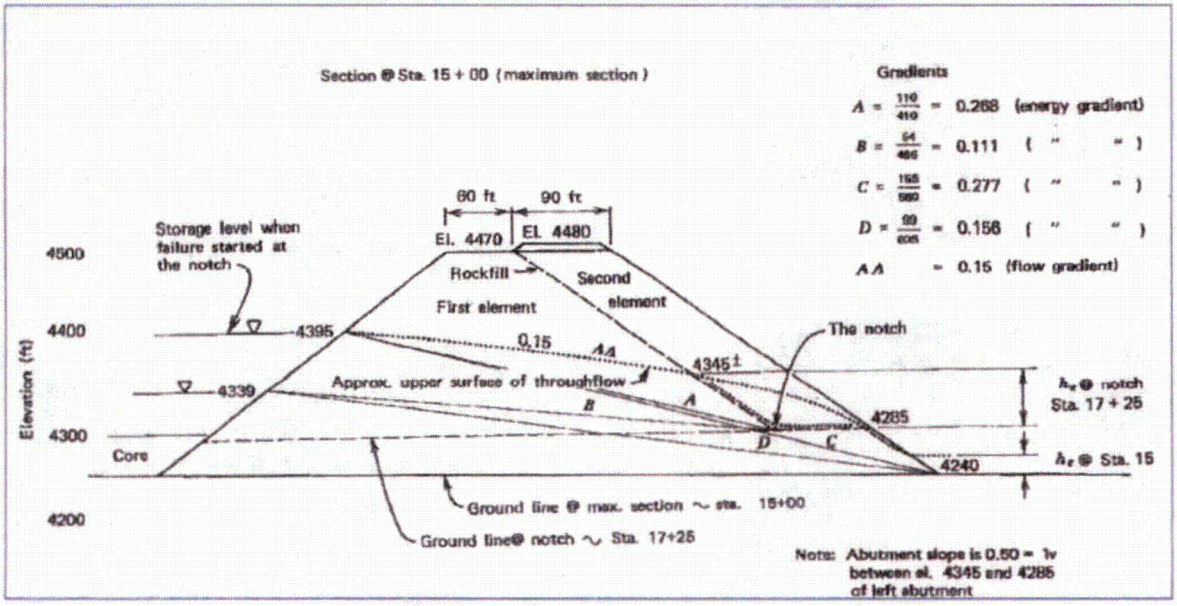

Hell Hole Dam Cross-Section

Failure of Hell Hole Dam

Construction of Hell Hole Dam on the Rubicon River in Placer County, California began in 1964. The dam failed during construction when the partially completed embankment was overtopped by a flood that was twice as big as the maximum flood of record.

The water emerging from the toe of the downstream rockfill shell at 3 pm on December 22, 1964. Some rock has been eroded.

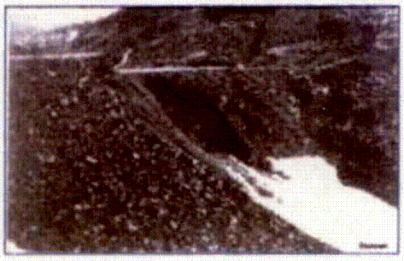

By 7 am on December 23rd, the flow had increased as the reservoir rose behind the dam, and a considerable portion of the downstream slope had been eroded away.

At 9:30 am on December 23rd, a gully had been eroded across the crest of the dam, and the reservoir began to spill over the top of the fill. When this happened the velocity of flow and the rate of erosion increased rapidly, and soon a major portion of the embankment was washed away and the reservoir was emptied.

At 3:30 pm on December 23rd, there was a gaping hole in the dam, and very little water in the reservoir.

Teton Dam

Teton Dam was essentially a homogeneous earth embankment dam constructed with the local wind-blown silts and sands and was therefore highly erodible. The outer slopes were somewhat protected by a mixture of coarse gravels and sands, which are highly erodible materials. The dam was founded on very porous rock conditions and contained voids and open jointing within the rock formations. Due to the poor design, foundation treatment and construction within the core trench and along the foundation contact, these factors facilitated piping of the core materials into the downstream rock formations. The movement and removal of core materials continued over a period of weeks and carried large volumes of core materials away from the core zone. This process was focused especially along the right abutment and caused a large cavity to be formed within the core of the dam (Osum 2013). That section of the core eventually collapsed as more and more material was removed and deposited within the rocks below the surface of the dam. This phenomenon was unnoticed during the core removal process. It was only when the removed materials began to fill the downstream voids that the flows exited along surface at the right abutment and began eroding the embankment itself.

The piping flows that carried the materials from the core rapidly increased and large amounts of water and soil materials exited from the face of the embankment. The local staff attempted to intervene by having bulldozers try to fill the developing openings and restrain the development of the openings, but to no avail. With the continued removal of materials the right abutment imploded into the large void that had formed within the core and the crest of the dam dropped into the opening.

This exposed the reservoir; a major breached developed, washed out the right abutment of the dam, and drained the reservoir. The unique undermining of the core by piping materials into the downstream rock voids was unnoticed and eventually formed the large cavity that collapsed. That collapse of the embankment into the void caused a premature collapse of the embankment leading to the breach. This premature collapse caused the dam to breach faster than if it were to form the breach by an erosion process. Thus, from a materials standpoint, and considering the foundation failure mechanism, and the rate of failure, the Teton Dam failure is not comparable to the rockfill materials, rate of erosion, and foundation geology at Jocassee Dam.

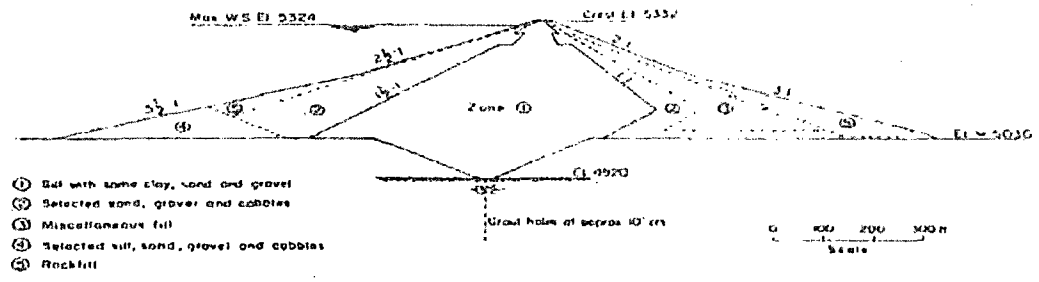

Fig.2. Cross-section through center portion of embankment founded on alluvium.

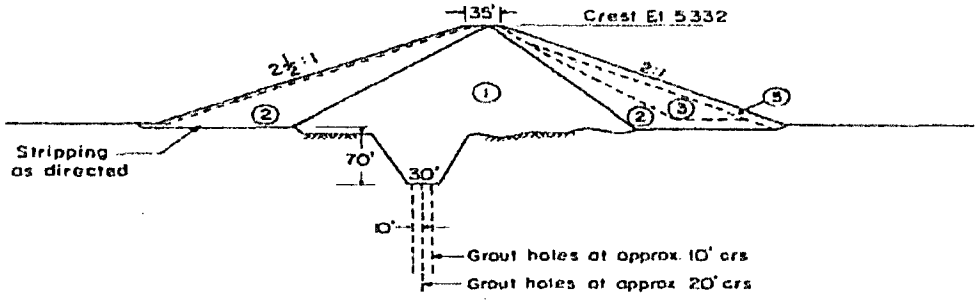

Fig.3. Typical cross-section over abutment sections founded on jointed rhyolite.

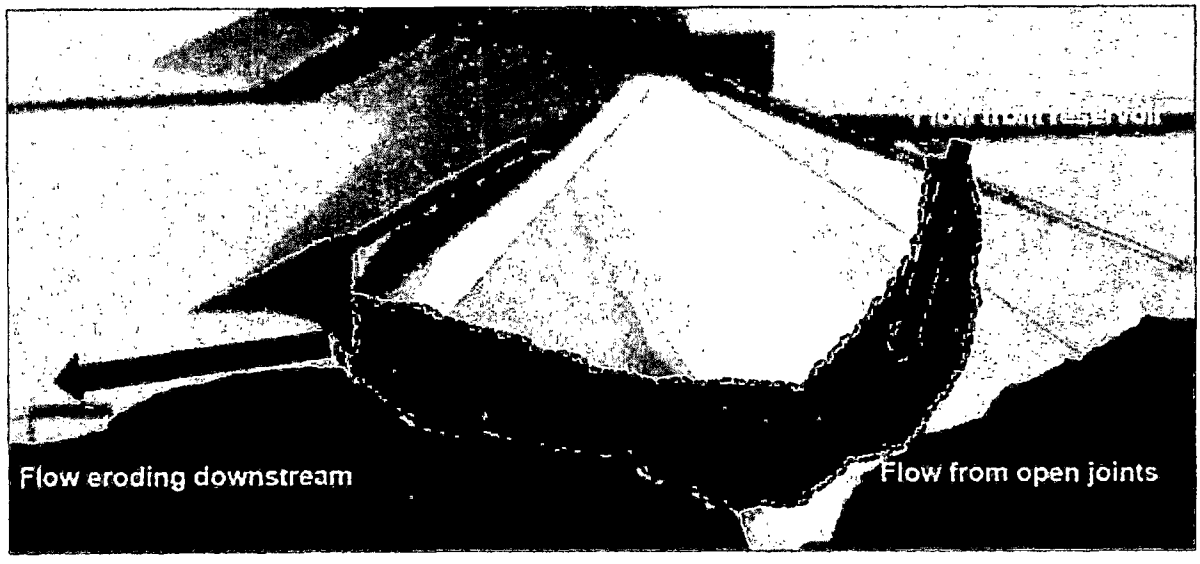

Taum Sauk Dam

Taum Sauk Upper Dam was a rockfill dam with an impervious upstream membrane. It was a dumped rockfill dam designed with very steep downstream slopes of 1.3H:1V and had a 10 foot high parapet wall along the crest. The rockfill was a dirty rockfill, which means the strength of the rockfill was not as high as a cleaner material, such as was used at Jocassee. Although just 100 feet high, it settled as much as two feet along various portions of its four mile length. This settlement had caused much distress to the reinforced concrete parapet wall and it had to be repaired several times during its operating life. Also, as a result of the embankment settlement, the upstream membrane suffered extreme cracking and eventually the entire upstream face of the dam was lined with a HDPE lining to reduce the water losses and improve the stability of the embankment and foundations. During the installation of the lining system a new instrumentation system was installed to record the reservoir levels. Unfortunately the system was not anchored properly along the interior slope of the dam and it moved during reservoir operations. This gave false readings to the operators and allowed the pumps to overfill the reservoir, which resulted in overtopping of the dam. The parapet wall along the crest of the dam was founded on and within the dam crest. The overtopping allowed the water to erode the crest along the downstream foundation of the parapet wall and caused the wall to overturn and fail. The wall failure caused a 10 foot surge of water to rapidly washout the toe of the downstream slope. This immediately caused instability and failed the over-steep slope. Since the downstream slope was marginally stable at 1.3H:1V it failed very quickly and released the reservoir. Thus, the Taum Sauk failure was not a typical overtopping dam breach caused by erosion; but instead it was a slope failure that released the reservoir. Therefore the dam breached very quickly, which is not a representative failure by erosion of a rockfill dam. Thus, the failure at Taum Sauk Dam should not be compared to the material quality, slope configuration or failure mechanism that is postulated for Jocassee Dam. At Jocassee Dam the embankment materials would have to be eroded and thus reduce the section to expose the core to the reservoir and form the open breach that would eventually fail.

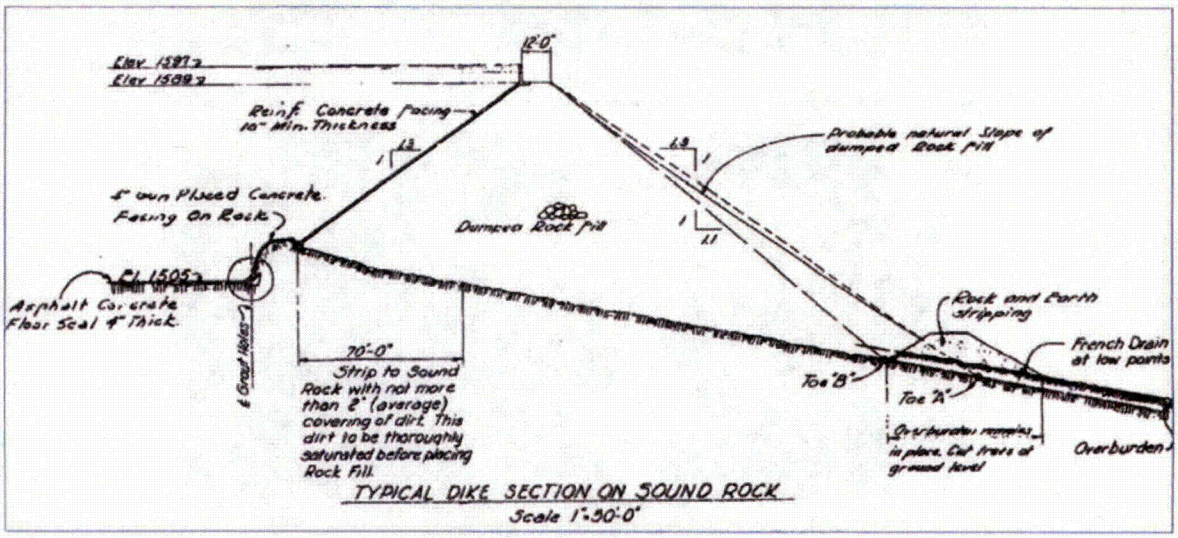

Taum Sauk Cross-Section

Taum Sauk Breach

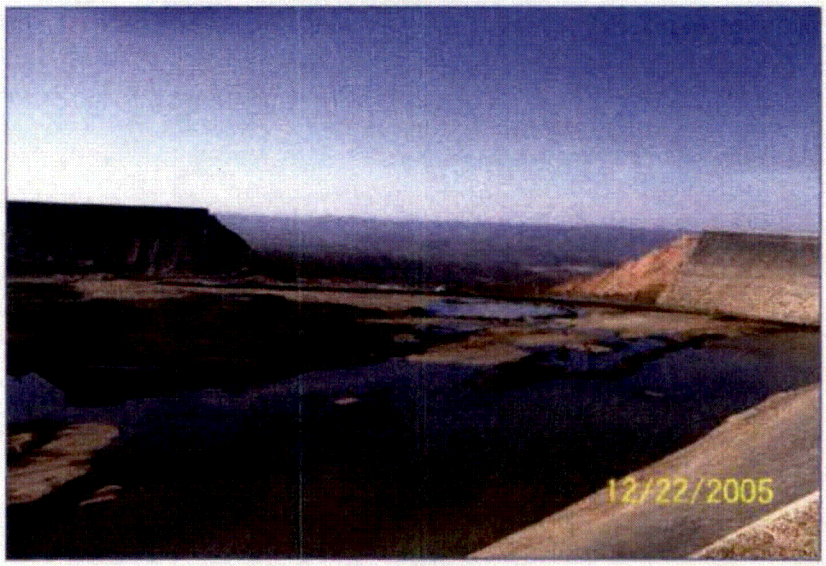

Taum Sauk Breach

Taum Sauk Breach

Tokwe-Mukosi Dam

The Tokwe-Mukosi Dam in Zimbabwe represents the most recent example, February 2014, of the low erodibility of rockfill dams. The project involves the construction of an 90 m (300 ft) high Concrete Faced Rockfill Dam (CFRD) on the Tokwe River and forming a large reservoir impounding 1.8 billion cubic meters (1.46 million AF); the largest reservoir in the Country of Zimbabwe . The Owner of the project is the Ministry of Water Resources Development and Management Harare – Zimbabwe. While the rockfill portion of the dam construction was approximately 60% complete (200 feet) an extreme flood occurred in the watershed and the upstream water level rose to within 5 feet of the crest of the rockfill. The construction on the rockfill continued throughout the flooding of the upstream reservoir and the partially constructed rockfill portion held back the waters while discharging water through the rockfill to the downstream.

Tokwe-Mukosi Dam is a Concrete Face Rockfill Dam (CFRD) under construction. It consists of compacted hard rockfill shell and had an upstream sloping transition rock surface in preparation for the future reinforced concrete facing, when the flood occurred. The dam was partially constructed when the rising waters during the extreme flooding came within five feet of the crest, infiltrated the rockfill and eventually washed through the rockfill in a long and extreme process. The rockfill passed extreme flows for an extended time (two weeks). With the long period of extreme flows, portions of the downstream slope began raveling but the rockfill embankment maintained overall stability.

Thus, the Tokwe-Mukosi Dam, a compacted rockfill shell embankment provided high resistance to erosion, even during extreme flows through the rockfill, similar to the Hell Hole example above. The dam withstood extreme flows for several weeks and only experienced local downstream raveling. Therefore, the Jocassee Dam, which is truly a rockfill dam, will provide the best resistance to erosion and can be considered a low erodibility dam.

Tokwe-Mukosi Dam

Construction of Tokwe-Mukosi Dam on the Tokwe River in Zimbabwe began in 1989. The dam experienced a flood during construction when the partially completed rockfill portion of the embankment was subjected to a flood that raised the upstream level to within five feet of the crest.

The water emerging from the toe of the downstream rockfill shell on February 2, 2014. Some rock has been eroded.

By February 4, 2014, the flow had increased as the reservoir rose behind the dam, and even with the extreme water flows through the rockfill it maintained its stability and resistance to erosion.

Even one week later February 9, 2014, when the flows had reduced, the rockfill maintained its stability and resistance to erosion.

The construction of the rockfill continued throughout the flood conditions and when the flood receded the rockfill would be restored and repaired.

The construction of the rockfill continued throughout the flood conditions and as the flood receded the rockfill was restored and repaired. See the following photos of the various stages of damage during the release of the floodwaters:


04 02 2014 12:46

Appendix D

Detailed Data Supporting Xu and Zhang Revisions

ANALYSIS OF DAM FAILURES AND DIAGNOSIS OF DISTRESSES FOR DAM REHABILITATION. Ph.D. thesis by Xiu Yao. 2010
75 CASE HISTORIES INCLUDED IN REGRESSION ANALYSIS
Froehlich 2008 and Wahl 1998 values interspersed for comparison
Changed values in red font

Dam No (RED ARE TO BE OMITTED)	Dam name	Location	Dam type	Dam height H_d (m)	Reservoir capacity Vd ($x10^6$ m^3)	Dam erodibility	Failure mode	Volume of water above breach invert V_w ($x10^6$ m^3)	Depth of water above breach invert H_w (m)	Breach geometry: Height H_b (m)	Top width B_t (m)	Bottom Width B_b (m)	Average width B_{ave} (m)	Side slope Z:1 (h:v)	Peak outflow rate Q_p (m^3/s)	Failure time T_f (hour)	Triangular Calculated Failure Time (Froehlich Defn)	Notes	Notes on Erodibility Classification and Reasons for Omissions: 1977 Chinese Dams: Erodibility based on year construct	1977 Chinese Dams: Erodibility assigned if different to previous column	1977 Chinese Dams: Changes	1965 Rockfill / 1950 Earthfill US and other non-Chinese dams: Erodibility based on year construct	1965 Rockfill / 1950 Earthfill US and other non-Chinese dams: Erodibility assigned if different to previous column	1965 Rockfill / 1950 Earthfill US and other non-Chinese dams: Changes	Other Information: From Wahl (1998) Rec database	Other Information:	Other Information: Year Constructed	Other Information: Year Failed	Data Source/Quality (All Chinese Dams are in Chinese Dam Failure Database, IWHE, Beijing,)
1	Apishapa	USA	HD	34.1	22.5	HE	SEP	22.2	28	31.1	91.5	81.5	86.5	0.44	6850	2.5	1.80	const 1920, poor compaction				HE			Piping	Homogeneous earthfill, fine sand	1920	1923	Froehlich 2008
Froehlich 2008					(like 22.5)			22.8					90			0.75													
Wahl 1998													80															
3	Baimalu	China	HD	8	0.2	ME	OT	0.2	8	8	40							homog silty clay const 1975, earthfill	HE	ME	silty clay justify ME						1975		
6	Banqiao	China	OC	24.5	492	HE	OT	697.5	31	28.5	372	210	291	0.3	78100	5.5	4.32	const 1953 poor compaction	HE								1953		Very detailed confidential investigative report in Chinese
Wahl CEATI																2.5													
7	Bayi	China	HD	30	30	ME	SEP	23	28	30	45	35	40	0.17	5000		2.56	clay L-M const 1957 M	HE	ME	clay justify ME						1957		Detailed confidential investigative report in Chinese
10	Castlewood	USA	DC	21.3	4.23	ME	OT	6.17	21.6	21.3	54.9	33.5	44.2	0.5	3570		0.96	earthfill w masonry core wall L-M, const 1890 M				HE	ME	OMIT masonry core wall	Overtop	Earthrockfill with masonry wall	1890	1933	Froehlich 2008
Froehlich 2008			E, M													0.5													
21	Chenyeng	China	HD	12	4.25	ME	OT	5	> 12	12					1200	1.83	2.31	clay L-M const 1955 M	HE	ME	clay justify ME						1955		
27	Coedty	UK	DC	11	0.31	HE	OT	0.311	> 11	11	67	18.2	42.7	2.22				const 1924, narrow clay core - local moraine (clayey silt/silty clay)				HE		OMIT - Wahl states "core wall"	Overtop	Earthfill with corewall	1924	1925	Froehlich 2008
Froehlich 2008									11							0.25													
Wahl 1998																short													
29	Dalizhuang	China	HD	12	0.8	ME	OT	0.6	12	12	40							const 1970 poor comp M, silty clay L-M	HE	ME	silty clay justify ME						1970		Chinese Dam Failure Database, IWHE, Beijing
30	Danghe	China	OC	46	15.6	LE	OT	10.7	24.5	25	90	20	58	0.66	2500	3	2.38	earthfill, conc core L, constr 1975 L	HE	LE	OMIT due to concrete core						1975		Investigative Report
32	Davis Reservoir	USA	FD	11.9	58	ME	SEP	58	11.58	11.9	21.3	15.4	18.3	0.25	510		63.18	CFEarthD poor constr., const 1914 fail 1914				HE	ME	OMIT since CFRD	Piping	Earth with concrete facing	1914	1914	
34	Delta	USA		18.3	13	HE	OT	13	18.3	18.3	112.8				5440	0.67	1.33	const 1908, poor const, glacial	HE			HE					1908		
33	Dongchuanliou	China	HD	31	27	HE	OT	27	31	31					21000		0.71	const before 1963, failed 1963, homog earthfill, poor const., rapid T -	HE								1963	1963	Investigative Report
36	Dushan	China	HD	17.7	0.67	ME	OT	0.67	17.7	17.7	70							silty clay L-M, const 1908 M	HE	ME	silty clay justify ME						1908		Chinese Dam Failure Database, IWHE, Beijing
38	Elk City	USA	DC	9.1	0.74	ME	OT	1.19	9.44	9.14	45.5	27.7	36.6	1		0.83		earthfill, conc wall, const 1925 (wall offsets year)				HE	ME	OMIT - concrete core wall	Overtop	Rolled sandy clay fill with concrete corewall	1925	1938	Froehlich 2008

ANALYSIS OF DAM FAILURES AND DIAGNOSIS OF DISTRESSES FOR DAM REHABILITATION. Ph.D. thesis by Xu Yao, 2010
75 CASE HISTORIES INCLUDED IN REGRESSION ANALYSIS
Froehlich 2008 and Wahl 1998 values interspersed for comparison
Changed values in red font

Dam No RED ARE TO BE OMITTED	Dam name	Location	Dam type	Dam height H_w (m)	Reservoir capacity Vd ($x10^6$ m^3)	Dam erodibility	Failure mode	Volume of water above breach invert V_w ($x10^6$ m^3)	Depth of water above breach invert H_w (m)	Breach geometry: Height H_b (m)	Breach geometry: Top width B_t (m)	Breach geometry: Bottom Width B_b (m)	Breach geometry: Average width B_{ave} (m)	Breach geometry: Side slope Z:1 (h:v)	Peak outflow rate Q_p (m^3/s)	Failure time T_f (hour)		Triangular Calculated Failure Time (Froehlich Defin)
42	Erlangmiao	China	HD	12.1	0.198	ME	OT	0.196	9	9	36	1.6	18.8	1.9				
44	Fengzhuang	China	HD	10	0.625	ME	OT	0.625	8	8	40	30	35	0.63				
46	Frankfurt	Germany	HD	9.8	0.35	LE	SEP	0.352	8.23	9.75	9.2	4.6	6.9	0.4	79	2.5		2.48
48	French Landing	USA	HD	12.2	-	HE	SEP	3.87	8.53	14.2	41	13.8	27.4	0.97	929	0.58		2.31
49	Frenchman Dam	USA	HD	12.5	21	ME	SEP	18	10.8	12.5	67	54.4	54.6	0.5	1420	3		6.26
50 Wahl 1998	Frias	Argentina	FD Homogeneous rockfill	15	0.25	ME	OT	0.25	15	15	62				400	0.25		9.35
54	Gouhou	China	FD	71	3.3	LE	SEP	3.18	44	48	138	61	99.5	1.27	2050	2.33		0.86
55 Froehlich 2008 Wahl 1998	Grand Rapids	USA	DC E, Z	7.6	0.22	ME	OT	0.256 0.0256	7.5 6.40d 6.4	7.5 6.4 6.4	12.2	9.1	10.7 19			0.5		
60	Hart	USA	HD	-	-	HE	SEP	6.35	10.7	10.8	106.8	41.2	73.9	3.03				
62	Hatfield	USA	-	6.8	12.3	HE	OT	12.3	6.8	6.8		6.1	91.5		3400	2		2.01
64 Froehlich 2008	Hell Hole	USA	Rockfill R, Z	87.1	30.6	ME LE	SEP	30.6	35.1	56.4	175.1	66.9	121	0.96	7360	0.75		2.31

Dam No RED ARE TO BE OMITTED	Notes	Notes on Erodibility Classification and Reasons for Omissions: 1977 Rockfill / 1960 Earthfill — Chinese Dams: Erodibility based on year construct.	Chinese Dams: Erodibility assigned if different to previous column	Chinese Dams: Changes	US and other non-Chinese dams: Erodibility based on year construct.	US and other non-Chinese dams: Erodibility assigned if different to previous column	US and other non-Chinese dams: Changes	Other Information: From Wahl (1998) Rec database		Year Construct	Year Failed	Data Source/Quality (All Chinese Dams are in Chinese Dam Failure Database, WHE, Beijing.)
42	dirty clay L-M, const 1966, poor const M	HE	ME	dirty clay justify ME						1966		
44	dirty clay L-M, const 1966, poor const M	HE	ME	dirty clay justify ME						1966		
46	const 1975, assume good quality, homog., relatively long T for very small volume released (and small breach width/breach height ratio)				ME	LE	LE, relatively long T for very small volume released (and small breach width/breach height ratio)	Piping	Earthfill	1975	1977	
48	const 1925, homog earthfill, v short T - see T				HE			Piping	Homogeneous earthfill	1925	1925	Froehlich 2008
49	const and fail 1952, Singh shows 244 m wide,				ME			Piping	Homogeneous earthfill	1952	1952	Froehlich 2008
50	CFRD, L, const 1940, H, overtop 1970 - used M				HE	ME	OMIT - CFRD	Overtop	Homogeneous rockfill	1940	1970	
54	CFRD const well except for connection between conc face and struct conc poor (K.Hoge 4 mm d50??), fail 1993, const 1990,	ME	LE	OMIT since CFRD						1990	1993	Very detailed investigative report
55	earthfill, puddle clay core, const 1874, fail 1900				HE	ME	puddle clay core	Overtop	Earthfill with clay corewall	1874	1900	Froehlich 2008
60	const 1920, homog dam, no other info				HE			Piping	Homogeneous earthfill	1920	1986	Froehlich 2008
62	const 1908, no other info, assumed poor comp				HE		OMIT - not representative, large vol, small hgt, rel long T and wide breach			1908	1911	
64	rockfill, const 1964,				ME		LE for rockfill	Piping	Rockfill	1964	1984	Froehlich 2008

~~Contains Security Sensitive Information - Withheld from public disclosure per 10 CFR 2.390(d)~~

ANALYSIS OF DAM FAILURES AND DIAGNOSIS OF DISTRESSES FOR DAM REHABILITATION. Ph.D. thesis by Xu Yao. 2010
75 CASE HISTORIES INCLUDED IN REGRESSION ANALYSIS
Froehlich 2008 and Wahl 1998 values interspersed for comparison
Changed values in red font

Dam No (RED ARE TO BE OMITTED)	Dam name	Location	Dam type	Dam height H_d (m)	Reservoir capacity Vol (x10^6 m^3)	Dam erodibility	Failure mode	Volume of water above breach invert V_w (x10^6 m^3)	Depth of water above breach invert H_w (m)	Breach geometry: Height H_b (m)	Top width B_t (m)	Bottom Width B_b (m)	Average width B_{ave} (m)	Side slope Z:1 (h:v)	Peak outflow rate Q_p (m^3/s)	Failure time T_f (hour)	Triangular Calculated Failure Time (Froehlich Defin)	Notes	Notes on Erodibility Classification and Reasons for Omissions: 1977 Chinese Dams: Erodibility based on year construct	1977 Chinese Dams: Erodibility assigned if different to previous column	1977 Chinese Dams: Changes	1965 Rockfill / 1950 Earthfill US and other non-Chinese dams: Erodibility based on year construct	1965 Rockfill / 1950 Earthfill US and other non-Chinese dams: Erodibility assigned if different to previous column	1965 Rockfill / 1950 Earthfill US and other non-Chinese dams: Changes	Other Information: From Wahl (1998) Rec database	Other Information:	Other Information: Year Construct	Other Information: Year Failed	Data Source/Quality (All Chinese Dams are in Chinese Dam Failure Database, IWHE, Beijing.)
67	Horse Creek	USA	FD	12.2	21	ME	SEP	12.8	7.01	12.8	76.2	70	73.1	0.83	3890	3	1.83	CFEarthD, const 1912 (1911? Wahl 1998), fail 1914 (Wahl 1998); Singh				HE	ME	OMIT CFEarthD	Piping	Homogeneous earthfill with concrete	1911	1914	Froehlich 2008
Froehlich 2008			E, H																										
68	Hougou	China	HD	8	0.24	ME	OT	0.24	8	8			20					const 1965; homog earthfill, no info on soil type; used ME because ratio of breach width to hgt = 2.5	HE	ME							1965		Chinese Dam Failure Database, IWHE, Beijing
71	Huoshaoshan	China	HD	13	0.22	HE	OT	0.22	16	16	45	15	30	0.94				poor const 1972, sandy silt	HE								1972		Chinese Dam Failure Database, IWHE, Beijing
72	Huyitang	China	HD	9.9	0.734	LE	SEP	0.424	5.1	9	12	3	7.5	0.6	50	4	4.71	narrow breach and 4 hr T - therefore LE, material?	HE	LE	OMIT Year built unknown								Chinese Dam Failure Database, IWHE, Beijing
77	Jiahesi	China	HD	18	80	HE	SEP	42	12	18	161							fail 1961, const before 1961, top width 10x breach hgt but large res - piped around conduit - used HE	HE								1961	1961	Chinese Dam Failure Database, IWHE, Beijing
80	Johnstown	USA	CF	38.1	18.9	ME	OT	18.9	24.6	24.4	128	61	84.5	1.38	8500		1.24	Zoned earth and rockfill, fail 1889, trash screen clogged with debris leading to Overtop				HE	ME	ME because of rockfill	Overtop	Zoned earth and rockfill	1853	1889	
82	Kelly Barnes	USA	HD	11.6	0.505	HE	OT	0.777	11.3	12.8	35	18	27.3	0.85	680	0.5	0.63	Homogeneous earthfill, const 1948, T=0.5 - relatively short				HE			Piping	Homogeneous earthfill	1948	1977	Froehlich 2008
Froehlich 2008 Wahl 1998			P Piping																										
84	Kodaganar	India	HD	11.5	12.3	ME	OT	12.3	11.5	11.5					1280		5.34	const 1977, earth dam, (long T - large res for small dam)				ME					1977		
89	Lake Frances	USA	HD	15.2	0.865	ME	SEP	0.789	14	17.1	30	10.4	18.9	0.65		1		Homogeneous earthfill, const and fail 1899				HE	ME	ME, Low av width/hgt ratio	Piping	Homogeneous earthfill	1899	1899	Froehlich 2008
91	Lake Latonka	USA	HD	13	4.59	ME	SEP	4.09	6.25	8.69	49.5	28.9	38.2	1.18	290	3	7.84	homog fill of coh clay - Singh p 90				ME		LE since homog clay fill	Piping	Homogeneous earthfill	1966	1986	Froehlich 2008
Froehlich 2008 Wahl 1998					1.58	LE		use 1.58									3.06												
97	Lyaju	China	HD	25	1.14	ME	OT	1.14	25	25					2950		0.21	const 1970, homog earthfill, no spillway/only a conduit.	HE	ME	HE due to short triang T						1970		Investigative Report
						HE																							

ANALYSIS OF DAM FAILURES AND DIAGNOSIS OF DISTRESSES FOR DAM REHABILITATION. Ph.D. thesis by Xu Yao, 2010
75 CASE HISTORIES INCLUDED IN REGRESSION ANALYSIS
Froehlich 2008 and Wahl 1998 values interspersed for comparison
Changed values in red font

Dam No (RED ARE TO BE OMITTED)	Dam name	Location	Dam type	Dam height H_d (m)	Reservoir capacity Vol (x10^6 m^3)	Dam erodibility	Failure mode	Volume of water above breach invert V_w (x10^6 m^3)	Depth of water above breach invert H_w (m)	Breach geometry: Height H_b (m)	Top width B_t (m)	Bottom Width B_b (m)	Average width B_{ave} (m)	Side slope Z:1 (h:v)	Peak outflow rate Q_p (m^3/s)	Failure time T_f (hour)	Triangular Calculated Failure Time (Froehlich Defin)	Notes	Notes on Erodibility Classification and Reasons for Omissions: 1977 Chinese Dams: Erodibility based on year construct	Erodibility assigned if different to previous column	Changes	1960 1995 Rockfill Earthfill: US and other non-Chinese dams: Erodibility based on year construct	Erodibility assigned if different to previous column	Changes	Other Information: From Wahl (1998) Rec database		Year Construct	Year Failed	Data Source/Quality (All Chinese Dams are in Chinese Dam Failure Database, IWHE, Beijing.)
99	Little Deer Creek	USA	HD	28.2	1.73	HE ME	SEP	1.36	22.9	27.1	49.9	9.3	29.6	0.75	1330	0.33	0.57	short T				ME	HE	WHI is low	Piping	Homogeneous earthfill	1952	1953	Froehlich 2008
101	Lupatar	China	DC	35.9	40.54	ME HE	OT	40.54	35.9	35.9					28000		0.80	earthfill w core const before 1963. T is short for ME	HE	ME	HE due to short inferred T						1963		Investigative Report
104	Longtun	China	DC	9.5	30	HE	OT	30	> 9.5	9.5	181							earthfill with inclined clay core M-H, fail 1959 during constr H, long breach top width	HE									< 1959	1959	Chinese Dam Failure Database, IWHE, Beijing
107 Froehlich 2008 Wahl 1998	Lower Otay	USA	DC	41.2	49.3	ME	OT	49.3	> 39.6	39.6	172	93.8	133	1		1 0.25		Singh p 91 - const 1897 dumped rockfill earth center steel plate embedded in cement mortar, fail 1916. See USGS ref fwd by Joe from Adam suggesting <2.5 hrs				HE	ME	OMIT because of uses plates and constraint of canyon walls, also Overtop described to fill d/s rockfill with water that started to ext at toe and failed rapidly (email pdf paper from Adam)			1897	1916	Froehlich 2008
108 Froehlich 2008 Wahl 1998	Lower Two Medicine	USA	HD	11.3	19.6	HE	OT P Piping	19.6 29.6	11.3	11.3	84	56	67	1.5	1800		6.05	Singh p 73: homog earthfill, long T, const 1913, fail 1964 (Froehlich 1995b has vol at 29.6 instead of 19.6, which Singh has on page 73)				HE		KEEP HE since WHI is large			1913	1964	Froehlich 2008
109	Lyman	USA	CF	19.8	49.5	HE	SEP	35.9	16.2	19.8	107	87	97	1				zoned earthfill, poor construction				HE			Piping	Zoned earthfill	1913	1915	Green Book
111	Lynde Brook	USA	DC	12.5	2.52	ME	SEP	2.88	11.6	12.5	45.7	16.3	30.5	1.22				earthfill with core wall L-M, const 1871 M				HE	ME	OMIT - due to core wall	Piping	Earthfill with corewall	1871	1876	Froehlich 2008
112	Mahe	China	HD	19.5	23.4	HE	OT	23.4	> 19.5	19.5					4950		2.63	homog earthfill, const before 1963, fail 1963	HE								1963	1963	Investigative Report
113 Wahl 1998	Mammoth	USA	DC	21.3	13.6	ME	OT Seepage	13.6	21.3	21.3			9.2		2520	3	3.00	const 1916, earthfill w core (Eng News ref - see Yao's list)				HE	ME	ME due to T=3	Seepage		1916	1917	Green Book
116 Froehlich 2008 Wahl 1998	Martin Cooling Pond Dike	USA	-	10.4	136	HE	SEP Foundtn Defect	136 125	8.53 5.06	12.8 9.14			188 183	0.1	3115	6	24.26	large vol, long T, silty sand				HE		silty sand - ok as HE	Foundtn Defect			1979	Wahl 1998

ANALYSIS OF DAM FAILURES AND DIAGNOSIS OF DISTRESSES FOR DAM REHABILITATION. Ph.D. thesis by Ku Yao. 2010
75 CASE HISTORIES INCLUDED IN REGRESSION ANALYSIS
Froehlich 2008 and Wahl 1998 values interspersed for comparison
Changed values in red font

Dam No (RED ARE TO BE OMITTED)	Dam name	Location	Dam type	Dam height H_d (m)	Reservoir capacity Vol ($x10^6$ m^3)	Dam erodibility	Failure mode	Volume of water above breach invert V_w ($x10^6$ m^3)	Depth of water above breach invert H_w (m)	Breach geometry: Height H_b (m)	Top width B_t (m)	Bottom Width B_b (m)	Average width B_{ave} (m)	Side slope Z:1 (h:v)	Peak outflow rate Q_p (m^3/s)	Failure time T_f (hour)	Triangular Calculated Failure Time (Froehlich Delbu)	Notes	Notes on Erodibility Classification and Reasons for Omissions: 1977 Rockfill / 1960 Earthfill — Chinese Dams: Erodibility based on year construct.	Erodibility assigned if different to previous column	Changes	US and other non-Chinese dams: Erodibility based on year construct.	Erodibility assigned if different to previous column	Changes	Other Information: From Wahl (1998) Rev. database		Year Construct	Year Failed	Data Source/Quality (All Chinese Dams are in Chinese Dam Failure Database, IWHE, Beijing.)
125	Nujiangyu	China	DC	10	0.16	LE	SEP	0.144	7.2	7.2	20	6	13	0.93		3		earthfill with clay core; const 1973, narrow breach basis for LE but 3 hrs likely includes init time	HE	LE				DART since 3 hrs may include init time			1973		Investigative Report
128	Oros	Brazil	CF	35.4	660	LE	OT	660	35.8	35.5	200	130	165	1	9630	8.5	38.08	Zoned earthfill and rockfill. Failed during construction and was very wide top width - core clayey sand accounting for about half of the top width, sand shells with narrow cobbles zones. If 5-12 hours - ASDSO/CEATI Wahl PPT				ME	LE	Change to ME	Overtop	Zoned earthfill and rockfill	1960	1960	Froehlich 2008
Froehlich 2008						ME																							
129	Otter Lake	USA	HD	6.1	0.15	ME	SEP	0.109	5	6.1	17.1	1.5	9.3	1.29				breach width/height				HE	ME	DART - due to lack of individual construction	Piping	Earthfill			Froehlich 2008
134	Potato Hill Lake	USA	HD		-	ME	OT	0.105	> 7.77	7.77	26.2	6.8	16.5	1.25				Homogeneous earthfill, const 1947, fail 1977, breach width/hgt ~2.5				HE	ME	DART due to lack of information	Overtop	Homogeneous earthfill	1947	1977	Froehlich 2008
Wahl 1998									7.77																				
135	Prospect	USA	HD		-	HE	SEP	3.54	1.66	4.42	91.4	85.4	88.4	0.69	116	2.5	16.95	const 1914 H. Homogeneous earthfill, wide breach				HE			Piping	Homogeneous earthfill	1914	1980	Froehlich 2008
Froehlich 2008																													
137	Qielinggou	China	HD	18	0.7	HE	OT	0.7	18	18					2000	0.17	0.19	earthfill, const 1972 and v short time is basis for HE	HE								1972		Investigative Report
138	Quail Creek	USA	HD	24	50	ME	SEP	30.8	18.7	21.3	72.1	67.9	70	0.1	3150		5.59	Homogeneous earthfill, const 1986, MATERIAL/REPORT				ME		Use T from Froehlich	Piping	Homogeneous earthfill	1986	1989	Froehlich 2008
Froehlich 2008																1													
142	Rio Manzanares	USA	HD	7.3	0.0247	HE	SEP	0.0247	4.57	7.32	19	7.6	13.3	0.77				Homogeneous earthfill, fail 1975, silty material H				ME	HE	HE - due to silty material	Piping	Homogeneous earthfill	1975	1975	Froehlich 2008
145	Schaeffer Reservoir	USA	DC	30.5	3.92	HE	OT	4.44	> 30.5	30.5	210	64	137	2.25	4500	0.5	0.55	Earthfill with concrete corewall, const fail 1921				HE			Overtop	Earthfill with concrete corewall	1921	1921	Froehlich 2008
Wahl 1998									30.5																				
148	Shangluzhuang	China	HD	14	0.11	ME	OT	0.11	14	14	30							const 1964, homog earthfill, not unusual breach top width to height ratio	HE	ME	Change to HE						1964		Chinese Dam Failure Database, IWHE, Beijing
						HE																							

ANALYSIS OF DAM FAILURES AND DIAGNOSIS OF DISTRESSES FOR DAM REHABILITATION, Ph.D. thesis by Xu Yao, 2010
75 CASE HISTORIES INCLUDED IN REGRESSION ANALYSIS
Froehlich 2008 and Wahl 1998 values interspersed for comparison
Changed values in red font

Dam No. RED ARE TO BE OMITTED	Dam name	Location	Dam type	Dam height H_d (m)	Reservoir capacity Vol ($x10^6$ m^3)	Dam erodibility	Failure mode	Volume of water above breach invert V_w ($x10^6$ m^3)	Depth of water above breach invert H_w (m)	Breach geometry: Height H_b (m)	Top width B_t (m)	Bottom Width B_b (m)	Average width B_{ave} (m)	Side slope Z:1 (h:v)	Peak outflow rate Q_p (m^3/s)	Failure time T_f (hour)	Triangular Calculated Failure Time (Froehlich Defin)	Notes	Notes on Erodibility Classification and Reasons for Omissions: 1977 / 1965 Rockfill / 1950 Earthfill — Chinese Dams: Erodibility based on year construct	Chinese Dams: Erodibility assigned if different to previous column	Chinese Dams: Changes	US and other non-Chinese dams: Erodibility based on year construct	US and other non-Chinese dams: Erodibility assigned if different to previous column	US and other non-Chinese dams: Changes	Other Information: From Wahl (1998) Rec database		Year Construct	Year Failed	Data Source/Quality (All Chinese Dams are in Chinese Dam Failure Database, IWHE, Beijing.)
149	Shanhu	China	HD	11.5	2.15	HE	SEP	1.78	12.5	13	58	24	41	1.31				poor construction, const 1975	HE								1975		Chinese Dam Failure Database, IWHE, Beijing
150	Sheep Creek	USA	HD	17.1	1.43	ME	SEP	0.91 / 2.91	14.02	17.1	30.5	13.5	22	0.5				[illegible], const 1969, fail 1				ME			Seepage	Earthfill	1969	1970	Green Book
Wahl 1998 152	Shilongshan	China	HD	14	2.06	ME / HE	OT	2.06	14	14	50							const 1971, homog earthfill	HE	ME							1971		Chinese Dam Failure Database, IWHE, Beijing
153	Shimantan	China	HD	25	94.4	HE	OT	117	27.4	25.8	446	288	367	0.32	30000	5.5	2.17	homog earthfill, poor compaction, const 1951, fail 1975	HE								1951	1975	Investigative Report
156	Spring Lake	USA	HD	5.5	0.135	HE	SEP	0.136	5.49	5.49	20	9	14.5	1				Homogeneous earthfill, clay and gravel, const 1887, fail 1889				HE			Piping	Homogeneous earthfill clay and gravel	1887	1889	Eng News Record Vol 47.25 507 1902
157	Statham Lake	USA	HD	5.5	-	ME	OT	0.564	5.55	5.12	23.8	18.2	21	0.54				Homogeneous earthfill, const 1955, fail 1994				ME			Overtop	Homogeneous earthfill	1955	1994	Froehlich 2008
133	Swift	USA	FD	57.6	37	ME	OT	37	47.85	57.6	221	225	225	0	24947		0.82	const 1914 (Eng News Record), CFRD, large crest breach - was it a slope failure?				HE	ME	OMIT - CFRD			1914		Eng News Record Vol 172:25:63 1964
Wahl 1998 160 Froehlich 2008	Teton	USA	CF	93	356	ME / HE	SEP	310	77.4	86.9	237.9	64.1	151	1	65120	short / 4 / 1.25	2.64	silty sand , no filters, piping cavity reduced failure time (Osmun PPT)				ME		HE/ME Brand	Piping	Zoned earthfill	1975	1976	Froehlich 2008
161	Tiemusi	China	HD	12	0.11	HE	OT	0.11	12	12	60							const 1968, fail 1975, poor const, homog earthfill	HE								1968	1975	Chinese Dam Failure Database, IWHE, Beijing
162	Tongshuyuan	China	HD	13	0.4	ME	OT	0.4	10	10	30							homog earthfill, const 1973, breach width to height about 3:1 and smaller breach for bigger res of Tiemusi is basis for ME	HE	ME	Breach width to height about 3:1 and smaller breach for bigger res of Tiemusi is basis for ME						1973		Chinese Dam Failure Database, IWHE, Beijing
163 Froehlich 2008	Trial Lake	USA	E H		-	ME	SEP	1.48	5.18	5.18	26.2	16.8	21	0.82				lack of info: breach width/height 4:1, const 1914, fail in 1980s. Also earlier dam that failed about 1890?				HE	ME	OMIT - lack of info/ inconsistent (Res. Cap. 3.02 mil m3, 18.3 m (Joe - url: State of MI WQ Stat'n)	Piping		1914	1980's	Froehlich 2008

~~Contains Security Sensitive Information - Withheld from public disclosure per 49 CFR 1.7(b)(4)~~

ANALYSIS OF DAM FAILURES AND DIAGNOSIS OF DISTRESSES FOR DAM REHABILITATION Ph.D. thesis by Xia Yao, 2010
75 CASE HISTORIES INCLUDED IN REGRESSION ANALYSIS
Froehlich 2008 and Wahl 1998 values interspersed for comparison
Changed values in red font

Dam No. RED ARE TO BE OMITTED	Dam name	Location	Dam type	Dam height H_d (m)	Reservoir capacity Vd ($\times 10^6$ m^3)	Dam erodibility	Failure mode	Volume of water above breach invert V_w ($\times 10^6$ m^3)	Depth of water above breach invert H_w (m)	Breach geometry: Height H_b (m)	Top width B_t (m)	Bottom Width B_b (m)	Average width B_{ave} (m)	Side slope Z:1 (h:v)	Peak outflow rate Q_p (m^3/s)	Failure time T_f (hour)	Triangular Calculated Failure Time (Froehlich Deltn)	Notes	Notes on Erodibility Classification and Reasons for Omissions: 1977 Chinese Dams: Erodibility based on year construct	Erodibility assigned if different to previous column	Changes	1965 Rockfill / 1950 Earthfill US and other non-Chinese dams: Erodibility based on year construct	Erodibility assigned if different to previous column	Changes	Other information: From Wahl (1998) Rec database		Year Construct	Year Failed	Data Source/Quality (All Chinese Dams are in Chinese Dam Failure Database, IWHE, Beijing.)
169	Upper Pond	USA	E, H	5.2	0.22	ME	OT	0.222	5.18	5.18	25.4	7.6	16.5	1.71				width/height 3:1				ME	ME	OMIT - lack of info	Overtop				Froehlich 2008
Froehlich 2008 169	Wanshangang	China	HD	13	1.5	ME	OT	1.5	> 12	12	50	30	40	0.83		—		fail 1975, homog earthfill, 4:1 width:height, hgt similar to previous two but res cap is much larger but breach only slightly larger than prev two Chinese	HE	ME	ME 4:1 width:height, hgt similar to previous two but res cap is much larger but breach only slightly larger than prev two Chinese dams						< 1975	1975	Chinese Dam Failure Database, IWHE, Beijing
170	Wilanson Lake	USA	DC	3.2	-	HE	SEP	0.533	3.57	3.72	35.5	22.5	29	1.74				Homogeneous earthfill with corewall, const 1956, fail 1984				ME	HE	OMIT due to core wall (correct hgt to Wahl 13.2)	Piping	Homogeneous earthfill with corewall	1956	1984	Froehlich 2008
171	Winston	USA	DC	7.3	0.664	LE	OT	0.662	6.4	6.1	21.3	18.3	19.8	0.2		5		Earthfill with corewall, earth with rubble core, const 1904, fail 1912				ME	LE	OMIT due to core wall	Overtop	Earthfill with corewall, earth with rubble core	1904	1912	Froehlich 2008
172	Yuanmen	China	HD	19.2	6.4	HE	OT	6.4	19.2	19.2						0.5		poor const, short fail T, const 1958	HE								1958		Chinese Dam Failure Database, IWHE, Beijing
180	Zhonghuaqu	China	HD	16	0.14	HE	OT	0.14	16	16						0.4		short T, poor comp, before 1980, dates?, narrow crest	ME	HE	Keep HE since constructed before 1980 with poor compaction						< 1980		Investigative Report
181	Zhuqou	China	DC	23.5	15.4	HE	OT	18.43	23.5	23.5	159	110	135	0.98	11200	0.43	0.91	short T, poor comp, const 1970	HE								1970		Investigative Report
182	Zuocun	China	DC	35	40	HE	OT	40	35	35					23000	1	0.94	short T, poor comp, fail 1963	HE								1963	1963	Investigative Report

Appendix E

Mark Morris Review

Jocassee Dam: Independent review of breach prediction methodology and supporting analyses outlined in the technical report:

Validation of HRR Breach Hydrograph for Jocassee Dam:
Through an in depth review of the Xu and Zhang breach parameter estimation methodology. March 2014

Objectives:

An independent review of the work undertaken to validate the approach taken for analysing the potential failure of the Jocassee Dam was undertaken and is reported here. This comprised a review of the technical report (Validation of HRR Breach Hydrograph for Jocassee Dam) and some of the associated / supporting material (as referenced in that report). The review was undertaken by Dr Mark Morris, who has extensive experience of both research into and industry application of breach analysis methodologies, see attached resume. The following provides a summary of key observations.

Observations:

1 Broadly – because of the nature of breach initiation and growth, it is impossible to predict the precise way in which a breach might form. Instead, a best prediction may be made, around which the degree of uncertainty and sensitivity should be examined. This is the approach which has been undertaken for the Jocassee Dam failure analyses, which is consistent with current good practice.

2 There are different degrees to which the breaching process might be analysed, ranging from pure judgement, through the use of equations based on historical failure data, through to more complex predictive modelling. For this analysis, the use of equations based upon regression analysis has been undertaken – and a potential flood hydrograph subsequently 'built' from this information. This decision defines the broad approach and hence the degree of detail that may be attributed to the hydrograph prediction and the associated uncertainty in the prediction.

3 Over the years there have been many equations developed to try to predict outflows in the event of a breach. The accuracy of these depends upon the parameters selected and the data upon which they are based (i.e. the types of dam, state of dam, failure mechanisms etc). A significant advance during the past 5-10 years has been a move to incorporate a measure of soil erodibility within both regression equations and predictive models. This is fundamental to predicting conditions associated with particular soil types and condition. The Xu and Zhang equations are the first time erodibility has been built into such equations, and are therefore considered current state of the art for this type of analysis (i.e. for using regression equations to predict breach failure).

4 Validation of regression equations can be undertaken by comparison against real events, controlled events and predictive models (that might be considered to more accurately reflect the breaching process). In the Jocassee study, an analysis of the development and validation

of the Xu and Zhang equations was undertaken. This analysis was extensive, covering the nature and quality of the base data used, as well as the method for equation development. This review was undertaken 'around the table' with the originators of the work, including Prof Briaud upon who's work the categories of erosion used were based. It is difficult to see how a more thorough review of the basis for the equations could have been undertaken.

5 Inclusion of material erodibility within the regression equations is a key advance, but then requires assignment of values of erodibility – in this case, high-medium-low, to appropriately represent the material type and state. The review by Prof Briaud addressed this important aspect, and provided independent assessment of the likely erosion category for Jocassee. This approach is consistent with industry good practice for breach analysis.

6 In addition to checking the original data and development of the predictive equations, new equations have been developed using openly accessible case data (i.e. excluding Chinese data which is not available outside of China). This removes any uncertainty relating to the quality of this data (even though that issue was addressed through careful consultation). The results from the new equations are broadly consistent with the earlier predictions.

7 Having undertaken an extensive assessment of the regression analysis methodology – including development and testing of revised equations based upon openly accessible data – it is worth remembering that there are practical limitations to the accuracy with which any regression equations can predict the breaching process. These have been carefully considered and discussed in the report; if a more detailed analysis of the potential processes is required then it is likely that this would only be achieved through undertaking more complex predictive modelling.

8 The approach adopted for prediction of the flood hydrograph makes use of the HEC RAS flow modelling software, within which there is a module designed to simulate growth of a breach and the associated production of a flood hydrograph. The approach has been to use parameters predicted by the Xu and Zhang equations as input to the HEC RAS breach module, and to adjust various breach parameters slightly to match the peak discharge predicted from the HEC RAS model to the Xu and Zhang equation. This approach is sensible and allows the creation of a realistic and representative flood hydrograph. There are likely to be some variations in the hydrograph descriptors in comparison to the regression analysis, since the two approaches accommodate different parameters. However, these differences should be within the typical ranges of uncertainty associated with breach prediction. Of all the parameters describing a breach flood hydrograph, the peak discharge is probably the most reliably predicted, hence tying the two methods via the peak discharge value and ensuring that the hydrograph volume matches the reservoir stored volume helps to limit uncertainties.

Conclusions:

The steps taken here to validate use of the Xu and Zhang regression equations for breach prediction have been very detailed and thorough. It is hard to see how more detailed analyses could be undertaken to support the recommended results without stepping from the level of regression analyses into more complex predictive breach modelling. The key aspects of (i) basis for the equations and (ii) representing the material erodibility have both been addressed in detail.

Mark Morris 14th April 2014
Mark.morris@samuifrance.com

Mark W Morris

Director

Company	**Samui France SARL**
Profession	Chartered Civil Engineer
Specialisation	Flood risk analysis (Dam and river engineering) Emergency planning Project management / Research coordination
Year of Birth	(b)(6)
Nationality	

Key Qualifications

- **Dam and Embankment Safety – Dam-break, Embankment Breach, Risk Assessment and Emergency Planning** – 20 years experience in dambreak analysis techniques, dam safety risk assessment and breach formation prediction at National and International levels supporting the development of emergency action plans. Studies include national and international research into fundamental processes and modelling tools, prioritisation of operational and research needs as well as consultancy studies.
- **Flood Defence and Flood Risk Assessment** – 25 years experience in conducting river engineering studies including desk, feasibility, design and environmental studies of river channels, hydraulic structures and flood plains. Experience in the assessment of flood risk, construction risk and the safety of hydraulic structures. Particular experience has been gained in the risk assessment of weirs and dams leading to failure of the structures and the analysis / prediction of breach development through embankments.
- **Project management, research coordination, training, technology transfer and dissemination** – 20 years experience in the management, co-ordination and implementation of international research projects, including various EU funded projects under FP4, FP5, FP6 and FP7. Experienced in the provision of technical courses, workshops and conferences on practical hydraulics and river engineering and in dissemination of research findings and applications to industry through production of industry guides, workshops and conference events. Specialist expertise in the development of web based tools and methods facilitating technical project management, and project communication and dissemination.

Career Summary

2011 – present	Director, Samui France SARL
2001 - 2011	Principal Engineer, Floods Group, HR Wallingford
1988 - 2001	Graduate to Senior Engineer, Various Groups, HR Wallingford
1987 - 1988	Graduate Engineer, Potable Water Dept., Sir M MacDonald & Partners, Cambridge

Education and Professional Status

PhD Breaching of earth embankments and dams. The Open University, 2012
BEng Hons (1st Class) in Engineering Science (Civil), Exeter University, 1987
Member of the Institution of Civil Engineers, 1993
Member of the Chartered Institution of Water and Environmental Management, 1993
Member of the British Dam Society Committee, 1999-2001, 2001-2005, 2005-2011
Member of the Reservoir Safety Advisory Group, 2007- present
Referee for journal publications including ICE and ASCE, 2006 – present
Member of the editorial committee for the BDS Journal of Dams and Reservoirs, 2008 - present
Member of the ASCE/EWRI task committee on dam / levee break fluvial processes, 2008 - 2012

Languages

	Speaking	Reading	Writing
English	Mother tongue	Mother tongue	Mother tongue
French	Good	Good	Reasonable

Current Practice

Mark Morris is Director of Samui France sarl, an independent consultancy established in France (Haute Savoie) focussing upon specialist research and consultancy supporting management of the environment, with a particular focus upon water. The core areas of work include specialist consultancy relating to reservoir safety, dam and levee performance (breach), and flood risk analysis and management.

In parallel, Mark collaborates extensively on European research projects, undertaking technical roles, project coordination and project communication and dissemination activities. Samui France, in conjunction with its sister company in the UK (Samui Design) develops web based tools and systems to support collaborative working and technical project communication and dissemination.

During 23 years of working at HR Wallingford, Mark developed world leading expertise in dam and levee breach analyses, leading to the development of the HR BREACH model, and supporting the more recent AREBA and EMBREA models. EMBREA arose from Mark's recent PhD studies into breach modelling. Mark was deputy coordinator of the European FLOODsite project, which supported implementation of the European Floods Directive. Within this project Mark also managed technical work on flood defence failure modes, and levee breach, much of which now underpins the fragility curves used to drive the UK Environment Agency system risk models. Mark also managed the FRMRCII work package relating to rapid breach model development (AREBA).

Selected Dam and Levee Projects

2009 – 2013 EUROPEAN FLOODPROBE PROJECT
European research investigating specific processes associated with urban flooding and levee performance. Specific research for levees includes the analysis of internal erosion processes, the performance of vegetation and the use of remote data for reliability analyses.

2012 DAMBREAK ANALYSIS FOR THE WLOCLAWEK DAM (VISTULA RIVER, POLAND)
Provision of expert advice to ARUP UK and ARUP Poland for the analysis of potential failure modes, breach and dambreak simulation for the Wloclawek Dam, River Vistula, Poland.

2011 – 2012 SMALL RESERVOIR RISK CATEGORISATION
With risk based reservoir safety legislation being introduced in England and Wales this project, commissioned by Defra, provided guidance and a simple risk assessment methodology aimed at owners of small reservoirs such that they could assess the risks posed by their existing or planned small reservoirs and hence take steps to minimise those risks through design and / or operation.

2011 – 2012 A GUIDE TO RISK ASSESSMENT OF RESERVOIRS
Following the earlier scoping study, development of a framework and recommended tiered approach for risk assessment for reservoirs in England and Wales. The project develops the methodology and produces industry guidance which builds upon the earlier Interim Guide and CIRIA Guide to risk assessment, including current international best practice.

2009 - 2010 DAMBREAK ASSESSMENT AND EMERGENCY PLANNING FOR KIO KHO MA DAM, THAILAND
Provision of expert advice on dam failure, flood routing and mapping, flood impact analysis, risk assessment and emergency planning for the Thai Kio Kho Ma Dam.

2008 - 2011 FLOOD RISK MANAGEMENT RESEARCH CONSORTIUM – FRMRC2
Task leader within the Infrastructure work package, developing a simplified breach model for use within system risk / reliability modelling.

2008 - 2011 INTERNATIONAL LEVEE MANUAL
Member of the UK steering committee for the development of an International Levee Manual, providing detailed guidance on the design, construction, maintenance and operation of flood levees.

2008 RESERVOIR INUNDATION MAPPING (RIM) PILOT APPLICATION
Trial application of the RIM methodology to selected dams, highlighting issues with the proposed methodology. Undertaken in partnership with Atkins.

2008 RESERVOIR INUNDATION MAPPING (RIM) METHODOLOGY
Expert guidance offered on methodology development as part of the project Quality Review Team.

2008 INTEGRATION OF THE HR BREACH MODEL AND THE INFOWORKS RS FLOW MODEL
The HR BREACH predictive breach model was integrated into the InfoWorks RS flow modelling package providing the first truly integrated commercial breach and flow modelling package.

2007 – 2009 DAM SAFETY INTEREST GROUP BREACH MODELLING PROJECT
Participation in this international R&D project aimed at reviewing, evaluating and developing a predictive breach model for industry use. Participation as developer of the HR BREACH model and evaluator of models.

2007 – 2008 DEVELOPING A STRATEGY AND PRIORITISED PROGRAMME FOR RESEARCH SUPPORTING UK RESERVOIR SAFETY
To review existing programmes of research supporting reservoir safety, develop an appropriate short and long term research strategy for the UK and to provide a prioritised list of recommended actions. This project supports the research programme being established by the Environment Agency through the Reservoir Safety Advisory Group. The research also considers different modes and sources of funding to support the research.

2006 – 2009 MODELLING EMBANKMENT PERFORMANCE (HR BREACH MODEL)
Second stage development of the HR BREACH model through detailed analysis of IMPACT project data and additional research via the FLOODsite project. This development project will enhance the accuracy and capabilities of the HR BREACH model for use in predicting breach growth through embankment dams and flood defence embankments.

2004 - 2009 EUROPEAN FLOODSITE PROJECT – TASK 4 (FAILURE MODES) AND TASK 6 (BREACH MODELLING)
Task Leader for FLOODsite Tasks 4 and 6 investigating failure modes for flood defence structures and breach initiation and growth processes. Outputs included a definitive collation of failure modes for use in reliability analysis, along with a state of the art review and development of predictive breach models.

2004 - 2009 EUROPEAN FLOODSITE PROJECT – INTEGRATED FLOOD RISK ANALYSIS AND MANAGEMENT METHODOLOGIES
Project Manager for the FLOODsite Project, for which HR Wallingford is the Co-ordinating organisation. FLOODsite is a European Commission Integrated Project under the Sixth Framework Research Programme comprising an extensive programme of research and application aimed at developing, drawing together and implementing an integrated European methodology for flood risk analysis and management. The project team comprises members from some 36 organisations drawn from 15 different countries with a total project value of ~€14M.

Selected Publications

Morris, M.W. (2011) Breaching of earth embankments and dams. PhD thesis. The Open University.

Morris, M.W., Hassan, M.A.A.M., Wahl, T.L., Tejral, R.D., Hanson, G.J. and Temple, D.M. (2012). Evaluation and development of physically based embankment breach models. FLOODrisk2012 conference, Rotterdam, Netherlands. 20-22nd November, 2012.

Van Damme, M., Morris, M.W., Borthwick, A.G.L. and Hassan, M.A.A.M. (2012). Rapid embankment breach modeling. FLOODrisk2012 conference, Rotterdam, Netherlands. 20-22nd November, 2012.

Tourment, R., Morris, M.W. and Royet, P. (2012). Levee failures related to structure transitions: typology, levee performance evaluation and improvements. FLOODrisk2012 conference, Rotterdam, Netherlands. 20-22nd November, 2012.

Morris, M.W., Hassan, M.A.A.M. and van Damme, M. (2012) 'Recent improvements in predicting breach through flood embankments and embankment dams'. British Dam Society 17th Biennial Conference, University of Leeds. 12-15th September, 2012.

Morris, M.W., Wallis, M., Brown, A.J., Bowles, D.S., Gosden, J., Hughes, A.K., Topple, A., Sayers, P.B. and Gardiner, K. (2012) 'Reservoir safety risk assessment – a new guide'. British Dam Society 17th Biennial Conference, University of Leeds. 12-15th September, 2012.

Morris, M.W., Goff, C. and Simm, J.D. (2012) 'Current European research relevant to reservoir safety: the FloodProBE and UrbanFlood projects'. British Dam Society 17th Biennial Conference, University of Leeds. 12-15th September, 2012.

Samuels, P.G. and Morris, M.W. (2010) 'Idealised model for flow towards a dam breach', First European Division IAHR Congress, Edinburgh. 4-6th May, 2010.

Samuels, P.G., Morris, M.W., Sayers, P.B., Creutin, J.-D., Kortenhaus, A., Klijn, F., van Os, A., Mosselman, E. and Schanze, J. (2010) 'A framework for integrated flood risk management', First European Division IAHR Congress, Edinburgh. 4-6th May, 2010.

Morris, M.W. and Hassan, M.A.A.M. (2009) 'Breach modelling research into practice: Conclusions from the HR Wallingford & European FLOODsite Projects', ASDSO Dam Safety 09, Hollywood, Florida, US2009.

Tagg, A.F., Morris, M.W., Lumbroso, D.M. and Di Mauro, M. (2009) 'Improved Emergency Planning and Evacuation through the use of a Loss of Life Model', ASDSO Dam Safety 09, Hollywood, Florida, US,

Simm, J.D., Morris, M.W., Gouldby, B.P. and Sayers, P.B. (2009) 'Levee fragility and breach growth analysis', ASFPM Conference 2009, Orlando, Florida, US,

Morris, M.W., Hassan, M.A.A.M., Ghataora, G.S. and Samuels, P.G. (2009) 'Breach formation: Identifying key physical processes to support improved breach numerical modelling', 33rd IAHR Congress, Vancouver, British Colombia,

Morris, M.W., Hanson, G.J. and Hassan, M.A.A.M. (2008) 'Improving the accuracy of breach modelling: why are we not progressing faster?' *Journal of Flood Risk Management*, Vol. 1 (No. 4), pp. pp. 150-161.

Morris, M.W. (2008) 'The impact of dambreak - managing the risks', *Dam Safety Management 2008*, Nanjing, China, 22-24th October, 2008.

Morris, M.W., Hassan, M.A.A.M, Kortenhaus, A., Geisenhainer, P., Visser, P.J. and Zhu, Y. (2008). Modelling breach initiation and growth. FLOODrisk 2008 conference, 30th September – 2nd October, 2008. Oxford, UK

Morris, M.W., Hughes, A.J. and Buijs, F (2008). Dambreak and emergency planning: Meeting end user needs. British Dam Society 15th Biennial Conference, Warwick, Sept 2008.

Morris, M.W., Hassan, M.A.A.M., Samuels, P.G. and Ghataora, G.S. (2008). Development of the HR BREACH model for predicting breach growth through flood embankments and embankment dams. Riverflow2008 International conference on fluvial hydraulics, 3-5th September, 2008. Izmir, Turkey.

Morris, M.W., Hassan, M.A.A.M., Buchholzer, Y. and Davies, T. (2008). HR BREACH: Developing a practical breach model to meet industry needs. US Society on Dams 28th Annual Meeting and Conference, April 28th - May 2nd Portland, Oregon.

Morris, M.W., Hassan, M.A.A.M and Vaskinn, K.A., (2007). Breach formation: Field tests and laboratory experiments. Journal of Hydraulic Research, Volume 45, Extra Issue (2007).